RELATIVE CONTRIBUTIONS OF THE STRINGENT

RESPONSE MEDIATORS (p)ppGpp and DksA TO

HAEMOPHILUS DUCREYI VIRULENCE IN HUMANS

Concerta Leigh Holley

Submitted to the faculty of the University Graduate School
in partial fulfillment of the requirements
for the degree
Doctor of Philosophy
in the Department of Microbiology and Immunology,
Indiana University

August 2015

Accepted by the Graduate Faculty, Indiana University, in partial
fulfillment of the requirements for the degree of Doctor of Philosophy.

_____
Stanley M. Spinola, M.D., Chair

_____
Margaret E. Bauer, Ph.D.

Doctoral Committee

_____
X. Frank Yang, Ph.D.

June 17, 2015

_____
Mark G. Goebl, Ph.D.

Acknowledgments

To my committee: Thank you for helping me transition between labs. Your guidance through those difficult times when the experiment just didn't quite work (Dr. Goebl), when I needed a radioactive home (Dr. Yang) or just needed a cup of tea and a chat (Dr. Bauer).

To my labmates (past and present): Kate, Dharanesh, Julia, Diane, Susan and Wei, and Lana. We've had so much fun these past years. I have learned so much from each of you. I know that we'll continue to be friends and collaborators long after my time in the lab has passed.

To Dr. Spinola: I was lucky to have found such a wonderful mentor who understood my career goals and supported me fully. I am a better person for having you in my corner and every future success I have is because you welcomed me into your lab.

I would like to thank my friends and my family for supporting me as I refused to get a real job. This would not have been possible without their steadfast support and encouragement.

To my Mom: I always said I'd dedicate my first book to you. It's not the dystopian novel I always promised – though that may still happen- but I hope this will do for now.

To my Husband: My tree root. I was never afraid to step out on a limb because you kept me grounded. Without your support, none of this would have been possible.

Concerta Leigh Holley

RELATIVE CONTRIBUTIONS OF THE STRINGENT RESPONSE MEDIATORS

(p)ppGpp AND DksA TO *HAEMOPHILUS DUCREYI* VIRULENCE IN HUMANS

Haemophilus ducreyi causes chancroid, a sexually transmitted genital ulcerative disease that facilitates the transmission of HIV-1. *H. ducreyi* also causes non-sexually transmitted cutaneous ulcers in children in tropical regions. During human infection, *H. ducreyi* is subject to a variety of stresses. The stringent response is a bacterial stress response system induced by nutrient limiting conditions and mediated by guanosine tetra- and pentaphosphate [(p)ppGpp] and the transcriptional regulator DksA. (p)ppGpp and DksA jointly interact with RNA polymerase to regulate genes critical for bacterial survival. We hypothesized that the stringent response is required for *H. ducreyi* virulence in humans. A Δ*relA*Δ*spoT* mutant, which is unable to synthesize (p)ppGpp, was partially attenuated for abscess formation in human volunteers. Loss of (p)ppGpp increased bacterial resistance to phagocytosis and stationary phase survival; however, the mutant was more sensitive to oxidative stress. A Δ*dksA* mutant was also partially attenuated in humans. The Δ*dksA* mutant behaved like the (p)ppGpp mutant in stationary phase survival and sensitivity to oxidative stress, but exhibited decreased resistance to phagocytosis. Both mutants had decreased adherence to fibroblasts, but the mechanisms underlying the adherence defect were distinct. To better understand the roles of (p)ppGpp and DksA in regulating gene expression, we performed transcriptome analysis of the parent and mutant strains. (p)ppGpp and DksA deficiency resulted in dysregulation of

multiple genes including several known virulence determinants. At stationary phase, (p)ppGpp and DksA targets were not identical but significantly overlapped; as the mutants were phenotypically distinct, this finding underscores both the unique and joint roles DksA and (p)ppGpp play in regulation of *H. ducreyi* virulence. We conclude that (p)ppGpp and DksA play significant roles in *H. ducreyi* pathogenesis. This is the first study to show that the stringent response has a direct role in the ability of a bacterial pathogen to cause disease in humans.

Stanley M. Spinola, M.D - Chair

Table of Contents

List of Tables

List of Figures

List of Abbreviations

ACT	Aspartate kinase, Chorismate mutase and TyrA (domain)
Amp/Amp^R	Ampicillin/ampicillin resistant
AP	Antimicrobial Peptides
BLAST	Basic Local Alignment Search Tool
Cat	Chloramphenicol
CDC	Centers for Disease Control
CFU	Colony Forming Units
CpxA	Two component sensor kinase protein
CpxR	Two component regulator protein
CUD	Cutaneous Ulcer Disease
DMEM	Dulbecco's Modified Eagle Medium
DNA	Deoxyribonucleic acid
DsrA	*H. ducreyi* serum resistance protein A
EDD	Estimated Delivered Dose
FBS	Fetal Bovine Serum
Flp	Fimbria-like protein
FRT	Flippase recognition target
GC	Gonococcal
GUD	Genital Ulcerative Disease
H_2O_2	Hydrogen peroxide
HBSS	Hank's Balanced Salt Solution
HFF	Human Foreskin Fibroblasts

HIV-1	Human Immunodeficiency Virus Type I
HP	Human Passaged
Kan/Kan^R	Kanamycin/kanamycin resistant
LOS	Lipooligosaccharide
LspA1	Large supernatant protein 1
LspA2	Large supernatant protein 2
Mab	Monoclonal antibody
MDM	Monocyte Derived Macrophages
mRNA	Messenger RNA
NHS	Normal Human Serum
OD	Optical Density
OMP	Outer Membrane Protein
ORF	Open Reading Frame
^{32}P	Radioactive monopotassium phosphate
(p)ppGpp	Guanosine tetraphosphate and guanosine pentaphosphate
PAL	Peptidoglycan Associated Lipoprotein
PBMC	Peripheral Blood Mononuclear Cells
PCR	Polymerase Chain Reaction
PEI	Polyethyleneimine
PMN	Polymorphonuclear leukocytes
qRT-PCR	Quantitative transcriptase polymerase chain reaction
RBS	Ribosomal Binding Site
RFAM	Database for annotating RNA

RPMI	Roswell Park Memorial Institute Medium
RNA	Ribonucleic acid
RNAP	RNA Polymerase
rRNA	ribosomal RNA
RT	Reverse Transcriptase
SCOTS	Selective Capture of Transcribed Sequences
Spec	Spectinomycin resistance cassette
sRNA	small RNA
STI	Sexually Transmitted Infection
Tad	Tight adhesion
TGS	Threonyl-tRNA synthetase, GTPase, and SpoT (domain)
Tet	Tetracycline
TLC	Thin Layer Chromatography
WCL	Whole Cell Lysates
WHO	World Health Organization
X-gal	5-bromo-4-chloro-3-indoyl-b-D-galactopyranoside

Chapter I:

Literature Review

Section I:

***Haemophilus ducreyi* and Ulcerative Disease**

Haemophilus ducreyi

Haemophilus ducreyi is a gram-negative coccobacillus belonging to the *Pasteurellaceae* family in the gammaproteobacteria class. Due to its requirement for hemin, *H. ducreyi* was originally placed within the genus *Haemophilus.* Compared to other members of this group, *H. ducreyi* is genetically unique. *H. ducreyi* lacks many of the genes involved in fermentation of carbohydrates but possesses genes encoding menaquinones not commonly found in the true *Haemophilus* group (1). *H. ducreyi* is most closely related to *Actinobacillus pleuropneumoniae*, a porcine respiratory pathogen, and ribosomal RNA analysis reclassified *H. ducreyi* in the *Actinobacillus* genus (2-4). This cluster, which also includes *Mannheimia haemolytica*, forms a distinct lineage from the other *Pasteurellaceae* (2).

Overall, *H. ducreyi* isolates exhibit a high degree of genetic homology (5). Based on differences in the migration of LOS, antigenicity, and *in vitro* growth characteristics, two classes of *H. ducreyi* clinical isolates have been defined (6, 7). Evidence suggests that these classes are still diverging. Recombination has introduced variant alleles that are

specific to each representative class. *lspA2, ncaA,* and *dsrA* alleles are different between the Class I and Class II strains (8). These genes produce proteins, which directly interact with the host and are likely exposed to more selective pressure than genes whose products are cytosolic. Analysis showed that the sequence of these genes alone can be used to distinguish between these two classes (8).

H. ducreyi is the causative agent of chancroid, a sexually transmitted genital ulcerative disease. Augusto Ducrey was the first person to identify the causative agent of chancroid in 1889 through a series of repetitive autoinoculation experiments (9). The organism was later named in his honor. However, *H. ducreyi* was not successfully isolated until 1900 when Bezancon and his group used purified bacteria to inoculate human volunteers (10).

Chancroid

Chancroid was first identified as a disease clinically distinct from syphilis in 1852 by Leon Bassereau (11). While syphilis, another ulcerative disease, causes hard ulcers, soft ulcers characterize chancroid. Papules develop on the genitals three to seven days after contact with an infected individual. The papules progress quickly into pustules that rupture into characteristic chancroidal ulcers. These ulcers often have ragged edges and a slightly rounded shape. The ulcer base is often covered by a necrotic, purulent exudate. In many cases, the infection progresses to include regional lymphadenopathy and bubo formation (12). *H. ducreyi* has never been reported to disseminate throughout the body and cause systemic infection. *H. ducreyi* grows best between 33°C and 35°C and likely cannot tolerate normal systemic temperatures (13). Lesions found outside of the genital

region or initial site of infection in a chancroid infected individual are often the result of autoinoculation.

Diagnosis requires identification of the bacterium on rich culture medium that is not widely available. Furthermore, due to lack of appropriate culture conditions, *H. ducreyi* cannot always be recovered from patients' lesions. Multiplex PCR is the most accurate test for diagnosis of *H. ducreyi*. It has a sensitivity of 95 to 98%, compared to the 75% sensitivity seen in culture-based diagnosis. A review of studies summarizing the prevalence of *H. ducreyi* in patients with GUD attending STI clinics showed that *H. ducreyi* is identified in 19.6% of GUD cases in endemic regions (14). Thus *H. ducreyi* is still a common cause of GUD.

Current CDC guidelines for treatment of chancroid include one of the following therapies: 1 oral dose of 1g Azithromycin; 250 mg of Ceftriaxone delivered intramuscularly; 500 mg oral Erythromycin given 3 times a day for 7 days; or 500 mg Ciprofloxacin given twice a day for 3 days.

Chancroid is an important disease because it facilitates acquisition of HIV-1. In fact, GUD is estimated to increase risk of HIV acquisition 25 fold (15). *H. ducreyi* infection induces an immune response that increases the number of CD4 positive T-cells and macrophages in the ulcerative region (16). CD4 positive cells are the primary targets for HIV infection. Compared to peripheral blood T cells and monocytes, lesional CD4 cells have increased expression of CCR5, and lesional macrophages have increased expression CCR5 and CXCR4, important co-receptors for HIV entry into CD4 positive cells (17). *H. ducreyi* also disrupts mucosal integrity, which increases the opportunity for HIV-1 acquisition. Chancroidal ulcers in HIV-1 positive patients heal slowly and poorly

compared to seronegative patients (18). HIV-1 infection is associated with an increased number of ulcers during *H. ducreyi* infection (19). Thus, the interaction between HIV-1 and *H. ducreyi* acquisition has global significance.

Patients infected with HIV and GUD have increased plasma HIV RNA levels (20). Furthermore, treatment of GUD reduces viral loads (21). In early stages of disease, no increase in viral loads was found in HIV-positive volunteers, who were experimentally infected with *H. ducreyi* (22). Together, this indicates that untreated GUD in the ulcerative stage results in increased HIV virion pools in the plasma and urogenital compartments, which increases the probability of transmission.

Due to an emphasis on syndromic management of genital ulcers in resource poor countries, the actual prevalence of chancroid is now unknown. The last estimate of chancroid prevalence by the WHO in 1995 was approximately 7 million cases per year worldwide (14). Chancroid prevalence appears to have substantially declined in resource-poor countries and Europe; nucleic acid amplification tests estimate that chancroid currently accounts for less than 1% of genital ulcers (23). Surveillance studies in southern Africa, however, suggest that chancroid remains an important cause of GUD in Lesotho, Madagascar, and Malawi (23).

Chancroid is rare in the United States and other industrialized nations but is endemic in resource poor countries. In order for chancroid to remain in a population, it has to be maintained in a population with a high sex-partner change rate. Thus, commercial sex workers allow for the maintenance of the disease in endemic areas. Targeting this reservoir of infection is thought to have caused an overall reduction in chancroid transmission. In fact, syndromic management and presumptive treatment of

high-risk populations worldwide have resulted in a substantial decline in chancroid and other sexually transmitted infections. Chancroid, however, remains endemic in Africa, Asia, and Latin America.

Cutaneous Ulcers

Although non-sexually transmitted cutaneous ulcers in children in the South Pacific islands and equatorial Africa are usually attributed to *Treponema palladium* subspecies *pertenue*, recent studies performed as part of a World Health Organization–directed yaws eradication campaign suggest that *H. ducreyi* is a major cause of this syndrome. The first case of cutaneous ulceration caused by *H. ducreyi* was reported in an adult from Fiji in 1989 (24). Subsequent cases of cutaneous ulcers in children due to *H. ducreyi* were reported from a wide range of the South Pacific islands (25-27). In three recent, large, cross-sectional community surveys in Papua New Guinea, the Solomon Islands, and Ghana, the prevalence of skin ulcers was between 2 and 4%. *H. ducreyi* DNA is detected in 60, 32, and 10% of lesions while *T. pallidum* DNA is detected in only 34, 0 and 0% (28-30). While the mode of transmission is unknown, CUD appears to be non-sexually transmitted. Considering the global prevalence of yaws, an estimated 2.5 million cases, extragenital lesions resulting from *H. ducreyi* infection may be much more common than was previously recognized. Thus, understanding the pathogenesis of *H. ducreyi* remains important from the point of view of public health.

Antibiotic Resistance and *Haemophilus ducreyi*

Controlling curable diseases such as chancroid is vital to minimizing HIV-1 transmission. Due to syndromic management, there is no current information about antibiotic resistance in *H. ducreyi* (14). Circulating *H. ducreyi* strains are thought to be universally susceptible to quinolones, macrolides, and ceftriaxone. However, *H. ducreyi* has a tendency to acquire antibiotic resistance factors. Several isolates of *H. ducreyi* have already been shown to be resistant to current or former lines of therapy (31). Chromosomal-mediated resistance has been described for trimethoprim, penicillin, and fluoroquinolones (32-34). Increasing MICs of ciprofloxacin and erythromycin have also been detected (34). Overall, this emphasizes the necessity of monitoring antimicrobial resistance of *H. ducreyi* strains.

The New Delhi metallo-beta-lactamase-1 (NDM-1), which confers resistance to quinolones and ceftriaxone, has been detected across the globe within the *Enterobacteriaceae* (35). If *H. ducreyi* acquires quinolones and ceftriaxone resistance from the NDM-1 plasmid, only macrolides will be available for treatment. Standard antibiotic treatment has been used to manage chancroid in the past, however, the potential for multidrug resistance makes understanding how *H. ducreyi* survives *in vivo* of the upmost importance.

Models of Chancroid Infection

In order to study *H. ducreyi* pathogenesis, the Spinola laboratory developed a human infection model (36). The human infection model very closely simulates early stages of natural infection. In the human challenge model, volunteers are inoculated with

H. ducreyi 35000HP and isogenic mutants. The Class I Strain 35000, originally isolated from a patient with chancroid, was then human passaged to make *H. ducreyi* 35000HP (Human Passaged) (36, 37). The bacteria are delivered into the epidermis and dermis of the upper arm through wounds made by the tines of an allergy-testing device. The model allows us to study *H. ducreyi* as it faces natural *in vivo* stresses because *H. ducreyi* is in its natural human host.

Phylogenetic analysis of cutaneous ulcer strains show that they are highly related to 35000HP (38). Data from our lab further demonstrates that CUD strains likely recently emerged from Class I strains (39). Overall, this suggests that the human inoculation model is relevant to the study of both chancroid and cutaneous ulcers.

Human infection models have been used to understand pathogenesis and the immune response to pathogens to test vaccines (40). Human experimental models allow us to define virulence factors of human pathogens in their natural settings. *H. ducreyi* is one of the few bacterial pathogens for which pathogenesis can be studied in humans. Human challenges have been done for several pathogenic bacterial species, including but not limited to *Streptococcus pneumoniae,* enterotoxigenic *E. coli,* and enteropathogenic *E. coli* (41-43). These models were used or developed for testing of vaccines or vaccine components. Human inoculation experiments with *Helicobacter pylori* were stopped for reasons including lack of need for vaccines and lack of a clear strategy for vaccine development in the United States; and potential for risk to volunteer – unsuccessful eradication of bacteria after trial (42). The usefulness of human infection models for understanding bacterial pathogenesis *in vivo* allows for the maintenance of studies whose focus is not vaccine development.

A temperature-dependent rabbit model does exist for *H. ducreyi*. In this model, rabbits are inoculated intradermally with 10^5 CFU of bacteria. When rabbits are housed at normal room temperature (23°C), they do not form lesions with this inoculum size. When rabbits are housed at 15-17°C, necrotic lesions form at the site of inoculation (44). A porcine model, in which pigs are inoculated in the ears using an allergy testing device similar to what is used in the human model, has also been established for chancroid (45). Finally, a macaque model of infection exists for *H. ducreyi*. Bacteria are injected into the foreskin of male macaques and the ulcers that are formed closely resemble those seen in humans (46). Female macaques, however, do not develop lesions at all and thus this model is gender limited.

These models allow study of the pathogen to the ulcerative stage of disease, which is impossible in our human model. However, there are also limitations of these models. In all 3 animal models, animals develop serum antibodies to *H. ducreyi*. In natural and experimental infection, however, antibodies do not develop in early disease (47). Additionally, rabbits develop protection from secondary challenge which does not happen in natural or experimental infection (48). A much larger inoculum is necessary for infection in the animal models (10^{4-7} CFU) versus the human challenge model (10^{1-2} CFU) likely because *H. ducreyi* is not a natural zoonotic pathogen (12). Lastly, a major problem with these models is that they are all clearance models; *H. ducreyi* is rapidly cleared from the animals making them unsuitable for the study of disease progression. In contrast, *H. ducreyi* replicates to a range of 10^{4-6} CFU in experimental pustules of human volunteers (49) .

Host – *Haemophilus ducreyi* Interactions

Experimental infection of *H. ducreyi* in humans mimics the time course of natural infection. After human experimental inoculation, fibrin and collagen are deposited in the wounds. Polymorphonuclear neutrophils and macrophages infiltrate the wounds at the site of infection thereafter (50). Within 48 hours, PMNs form an abscess at the site of infection that ultimately forms an ulcer within 7 days in the epidermis. Below the abscess, myeloid dendritic cells, CD4 and CD8 T cells and activated natural killer cells infiltrate the dermis. *H. ducreyi* is found within the abscess and within the dermis in pustules where it associates with fibrin, collagen, PMNs, and macrophages. During natural infection, *H. ducreyi* also colocalizes with fibrin and PMNs (51). Importantly, *H. ducreyi* is not found within phagocytes at the site of infection.

Pustules caused by *H. ducreyi* contain several cell types. The majority of the pustule is comprised of PMNs; however macrophages, T-cells, dendritic cells and some B cells can also be found in the lesion (12, 50). Furthermore, collagen and fibrin deposition at the site of infection forms scaffolding, which ultimately supports pustule formation (12, 50). A macrophage collar forms at the base of the abscess (12, 50).

In both natural and experimental infection, *H. ducreyi* associates with both PMNs and macrophages, but resists phagocytic uptake (12, 50, 52). Dendritic cells, however, do phagocytize *H. ducreyi*. The dendritic cells become partially activated, which stimulates the immune response (53, 54). CD4+ memory cells are recruited in naive volunteers to the site of infection, indicating a delayed-type hypersensitivity reaction, even in naïve volunteers (12, 55). The CD4+ memory cells produce IFN-gamma and IL-10. IL-10 is

thought to inhibit phagocytic activity, which prevents effective clearance of *H. ducreyi* (12, 53).

In experimental infection, some volunteers repeatedly resolve infection (resolvers) while others repeatedly form pustules (pustule formers) (47). Pustule formation in individuals is dependent on both the host immune response and gender (47, 56). Subsequently, interest in identifying the underlying differences between pustule formers and resolvers has deepened. Microarray analysis indicated that challenge with *H. ducreyi* results in distinct immune response between pustule formers and resolvers (53, 56). Pustule formers have a mixed hyper inflammatory and regulatory transcriptional profile while resolvers exclusively expressed differentially regulated unique transcripts that should promote only a Th1 response or allow for expansion of Th17 cells (53).

Recently, our lab conducted a study to determine if the skin microbiome dictated the outcome of experimental infection in volunteers. We did identify some potentially protective species (species associated with resolvers) and some potentially deleterious species (associated with pustule formation). Overall, after exposure to *H. ducreyi*, the microbiomes of sites on pustule formers were more similar to one another while sites on resolved persons were more dissimilar (van Rensburg, submitted). Thus, although the microbiome may exert some effect, the final outcome of the volunteers is still largely driven by host factors.

Section II:

***Haemophilus ducreyi* Virulence**

Virulence Determinants of *H. ducreyi*

The experimental human inoculation model has revealed genes critical for virulence of *H. ducreyi*. Not including this study, to date 32 isogenic mutants have been tested in the human challenge model. 10 mutants were fully attenuated (absolutely required for pustule formation) and 6 were partially attenuated. The remaining mutants encode genes that do not contribute to virulence; thus, the following discussion is largely limited to mutants found fully or partially attenuated in the human challenge model of *H. ducreyi* infection.

Many of the known virulence factors of *H. ducreyi* are located in the outer membrane. For example, PAL is an OMP thought to play a critical role in stabilization of the membrane (57). In addition to decreased pustule formation rates, loss of PAL was associated with increased sensitivity to antibiotics, suggesting that the *pal* mutant exhibits an unstable outer membrane (12).

The TonB dependent hemoglobin receptor HgbA is another OMP required for virulence (58). HgbA binds to hemoglobin, which is the sole heme source required for *H. ducreyi* infection *in vivo* (59). Loss of HgbA likely results in heme starvation, even when hemoglobin is readily available. Two additional TonB dependent heme receptors have been identified in *H. ducreyi*, TdhA and TdX. A *tdX tdhA* double mutant is fully virulence in the human model indicating that these receptors are likely dispensable *in*

vivo (59). This suggests that expression of HgbA is critical for heme acquisition in *H. ducreyi.*

H. ducreyi also contains homologues of genes required for synthesis of enterobacterial common antigen (ECA). ECA is an outer membrane glycolipid commonly found on lipopolysaccharide (LPS) O-antigen or in capsule of Gram-negative enterobacterial species. The first enzyme in the ECA synthesis pathway, WecA, transfers N-acetylglucosamine to undecaprenyl-P. Although *H. ducreyi* does not express O-antigen or capsule, the *wecA* mutant was partially attenuated (60). This suggests that *H. ducreyi* may express a putative ECA-like glycoconjugate that is required for infection.

Phagocytosis is a critical element of the innate immune response that enables pathogens to be rapidly contained and cleared. Although *H. ducreyi* colocalizes with polymorphonuclear leukocytes and macrophages, it evades phagocytosis. Evasion results from secretion of two large secreted proteins, LspA1 and LspA2. The two proteins are secreted by LspB; the *lspB* mutant was attenuated in the rabbit model of infection indicating that the ability to secrete LspA1 and LspA2 is necessary for virulence (61). LspA2 and LspA1 suppress Src family protein tyrosine kinase activity, which ultimately inhibits phagocytosis (62, 63). Furthermore, LspA1 was found to bind the C-terminus of Src kinase, which stimulates Src's catalytic activity inhibiting Src activity (64). The *lspA1 lspA2* double mutant is fully attenuated in both the rabbit and human models of infection (65, 66). Taken together, these studies suggest that expression of LspA1 and LspA2 allow *H. ducreyi* to resist phagocytosis.

To combat bacteria, the innate immune system also produces APs whose purpose is to kill bacteria, which they are thought to do by primarily disrupting membrane

integrity. Bacteria have evolved multiple resistance strategies to avoid AP-mediated killing. One mechanism is the sensitive-to-antimicrobial-peptides (Sap) uptake transporters. SapA, the periplasmic binding protein, binds the AP and brings it to the periplasmic membrane. The SapBC proteins, which encode the periplasmic permease complex, translocate the APs into the cytoplasm. The APs are subsequently degraded by cytoplasmic peptidase. In *H. ducreyi*, a *sapA* mutant is partially attenuated for virulence while a *sapBC* mutant is fully attenuated (67, 68). Additionally, the *sapA* mutant is less susceptible to APs than the *sapBC* mutant. Taken together, these data suggest that the transport machinery remains active in the *sapA* mutant and thus, may still confer partial resistance to antimicrobial peptides.

The *H. ducreyi* genome contains a large operon which has high homology to the tight adhesin (tad) operon of *Aggregatibacter actinomycetemcomitans* (69). Components of this operon, which is homologous to type IV secretion system NTPases, have been well characterized in the human challenge model. The three fimbriae-like proteins, Flp1-3, are required for pustule formation (70). These proteins mediate adherence to human foreskin fibroblasts and microcolony formation *in vitro*. The Flp proteins are transported to the outer membrane by the Tad proteins, including TadA. TadA encodes an ATPase that is required for fibril production in *A. actinomycetemcomitan* (71). The *tadA* mutant is also fully attenuated in humans (72). Taken together, these results indicate that the ability to express the Flp proteins on the outer membrane is critical for pathogenesis.

During experimental infection, *H. ducreyi* associates with fibrin and collagen in the papular and pustular stages and fibrin in the ulcerative stage (51, 73). *In vitro* studies show that *H. ducreyi* binds extracellular matrix proteins fibronectin, laminin, and type I

and III collagen (74). The necessary for collagen adhesion protein A, NcaA, as its name implies, is required for collagen binding *in vitro.* Expression of *ncaA* was absolutely required for pustule formation in humans, highlighting the additional importance of collagen binding *in vivo* (75).

Resistance to serum-mediated killing is an important virulence mechanism for *H. ducreyi*. The outer membrane ducreyi serum resistance A (DsrA) protein has been identified as the primary mediator of serum resistance (76). DsrA functions by blocking binding of IGM, which is critical for activating the classical complement pathway (77). DltA, the *ducreyi* lectin A protein, provides partial serum resistance for *H. ducreyi* (78). Similar to the *dsrA* mutant, the *dltA* mutant is more susceptible to serum mediated-killing than the parent strain. Unlike the *dsrA* mutant, however, the *dltA* mutant is only partially attenuated in the human challenge model underscoring the fact that DsrA is the primary mediator of serum resistance in *H. ducreyi* (79).

An *fgbA* mutant was partially attenuated in the human challenge model suggesting that fibrinogen binding plays a role *in vivo* (80). The gene encoding FgbA was originally identified using SCOTS to identify genes preferentially expressed in experimental pustules (73). The gene product was subsequently identified in a ligand blot assay with denatured proteins as a fibrinogen binding protein. However, recently, fibrinogen was shown to interact specifically and in a dose-dependent manner with DsrA at the surface of viable *H. ducreyi* cells (81). Under non-reducing conditions, fibrinogen did not bind FgbA indicating that its role in *H. ducreyi* virulence is unclear.

Quorum sensing is a process, which allows individual bacteria to regulate gene expression based on the local bacterial cell density. In this way, quorum sensing serves as

14

a potent indicator of population density. Autoinducers, such as AI-2, are signaling molecules involved in quorum sensing (82). Inactivation of *luxS,* a critical component in synthesis of AI-2, decreases virulence of *Vibrio cholerae* and *A. actinomycetemcomitans* (82, 83). *luxS* is necessary for full virulence of *H. ducreyi* (84). The virulence defect of the *luxS* mutant is a direct result of decreased production of AI-2. Importantly, *H. ducreyi* produces AI-2 that functions in a *Vibrio harveyi*-based reporter system suggesting that *H. ducreyi* may have a functional quorum sensing mechanism (85).

The remaining three genes required for virulence are *cpxA, hfq*, and *csrA*. These genes are putative regulators of the aforementioned virulence determinants and are discussed in further detail in the next section.

Haemophilus ducreyi regulators of virulence

Unlike *E. coli* and many other gammaproteobacteria, *H. ducreyi* does not have an extensive stress response system. In comparison to *E. coli,* the *H. ducreyi* genome is relatively small (4.6 vs. 1.7 Mbp). *H. ducreyi* must use its smaller genome efficiently. For example, most bacterial species have multiple 2-component signal transduction systems that allow response to stress by altering gene expression (86). In contrast, *H. ducreyi* only appears to have one 2-component system, named CpxRA (85). In *E. coli*, CpxRA senses and responds to envelope stress signaled by misfolded proteins in the periplasm. CpxA is a sensor kinase that autophosphorylates when it senses envelope stress. CpxA then donates a phosphate group to the response regulator CpxR (which catalyzes the transfer), leading to a conformational change that ultimately results in regulation of target genes. For example, activation of the system in *E. coli* stimulates expression of chaperones to

alleviate accumulation of misfolded proteins. The *H. ducreyi* CpxRA system was found to downregulate at least 7 genes that encode known virulence factors including *dsrA* and *lspA2* (85). In the human challenge model, activation of CpxR by deletion of *cpxA* resulted in complete attenuation of the mutant, while inactivation of the system by deletion of *cpxR* did not affect virulence (87). These data led us to look at other stress response systems that may be important for *H. ducreyi* virulence.

Cyclic-di-GMP is a small nucleotide important for signal transduction and gene expression and has been shown to regulate expression of genes critical for adapting to changes in the environment (88). The *H. ducreyi* genome lacks homologues of diguanylate cyclases such as YdeH that synthesize cyclic-di-GMP.

In the transition from nutrient abundance to starvation, the limited amount of available RNAP is redistributed to transcribe genes involved in maintenance and survival. Alternative sigma factors are specialized regulatory factors that respond to unique environmental stress conditions and increase transcription of genes necessary for each stress. Within *E. coli*, there are 6 such factors: RpoE (Extracytoplasmic/oxidative), RpoH (Heat shock), RpoN (Nitrogen stress), RpoS (Stationary/Starvation), RpoF (Flagella/motility), and FecI (Iron starvation). The function of these factors is to help switch transcriptional activity in response to a large variety of environmental signals. As these are highly specialized they are required only for certain physiologically roles.

Of the above described alternate sigma factors, the *H. ducreyi* genome has homologues of only RpoH and RpoE. RpoS, *E. coli*'s primary alternate sigma factor, is not present. This indicates that unlike *E. coli*, *H. ducreyi* must have evolved other mechanisms to regulate gene expression without the use of a multitude of sigma factors.

Our lab found that RpoE and CpxRA regulate distinct sets of genes in *H. ducreyi*. Interestingly, the sets of genes regulated by RpoE and CpxRA ultimately complement one another in an effort to stabilize a stressed membrane (89). RpoE is a major regulator of envelope maintenance and repair factors, while CpxRA appears to regulate *H. ducreyi* virulence genes.

Hfq is an RNA chaperone that binds small regulatory RNA (sRNAs) and mRNAs to facilitate mRNA translational regulation in response to envelope stress, environmental stress, and changes in nutrient concentrations (90). Hfq functions as a global RNA regulator interacting with several hundred different sRNA and mRNA species (91, 92). Hfq modulates a myriad of cellular functions; inactivation of *hfq* significantly impairs pathogenicity of several bacterial species. In the absence of an RpoS homolog, Hfq likely serves as a major contributor of stationary phase gene regulation in *H. ducreyi* (93). Hfq positively regulates the expression of several virulence determinants including *lspB-lspA2*, *flp1-3*, and *dsrA* (93).

In *E. coli,* CsrA is a global regulator of carbon metabolism. An *H. ducreyi csrA* mutant was partially attenuated and exhibited several profound phenotypic changes in stationary phases including increased susceptibility to oxidative stress (94). Furthermore, deletion of *csrA* resulted in downregulation of *flp1* and *tadA* transcripts and Flp1 and Flp2 proteins (94). Taken together, this suggests that CsrA, similar to *hfq,* may be a regulator of virulence; however, it is unclear if CsrA regulates any other virulence determinants in *H. ducreyi*.

H. ducreyi has homologues to another system with well-characterized roles in nutrient stress, the stringent response. Despite its reduced genome size, *H. ducreyi* has

homologues for all 3 stringent response mediators previously identified in *E. coli*. The *H. ducreyi* RelA, SpoT and DksA proteins are 59, 69, and 70% identical to their *E. coli* homologues, respectively. Structural organization of the *E. coli* and H. *ducreyi* homologues is depicted in Figure 1. The subject of this thesis was to characterize the role of the stringent response in *H. ducreyi* pathogenesis.
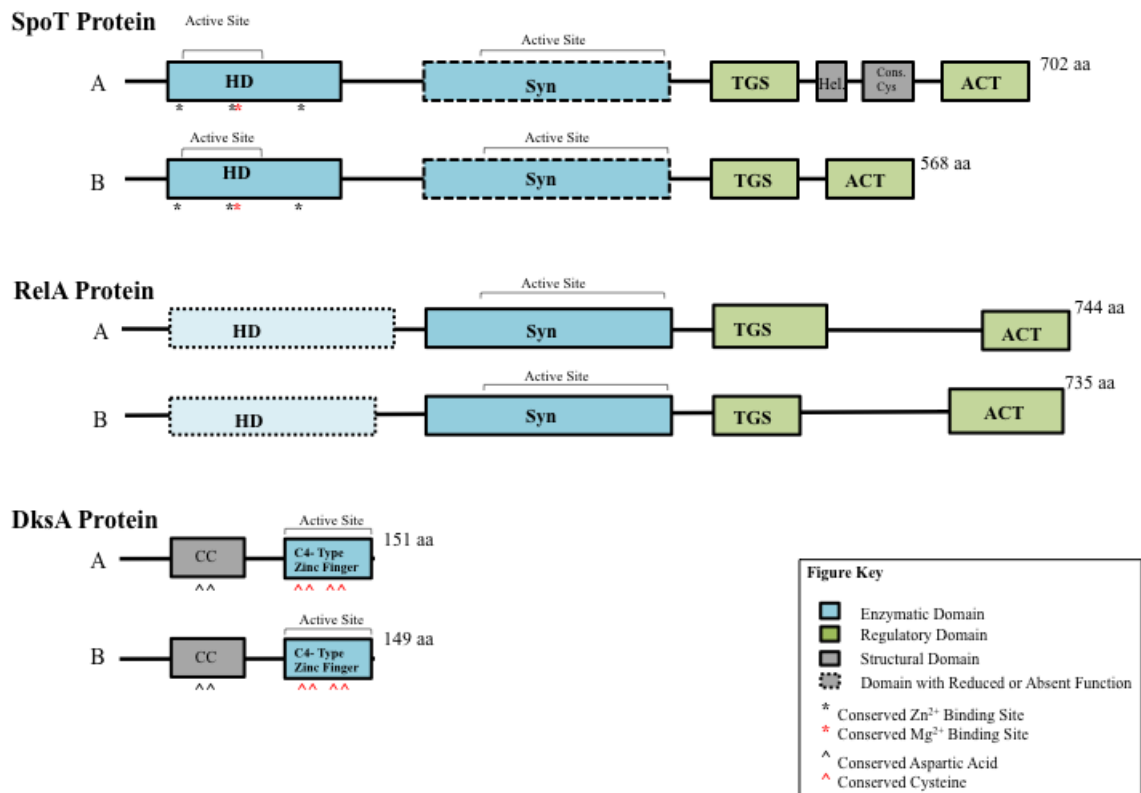
Figure 1. Structure of the enzymes that mediate the stringent response in *E. coli* (A) and *H. ducreyi* (B). Four functional regions have been identified: the Syn, synthetase domain, the HD, hydrolase domain, and the TGS and ACT domains. Functional domains with reduced or absent activity are indicated with dashed lines. The bifunctional SpoT protein contains both synthetase and hydrolase activities. As depicted in the diagram, the *H. ducreyi* SpoT protein has a deletion of the structural helical and Conserved Cysteine domains. *RelA* is a monofunctional synthetase; the HD domains in the RelA proteins lack the metal ion binding sites that give the domain activity. The activity of the SpoT and RelA proteins are controlled through their TGS and ACT domains. The DksA functional domain is a C4-Type Zinc Finger but the Coiled Coil Domain (CC) interacts with RNAP. Note that the structures show approximate locations of domains.

Section III:

The (p)ppGpp–mediated Stringent Response

The stringent response

An abscess is a localized accumulation of leukocytes with necrosis and partial liquefaction of cells and tissue (95). There is high protein content in the abscess that is likely the result of cell and tissue decay. The release of contents from within the cells may result in localized changes of nutrient content within the abscess. Stationary phase bacteria, cellular exudate, and anaerobic conditions are common in abscesses (96, 97). The abscess microenvironment may induce alterations in gene expression as a result of entry into stationary phase, anaerobic conditions, changes in pH, and nutrient availability.

To our knowledge, there are no studies that detail the nutrient content of the skin abscess. Understanding the nutrient content of the abscess is important because during human infection *H. ducreyi* will only have access to nutrients within the abscess. There are a few studies that determine various contents of abscesses in other locations that can give some insight into what may be occurring in a skin abscess. A study of amino acid content in brain abscesses found an increased concentration of valine and leucine (8.16 mMol/L) within the abscess as compared to outside the abscess (2.57 mMol/L) (98). Most of the other amino acids found within the abscesses are below 1 mMol/L, which may lead to amino acid starvation in the invading bacteria. In terms of fatty acid content, the majority of fatty acids detected in pyogenic liver abscesses are volatile short chain fatty acids such as butyric and acetic acid that perturb fatty acid biosynthesis in bacteria

(99, 100). Concentrations of other nutrients are unknown. The abscess, therefore, is likely a nutrient limiting environment.

In bacteria, nutrient starvation induces the stringent response. The response is mediated by the alarmone guanosine tetraphosphate (ppGpp) and guanosine pentaphosphate (pppGpp), collectively referred to as (p)ppGpp. (p)ppGpp synthetases and hydrolases are highly conserved in β- and γ-proteobacteria (101). The stringent response is induced by amino acid, fatty acid, carbon, phosphate, and iron starvation, and heat shock (102-105). The mechanism by which ppGpp levels are controlled is well characterized in *E. coli* (Figure 2).

The enzyme RelA synthesizes (p)ppGpp from ATP and GTP during amino acid starvation. (p)ppGpp then interacts with RNA polymerase (RNAP) to regulate gene expression. Through recognition of specific discriminator regions upstream of transcription start sites, (p)ppGpp upregulates genes critical for survival and increases usage of alternative sigma factors, while genes involved in protein synthesis are downregulated. To turn off the response, *E. coli* utilizes the bifunctional enzyme SpoT. SpoT can synthesize (p)ppGpp but is primarily involved in hydrolysis of ppGpp back to GTP and ATP.
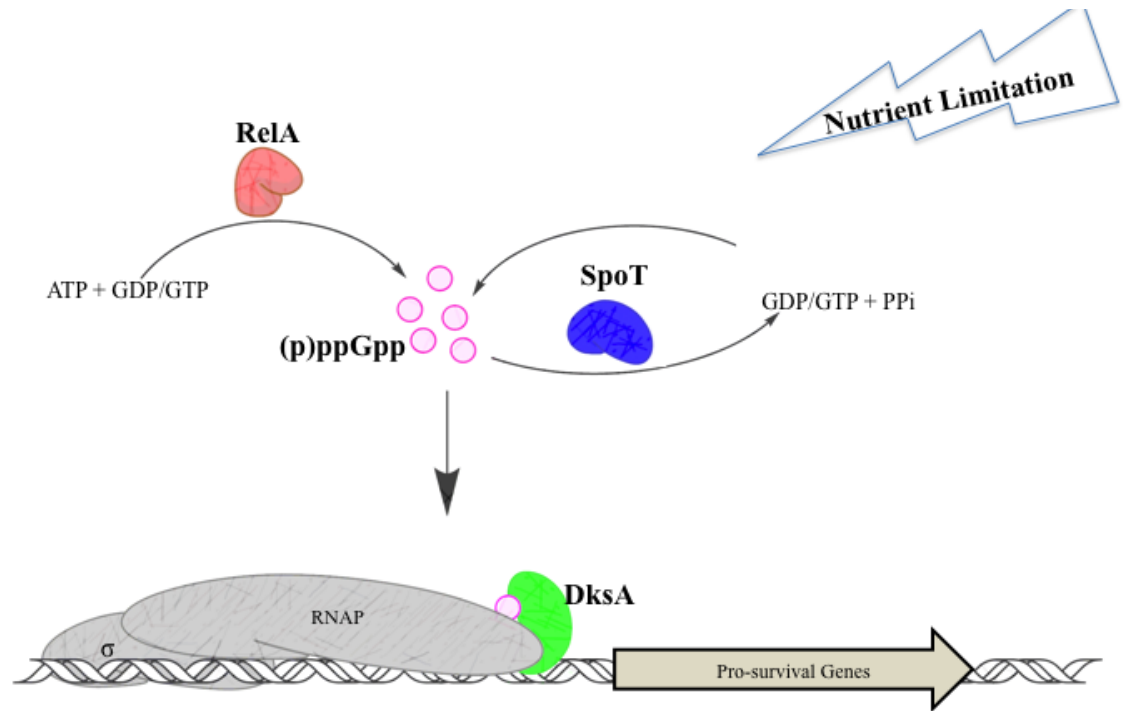
Figure 2.   Diagram of the bacterial stringent response system. Two parallel pathways synthesize (p)ppGpp from ATP and GTP in response to any of several nutrient stress signals. Together with DksA, (p)ppGpp alters gene expression through direct interaction with RNAP. PP_i, pyrophosphate.

   To enhance the stringent response, (p)ppGpp interacts with a co-factor known as DnaK Suppressor, or DksA, that helps to stabilize (p)ppGpp's interaction with RNAP by interacting with the secondary channel of RNAP (106). In addition to its role in the stringent response, DksA can act independently of (p)ppGpp. DksA is involved in multiple processes in bacteria including quorum sensing and regulation of cell division. DksA functions similarly to transcription factors; however, unlike most transcription factors, DksA does not bind DNA (107). Interestingly, DksA is required for repair of double stranded breaks in the chromosome when there are two or more damaged locations (108). DksA is also hypothesized to help replication because it removes

21

transcription roadblocks; this is why DksA is thought to be so critical for replication *in vitro*. In fact, *in vitro* transcription models suggest that halted replication occurs in *dksA* mutants more frequently than in wild type bacteria (109). It is also important to note that DksA helps facilitate binding of the housekeeping sigma factor, σ^{70}, to promoter DNA during all phases of growth (110, 111). Thus, DksA is considered a major contributor to bacterial transcription as well a global regulator of gene expression.

(p)ppGpp also regulates gene expression indirectly. (p)ppGpp binds to the core domain of RNAP and competes with σ^{70}. This interaction allows RNAP to bind to alternative sigma factors (112). Additionally, (p)ppGpp induces expression of mRNAs in *Legionella pneumophila* and *E. coli* that regulate activity of the carbon storage regulator A (CsrA) (39). CsrA binds regulatory RNA to control processes such as protein secretion. Thus, through regulation of RNAs that regulate CsrA, (p)ppGpp indirectly controls gene expression. (p)ppGpp also prolongs the half-lives of mRNA by inhibiting transcription of *pcnB* (poly(A) polymerase) in *Actinomycetes* (113). (p)ppGpp interacts with and modifies the activity of two translational GTPases in *E. coli*, EF-G and IF2 (114). (p)ppGpp inhibits the activity of these GTPases, thereby indirectly inhibiting translation. (p)ppGpp also inhibits DNA primase, which is responsible for initiating DNA replication in *Bacillus subtilis* (82).

In *E. coli,* both (p)ppGpp and DksA directly affect activities of RpoH, RpoS, RpoE, and RpoN (115-117). Induction of the stringent response, helps shift bacteria away from active growth and σ^{70}-mediated transcription and redistribute RNAP to promoters of maintenance and survival-related genes. Through their interaction with RNAP, (p)ppGpp and DksA facilitate transition to the alternate sigma factors and allow for more effective

competition against σ⁷⁰. For example, stringent response activation increases stationary phase synthesis of RpoS in *E. coli* (118, 119). DksA in particular has a key interaction with RpoS in stationary phase and during the stringent response (92, 107, 119). The affinity of DksA to the core RNAP is ten times greater than to the open complex suggesting that DksA's interaction with RNAP is not limited to the stringent response (120). Critical for this study, DksA and (p)ppGpp also stimulate transcription of RpoE and RpoH promoters (117). As RpoE and RpoH are the only alternative sigma factors *H. ducreyi* possesses, this may indicate a role for the stringent response in alternative sigma factor usage in *H. ducreyi*.

The stringent response is also involved with Hfq. DksA is involved in regulation of transcription of Hfq in exponential phase as well as stringent response (121). The enzyme RelA directly interacts with the Hfq protein. In *E. coli,* Hfq functions as a homohexameric ring in RNA binding. RelA is required for stimulation of multimerization of Hfq, increases the levels of the active form of Hfq, which enables binding of RNAs (122). It is unknown if this stimulation is a stoichiometric or catalytic reaction. Importantly, (p)ppGpp does not appear to directly interact with Hfq, however, (p)ppGpp interaction with RNAP may increase expression of an Hfq regulator. Thus, both (p)ppGpp and DksA have significant roles beyond the stringent response.

Bacterial virulence and the stringent response

The (p)ppGpp mediated stringent response has been shown to be important for virulence in pathogenic *E. coli* and several other pathogenic bacterial species. (p)ppGpp°mutants of *Yersinia pestis*, Salmonella *enterica* serovar Typhimurium, and *Borrelia*

burgdorferi are completely avirulent in animal models of infection (123-125). (p)ppGpp°

mutants of *Staphylococcus aureus*, *Pseudomonas aeruginosa*, *Mycobacterium*

tuberculosis, and *Enterococcus faecalis* are partially attenuated in their wild-type parents

in their respective animal models of infection (126-129). Uropathogenic *E. coli*, a leading

cause of acute urinary tract infections, require type 1 fimbriae for adherence to

uroepithelial cells. (p)ppGpp is required for activation of the *fim* operon, which confers

expression of the Type 1 fimbriae (130). SpoT is required for expression of *Yersinia's*

secreted virulence factors (83). The (p)ppGpp-mediated stringent response is essential for

expression of Pla, a key protease responsible for promoting invasion of *Yersinia* into

epithelial cells (124). *Vibrio cholerae* required RelA for expression of virulence genes

needed to help it adapt to changing environments during transmission (131).

DksA plays a role in bacterial virulence separate from (p)ppGpp. In *E. coli*, *in*

vitro studies show that DksA protein levels remains constant throughout bacterial growth.

dksA mutants have defects in chaperonin function, gene expression, cell division, amino

acid biosynthesis, quorum sensing and virulence (107). In *Shigella flexneri,* DksA is

essential for regulation of *hfq*, which is an important regulator of *S. flexneri* virulence

genes (121). DksA expression is typically increased under acidic conditions and

oxidative stress. *Shigella flexneri dksA* mutants have increased sensitivity to acidic and

oxidative stress (132). DksA also contributes to the resistance of *S. enterica* serovar

Typhimurium to reactive nitrogen species produced by inducible nitric oxide synthase

(iNOS) and Nitric Oxide (NO) (133). In UPEC, DksA is important for the regulation of

cell-to-cell adhesion between bacterial cells and adherence to eukaryotic cells

independent of (p)ppGpp (134). DksA regulates motility, expression of the hemagglutinin

24

protease, and production of cholera toxin in *Vibrio cholerae,* all processes related to virulence (135). DksA is also involved in the posttranscriptional control of rhamnolipids and LasB elastase, which are involved in quorum sensing in *Pseudomonas aeruginosa* (136).

During human infection, multiple genes involved in stress response are upregulated in *H. ducreyi* (73). Genes critical for DNA repair such as *mutL* (DNA mismatch repair protein) and *recB* (dsDNA break repair) are upregulated *in vivo.* Likewise several stress response components including *rpoE* (alternative sigma factor), *htpX* (probable heat shock protein) and *relA* (a component of the stringent response) are also upregulated during human infection (73). In addition, the doubling time of *H. ducreyi* in nutrient-rich media is 2 hours while the estimated doubling time is 16 hours in human lesions (49). During human infection, the environment is hostile and *H. ducreyi*, like other pathogens, might need to modify gene expression to survive.

Hypothesis

We hypothesized that the stringent response is required for virulence of *H. ducreyi* in humans. The rationale for this hypothesis is derived from three sources. First, the *H. ducreyi* genome encodes genes with high homology to *relA, spoT,* and *dksA;* previously identified as key players in the stringent response. Second, the minimum estimated doubling time of *H. ducreyi in vivo* is approximately 16 hours while the *in vivo* doubling time in nutrient rich media is 2 hours. This suggests that *H. ducreyi* experiences nutrient limitation in the human host. Lastly, the *relA* homolog is upregulated in pustules from infected volunteers, strengthening the hypothesis that *H. ducreyi* experiences nutrient limitation *in vivo*.

Taken together, these data suggest that *H. ducreyi* might utilize the stringent response to adapt to nutritional stress during human infection. To address this hypothesis, our Specific Aims were to: (1) Construct and characterize *in vitro* virulence-associated phenotypes of Δ*relA*, Δ*relA*Δ*spoT* and Δ*dksA* mutants; (2) Evaluate Δ*relA*Δ*spoT* and Δ*dksA* mutants for abscess formation compared to the parent strain in human volunteers; (3) Determine the transcriptome of the (p)ppGpp and DksA deficient mutants compared to the parent strain.

Chapter II:

Materials and Methods

Bacterial strains and growth conditions. The bacterial strains used in this study are listed in Table 1. *H. ducreyi* strains were grown on chocolate agar plates supplemented with 1% IsoVitalex at 33°C with 5% CO_2 or in GC broth supplemented with 5% fetal bovine serum, 1% IsoVitalex and 50 μg/ml hemin (Aldrich Chemical Co.) at 33°C. *H. ducreyi* 35000HP was grown to mid-log (optical density at 660 nm [OD_{660}] = 0.2), transition (OD_{660} = 0.35), or stationary phase (OD_{660} = 0.5); mutant strains were harvested when the OD_{660} of 35000HP was in the appropriate range for each phase of growth. *E. coli* strains were grown in Luria-Bertani medium at 37°C with the exception of strain DY380, which was maintained in low salt broth or agar at 32°C and grown at 42°C for induction of the lambda red recombinase. When necessary, medium was supplemented with kanamycin (20 μg/ml for *H. ducreyi;* 50 μg/ml for *E. coli*) or spectinomycin (200 μg/ml for *H. ducreyi*; 50 μg/ml for *E. coli*). For *H. ducreyi* strains containing a pACYC177 backbone, medium was supplemented with 30 μg/ml kanamycin.

Characterization of the *relA*, *spoT* and *dksA* genes. The Basic Local Alignment Search Tool (BLAST) was used to identify putative homologues of *relA, spoT* and *dksA* in *H. ducreyi* (GenBank accession no. AE017143). RT-PCR was conducted to determine if target genes were in operons with surrounding genes. Primers used for RT-PCR are found in Table 2.

Table 1. Bacterial strains used in this study

Strain(s)	Description[a]	Source or reference(s)
***E. coli* strains**		
DH5α, Top10, and DY380	Strains used for general cloning procedures	Invitrogen
	DH10B derivative containing a defective λ prophage in which the *red, bet,* and *gam* genes are controlled by the temp-sensitive λ*cI857* repressor	(137)
CF1693	*ΔrelAΔspoT* deletion mutant in MG1655	(138)
CF1652	*ΔrelA* deletion mutant in MG1655	(138)
MG1655	Wild type strain *E. coli* strain	(138)
***H. ducreyi* strains**		
35000HP	Human-passaged variant of strain 35000	(37)
35000HPΔ*dksA*	Unmarked, in-frame *dksA* deletion mutant	This study
FX517	35000HPΔ*dsrA:: cat* insertion mutant	(77)
35000HPΔ*flp1-3*	Unmarked, in-frame *flp1-2-3* deletion mutant	(70)
35000HP.400	35000HPΔ*tadA:: cat* insertion mutant	(72)
35000HPΔ*relA*	Unmarked, in-frame *relA* deletion mutant	This study
35000HPΔ*relA*Δ*spoT*	Unmarked, in-frame *relA* and *spoT* double deletion mutant	This study
35000HPΔ*sodC*	35000HPΔ*sodC:: cat* insertion mutant	(139)
HD183	Class I isolate; Singapore 1982	---
82-029362	Class I isolate; California 1982	---
33921	Class II isolate; Kenya, unknown	---
CIP542	Class II isolate; Hanoi 1954	---
NZS3	CUD Isolate; Samoa 2006	---
NZS4	CUD Isolate; Samoa 2007	---

Table 2. Primers used in this study

Primer	Gene	Purpose	5' to 3' sequence[a]
P1	*dnaE* int 5'	colony hybridization, qRT-PCR	AACGTTACCTTCAGCAAGCGGTTC
P2	*dnaE* int 3'	colony hybridization, qRT-PCR	GGCGTTTGGGATCGTCGAGTGTAT
P3	*relA* int 5'	mutagenesis, colony hybridization	CGCGCGGTACGGGTGATTGT
P4	*relA* int 3'	mutagenesis, colony hybridization	TGGCGCGCGCTTTTGAGGTA
P5	*spoT* int 5'	mutagenesis, colony hybridization	CCAGTCGCGGTTGCCACCAT
P6	*spoT* int 3'	mutagenesis, colony hybridization	CACGCCCGTAAACACGGCCT
P7	*relA-dxr*, 5'	RT-PCR	GCGATGTAAGTGCTGTGATGGCAA
P8	*relA-dxr*, 3'	RT-PCR	TTCGCCGGTTAATACTTGGGTGGT
P9	*recG-rpoZ*, 5'	RT-PCR	TGGCACTAAACAAACGGGTATGGC
P10	*recG-rpoZ*, 3'	RT-PCR	ATCGCTTCTTGTTCAGCCACCTCT
P11	*rpoZ-spoT*, 5'	RT-PCR	TAACCGTCCAAGAAGCTGCCGATA
P12	*rpoZ-spoT*, 3'	RT-PCR	AAGGCTCACCACTAGAGCGAGTTT
P13	*spoT-menB*, 5'	RT-PCR	AATTGATCAGAGTCCGCGGTGTGA
P14	*spoT-menB*, 3'	RT-PCR	ATGATCGACCCATTCAATCGGAGC
P15	RelA Homology 1	*relA* and mutagenic cassette homology primer, Forward	ACTGTGTAAGCAGTTCAATTCTCT CATTATTTTGCAAAGGAGGTTTTA TG**ATTCCGGGGATCCGTCGACC**
P16	RelA Homology 2	*relA* and mutagenic cassette homology primer, Reverse	TTGCTACTTAAAACTGACCGCTTA TTCAATTAGTTTGCTAGCCGTTTTG C**TGTAGGCTGGAGCTGCTTCG**
P17	*relA* amplification, F	*relA* ORF and 500bp upstream	ATATAT<u>ACTAGT</u>CTGCAATATTAG CATGGCCATATTTACGGT
P18	*relA* amplification, R	*relA* ORF and 500bp downstream	ATATAT<u>ACTAGT</u>TGCCCGCATGTC ACTAAAGATTC
P19	SpoT Homology 1	*spoT* and mutagenic cassette homology primer, Forward	AGCCTTATATTACTCATCCAGTCG CGGTTGCCACCATTATTGCTGAAA TG**ATTCCGGGGATCCGTCGACC**
P20	SpoT Homology 2	*spoT* and mutagenic cassette homology primer, Reverse	AGATTTGCGAATGAGACCGCTTGT AACGACTAGGCGCTGACTTTTGCC AC**TGTAGGCTGGAGCTGCTTCG**
P21	*spoT* amplification, F	*spoT* ORF and 500bp upstream	ATATAT<u>ACTAGT</u>ATTACAACTTCA CGTTCGTGAGCCGC
P22	*spoT* amplification, R	*spoT* ORF and 500bp downstream	ATATAT<u>ACTAGT</u>CTGCTACCATTG CTACTACGGGTT
P23	*spec,* 5'	mutagenesis	ATTCCGGGGATCCGTCGACC
P24	*spec,* 3'	mutagenesis	TGTAGGCTGGAGCTGCTTCG
P25	*relA,* 5'	qRT-PCR	TACACCGCGTGGTGAAGTGATTGA
P26	*relA,* 3'	qRT-PCR	TAGCGCCTATACAACGATGCCCAA

P27	*spoT*, 5'	qRT-PCR	CTTTCAAGCCATGCATCCTTATC
P28	*spoT*, 3'	qRT-PCR	CACGGATTTGGTATGGTCTAGG
P29	*dxr* 5'	qRT-PCR	AGTTATGGCAGCGATTGTTGGTGC
P30	*dxr* 3'	qRT-PCR	ACTTGCGTTAAATAGCCAGCGTGC
P31	*menB* 5'	qRT-PCR	TGGTCCGAAAGTCGGTTCCTTTGA
P32	*menB* 3'	qRT-PCR	ATAGAACAGCATGGTTGCGTTGCC
P33	cat promoter, R	*cat* promoter of pACYC184 for complement (#1), upstream	CATATGATATCTAGAATATTTAGCTTCCTTAGCTCCTG
P34	cat promoter, F	*cat* promoter of pACYC184 for complement (#1), downstream	ATCCTGTCGGCTGTGGCACAGGCTGAACGCCGGAGGATCCGTTGATACCGGGAAGCCCTGGGCCAAC
P35	*spoT* ORF, F	*spoT* fragment (#2) for complement, upstream	GGAGCTAAGGAAGCTAAATAT<u>TCTAGA</u>TAT<u>CATATG</u>AATTGCCATATTGTGAGGTGAAATTTG
P36	*spoT* ORF, R	*spoT* fragment (#2) for complement, downstream	CATATGATACTAGGCGCTGACTTTTG
P37	*relA* ORF, F	*relA* fragment (#3) for complement, upstream	GCAAAAGTCAGCGCCTAGTAT<u>CATATG</u>AGTTCAATTCTCTCATTATTTTGCAAAGGAGGTTTT
P38	*relA* ORF, R	*relA* fragment (#3) for complement, downstream	TTTGCTTCCTGTCGGCCCTCATTCGTGCGCTCTAGGATCCTCTAGAATACTATTATCCTTCATTTTTTATACAA
P39	*tbpA-dksA*, 5'	RT-PCR	ACGGAAGTGGATCCAGCATTTGTC
P40	*tbpA-dksA*, 3'	RT-PCR	TAGCACGATCAGGATCAGCAA
P41	*dksA-pcnB*, 5'	RT-PCR	TCGTCCGACTGCGGATATGTGTAT
P42	*dksA-pcnB*, 3'	RT-PCR	TTCGCTTTGCTAAGGCTTCACTGC
P43	*pcnB- folK*, 5'	RT-PCR	GTTGAATTATCGGCGTGGTGGCAT
P44	*pcnB- folK*, 3'	RT-PCR	TGTGGCCCTATTGGCTGACTACAA
P45	*dksA* int, 5'	mutagenesis, colony hybridization	TGCTGATCCTGCTGATCGTGCT
P46	*dksA* int, 3'	mutagenesis, colony hybridization	TCCGCAGTCGGACGAGCTTCT
P47	*dksA* amplification, F	*dksA* ORF and 500bp upstream	ATATAT<u>ACTAGT</u>GGCTGCTGAATTTGAAGAAGGCCA
P48	*dksA* amplification, R	*dksA* ORF and 500bp downstream	ATATAT<u>ACTAGT</u>CAGGTTTAGCATTAGTGGCAATATCC
P49	DksA Homology 1	*dksA* and mutagenic cassette homology primer, Forward	AGTTATATTCAAAGATCAGGCTGACTTATCCAACAAGGAGTGCAATTATG**ATTCCGGGGATCCGTCGACC**
P50	DksA Homology 2	*dksA* and mutagenic cassette homology primer, Reverse	CATTGTCCATTCCTATGTACCTATACTAACTAAAGCCCCATTTGTTTCTC**TGTAGGCTGGAGCTGCTTCG**

P51	*dksA* ORF, F	*dksA* fragment (#2) for complement, upstream	ATATAT<u>TCTAGA</u>CAAAGATCAGGCTGACTTATCATG
P52	*dksA* ORF, R	*dksA* fragment (#2) for complement, downstream	ATATAT<u>TCTAGA</u>ATTCCTATGTACCTATACTAACTA
P53	*tbpA,* 5'	RT-PCR	ATGCCTGAGGCGGTTAAAT
P54	*tbpA,* 3'	RT-PCR	GCTCGTGCCAATAATGGTATAAAG
P55	*dksA*, 5'	qRT-PCR	GTGCATGGCACGTGCAAATTATGG
P56	*dksA*, 3'	qRT-PCR	TCTTCTTGGGTAGCACGATCAGCA
P57	*pcnB*, 5'	qRT-PCR	AGTGGGTGGGTGTATCCGTGATTT
P58	*pcnB*, 3'	qRT-PCR	TAAATCGCACCGCGCGTAACATTC
P59	*lspB*, 5'	qRT-PCR	AGCTAGAGCGGCTGACCCATTAAA
P60	*lspB*, 3'	qRT-PCR	GTGAGAAATTGCTCCGCTTTGGCT
P61	*flp1, 5'*	qRT-PCR	GGTTAATTGCAGTCGCAGTTGCT
P62	*flp1*, 3'	qRT-PCR	GTGCCATTAGCGCTACTTATACCA
P63	*tadA,* 5'	qRT-PCR	AATCAATGCCTTGCGTATGCGTCC
P64	*tadA*, 3'	qRT-PCR	TGTATTGGCGTGCAGGGTAGACAT
P65	*cpxA* 5'	qRT-PCR	GCCATTCCTAATTTCGATGCGCGT
P66	*cpxA* 3'	qRT-PCR	TTTGAGTGGCTACAGAAAGGCGAC
P67	*oxyR* 5'	qRT-PCR	CTTGTTGAACAGGCCAAAGCGGTA
P68	*oxyR* 3'	qRT-PCR	GTGCAATGGGCCAGACATTTCCTT
P69	*sodC* 5'	qRT-PCR	GGCCATTGGGATCCAAAGCAAACT
P70	*sodC* 3'	qRT-PCR	CAGGCGTTGTTGCTGAACCATCAT
P71	*ccmD,* 5'	qRT-PCR	CGCAGATTTCTTTGCGATGGGA
P72	*ccmD*, 3'	qRT-PCR	CTCGGTAAGACAACCAAATTAGCC
P73	*HD1577,* 5'	qRT-PCR	TAAATCAAGCGCTCGCACCGAAAC
P74	*HD1577*, 3'	qRT-PCR	AAACACACATTGTGGCGTGCCTTC
P75	*sapF,* 5'	qRT-PCR	TATTGGGCAGATTCTTGATGCGCC
P76	*sapF*, 3'	qRT-PCR	CCCTTGCAAGTGCAATCCGTTGTT
P77	*HD1904,* 5'	qRT-PCR	AGCTAACTATTCATTAGACGACCT
P78	*HD1904*, 3'	qRT-PCR	AAGGCAATTTGTGGGAAATACT
P79	*tadB,* 5'	qRT-PCR	GCAACCTCTTCAGGTGTTAGT
P80	*tadB*, 3'	qRT-PCR	GCTTCTGCTGTCATTGCTTTC
P81	*rfaD,* 5'	qRT-PCR	TATATGCTTCTAGCGCGGCCACTT
P82	*rfaD*, 3'	qRT-PCR	CGCTTGCCATCGACCCTTTATGTT
P83	*HD0457,* 5'	qRT-PCR	GCGTAATGATGGAAATGTCTCAAA
P84	*HD0457*, 3'	qRT-PCR	TCCGCTAACTCTTTAGCTTTCTT
P85	*lspA1,* 5'	qRT-PCR	CCGGAATTAAGTGGCTATGGT
P86	*lspA1*, 3'	qRT-PCR	GCGATAAGCGCGGTCAATA
P87	*glpF,* 5'	qRT-PCR	CGCCTGTATCGCAGAATGTAT
P88	*glpF*, 3'	qRT-PCR	ACAAGTGCCGCAGCTAAA
P89	*degP,* 5'	qRT-PCR	AGGGCAAACGGTGACATCTGGTAT
P90	*degP*, 3'	qRT-PCR	AACTCACCGCCTTTAATGCCCAAC
P91	*HD1218,* 5'	qRT-PCR	GCTCAGAGAATGAAATCACCAAA
P92	*HD1218*, 3'	qRT-PCR	TTATCGTTGGCTAGGAGTGTTG

P93	*hfq, 5'*	qRT-PCR	TCGAGAGCGTATTCCCGTCTCAAT
P94	*hfq, 3'*	qRT-PCR	TGTACGGCTTGTTGAGGAGCTTGT
P95	*ompP2A 5'*	qRT-PCR	TGCTAAAGGAGAAGCGTTAGAC
P96	*ompP2A 3'*	qRT-PCR	TAGCCAAGCGCCATTTGA
P97	*HD0098 5'*	qRT-PCR	ACAAAGAATTGTCAGGATTGGC
P98	*HD0098 3'*	qRT-PCR	GAGTAGTAACAACAGCTCCATCA

[a]Boldfaced text represents sequences with homology to the mutagenic cassette. Underlined text indicates regions corresponding to restriction enzyme sites as mentioned in the text. *H. ducreyi* sequences are from GenBank accession no. AE017143.

Recombineering in *H. ducreyi*. Unmarked, in-frame deletion mutants were constructed using the λ red and FLP recombinase method described previously (85, 140). The method is summarized in Figure 3. To construct a deletion mutant, PCR was used to amplify the spectinomycin resistance cassette (*spec*) flanked by flippase recognition target (FRT) sites from pRSM2832. The forward primer includes 47 bp upstream of and the ATG start codon of the target gene. The reverse primer includes the final 21 bp at the 3' end of the target, the stop codon and 29 bp downstream. Plasmids constructed and used for mutagenesis are found in Table 3.

The coding region of the target along with a 0.5-kb flanking region on either side of the gene was amplified. The product was cloned into pCR-XL-TOPO® and then electroporated into *E. coli* DY380, which contains a temperature sensitive λ red recombinase. The *spec* cassette containing PCR product was electroporated into the DY380 strain generated above. Following induction of the recombinase, the target gene was replaced with the *spec* cassette with the exception of the start codon and the last 21 bp of the gene. The *spec* cassette containing the flanking regions was digested with SpeI and cloned into the suicide vector pRSM2072. This construct was electroporated into 35000HP. Chocolate agar containing spectinomycin and X-gal was used to select clones

in which allelic exchange had occurred. PCR and sequence analysis confirmed replacement of the target gene with the *spec* cassette.
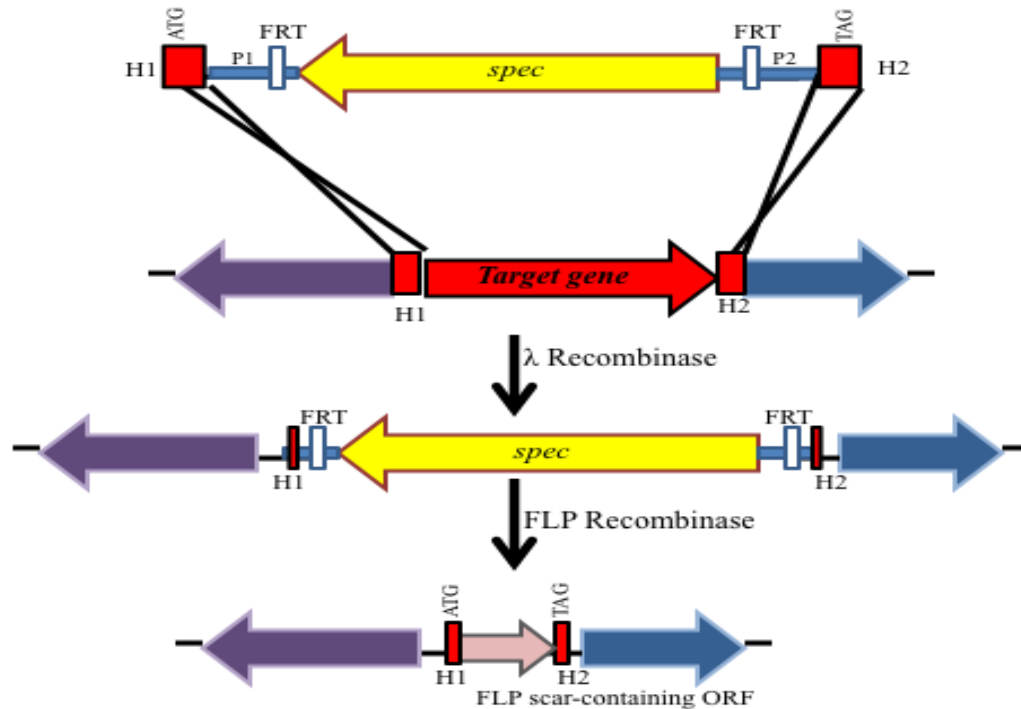
Figure 3. Mutagenesis strategy in *H. ducreyi.* Gene knockout primers have 20- to 30-nucleotide ends for priming upstream (P1) and downstream (P2) of the FRT sites flanking the resistance gene and 500-nucleotide ends homologous to upstream (H1) and downstream (H2) chromosomal sequences for the target genes. H1 includes the target start codon. H2 includes codons for the six C-terminal residues, the stop codon, and 21 nucleotides downstream.

FLP recombinase was used to remove the *spec* cassette as described previously (140). In place of the target ORF, the final mutant carries a scar ORF which contains the target gene's start codon, the FRT sequence, and the last 21 nucleotides of the target including the stop codon. PCR and sequence analysis then confirmed removal of the *spec* cassette. qRT-PCR was performed to ensure that the gene deletion was non-polar.

Table 3. Plasmids used in this study

Plasmid Name	Description	Source or
Plasmids[a]		
pRSM2832	Plasmid containing spectinomycin resistance cassette flanked by the FRT sites	(141)
pRSM2072	*H. ducreyi* suicide vector	(140)
pRSM2975	Plasmid containing the origin of replication and kanamycin-resistance gene from pLS88, FLP recombinase gene from pFT-A and a point mutation conferring a temp-sensitive phenotype in *H. ducreyi*	(87)
pCH1	pCR-XL-TOPO containing the *relA*-coding region along with 0.5- kb flanking regions	This study
pCH11	pCR-XL-TOPO containing the *spoT*-coding region along with 0.5- kb flanking regions	This study
pACYC177	Cloning vector, Kan^r Amp^r for complementation	New England Biolabs
pACYC184	Cloning vector, Cm^r Tet^r	New England Biolabs
pCH4	pACYC177 containing the 35000HP *relA* gene with the *cat* promoter from pACYC184	This study
pCH30	pACYC177 containing the 35000HP *relA* and *spoT* gene with the *cat* promoter from pACYC184	This study
pCH21	pCR-XL-TOPO containing the *dksA*-coding region along with 0.5- kb flanking regions	This study
pCH24	pACYC177 containing the 35000HP *dksA* gene with the *cat* promoter from pACYC184	This study
pCH31	pACYC177 containing the *cat* promoter from pACYC184	This study

[a]Plasmids are listed in the order in which they appear in text.

RNA isolation and quality assessment. Total RNA was extracted from 35000HP, 35000HPΔ*relA*Δ*spoT,* and 35000HPΔ*dksA* in the mid-log, transition, and stationary growth phases using TRIzol reagent (Invitrogen) according to the manufacturer's protocol. RNA isolation was performed on four independent bacterial cultures for each strain in each growth phase. RNA was treated twice with the TURBO DNA-free DNase (Ambion). The integrity and the concentration of RNA were determined using the Agilent 2100 Bioanalyzer (Agilent Technologies) and the NanoDrop ND2000 (ThermoScientific), respectively. The efficacy of DNase treatment was confirmed by reverse transcriptase PCR (RT-PCR) analysis of *dnaE* with the primer pair P1/P2 (Table 2).

Reverse transcriptase PCR (RT-PCR) and quantitative RT-PCR (qRT-PCR). cDNA was synthesized from total RNA using Advantage RT-for-PCR kit (Clontech). RT-PCR was performed using the cDNA and FastStart PCR Master mix (Roche). qRT-PCR was performed using the QuantiTect SYBR Green RT-PCR kit (Qiagen) and a Mastercycler® Ep Realplex 4 (Eppendorf). All primer pairs used for qRT-PCR (Table 2) had greater than 95% amplification efficiency. Relative expression was calculated as $[(E_{target}^{\Delta CTtarget})/(E_{referencce}^{\Delta CTreference})]$, where E is the amplification efficiency (10^{-1}/slope) and the ΔCT is the change in cycle threshold. *dnaE* was amplified to normalize the expression levels of target genes.

Construction of complementation plasmids. To complement the ΔrelAΔspoT and

ΔdksA mutants, genes were expressed under the control of a constitutive *cat* promoter

from pACYC184 in the expression vector pACYC177. The *cat* promoter was amplified

from pACYC184. Specific fragments used to construct the individual complementation

plasmids are described in subsequent chapters. The PCR fragments were combined with

BamHI digested pACYC177 in a Gibson assembly reaction (142). Briefly, the three

fragments were incubated in a reaction mixture (kindly provided by M. Goebl, Indiana

University) that contained T5 exonuclease (Epicentre), Phusion Taq (New England

Biolabs), and Taq DNA ligase (New England Biolabs) at 50°C for 1 hour. The final

constructs were confirmed by PCR and sequence analysis. Strains containing pACYC177

were used as controls.

Although all transformed strains grew well on antibiotic supplemented plates, *H.

ducreyi* strains containing pACYC177 grew poorly in antibiotic-supplemented broth.

Kanamycin dose response growth curves confirmed that only the 35000HP pACYC177-

containing strains grown in the absence of kanamycin grew as well as 35000HP in broth

(Figure 4). Furthermore, strains transformed with pACYC177 could be grown in broth

without antibiotics for only 6 hours before losing the plasmid. Thus, use of the

complemented strains was limited to those assays using cells that had been grown or

maintained in broth without antibiotics for 6 hours or those that had been grown on plates

supplemented with antibiotics.
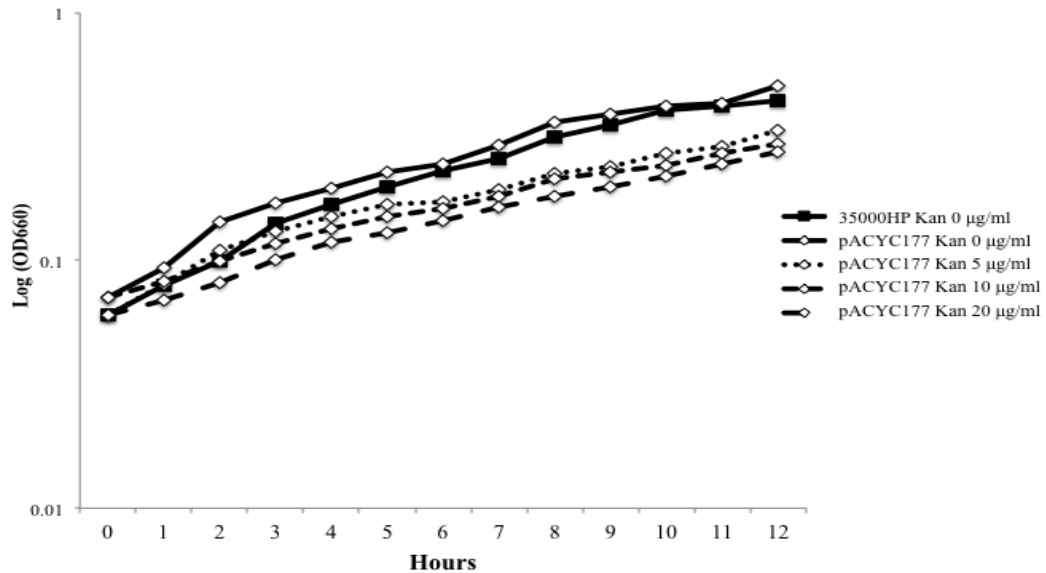
Figure 4. Growth curve of 35000HP containing pACYC177 in increasing concentrations of kanamycin compared to 35000HP grown in the absence of kanamycin.

Human inoculation experiments. Human inoculation experiments were conducted according to the guidelines of the U.S. Department of Health and Human Services and the Institutional Review Board (IRB) of Indiana University. All volunteers gave written, informed consent for participation and HIV-1 serology. The procedures for the human inoculation experiments, including calculation of the estimated delivered dose (EDD), are described in detail elsewhere (47). Briefly, healthy adult volunteers are inoculated with *H. ducreyi* at multiple sites on the upper arm using an allergy testing device. Based on the delivery characteristics of the allergy testing device, the EDD is calculated by dividing the CFU loaded on the device by 1000 (12). Volunteers remain infected until one of three clinical endpoints is reached: (1) resolution of disease at all sites, (2) development of a pustule that is either painful or > 4 mm in diameter, or (3) 14 days after

inoculation. At endpoint, all volunteers are treated with one dose of oral ciprofloxacin. Papule and pustule formation rates for parent and mutant inoculation sites were compared using logistic regression with generalized estimating equations (GEE) as previously described (72). Ninety-five percent confidence intervals (95% CI) for papule and pustule formation rates were calculated using GEE-based sandwich standard errors.

To ensure that there was no cross contamination of samples, colony hybridization was performed on colonies derived from the inocula, surface cultures, and biopsies. Probes specific for the deleted gene(s) and *dnaE* were designed and the DIG DNA labeling kit (Roche Applied Sciences) used to label the probes with digoxigenin. The DIG Easy Hyb protocol was performed according to manufacturer's instructions (Roche Applied Sciences).

LOS preparation. Bacterial suspensions in 50 mM NaH_2PO_4/ 5 mM EDTA were sonicated and incubated with 1 mg/ml lysozyme at room temperature with stirring. A mixture of 50 mM NaH_2PO_4/ 45 mM $MgCl_2$, 4 mg/ml lysozyme, 30 μg/ml DNase and 30 μg/ml RNase was added and incubated overnight at 37°C. Proteinase K was added and the mixture incubated at 56°C for 2 hours, then 75°C for 1 hour. The bacteria were pelleted and the mixture suspended in 300 μl dH_20. The liquid was transferred to a dram vial with a micro stir bar. An equal volume of hot 90% phenol was added to a dram vial and the mixture was stirred vigorously for 15 mins at 65°C, incubated on ice for 10 mins, and then centrifuged for 10 mins at 4°C. The top aqueous phase was extracted twice, then the preparations were ethanol-precipitated, resolved on LOS gels and silver stained to visualize the LOS bands.

Outer membrane preparation. Bacteria were grown in 225 ml broth culture in side arm flasks for 16 hours. The culture was collected and centrifuged at 10000 x *g* for 20 mins at 4°C. The pellet was washed in cold 10 mM HEPES and centrifuged. The preparations were sonicated for 10 mins on ice and spun at 7000 rpm for 30 mins at 4°C. The supernatant was collected and transferred to ultracentrifuge tubes and centrifuged at 100000 x *g* for 60 mins at 4°C. To separate the outer membrane proteins, the pellet was suspended in an equal volume of HEPES buffer and 2% sodium lauryl sarcosinate in HEPES and incubated at room temperature for 30 mins with gentle rocking. After incubation, the tubes are centrifuged.. The supernatant is removed and the pellet was incubated with dH_20 at 4°C overnight.

Antibodies and immunoblots. Polyclonal antibodies against OmpP2A, OmpP2B, Flp1/2, and DsrA were used in this study. Anti-sera for Flp1/2 (kindly provided by E. Hansen, University of Texas Southwestern), OmpP2A and OmpP2B (A. Campagnari, SUNY-Buffalo), and DsrA (C. Elkins, University of North Carolina) were used to detect their respective proteins. Mabs 3B9 and 2C7 were used to detect PAL and MOMP/OMPA2 respectively and are described elsewhere (143, 144). Immunoblots were performed on whole cell lysates and purified outer membranes.

Tandem mass spectrometry (LC-MS/MS). An 8% SDS-PAGE gel containing purified outer membranes of 35000HP and 35000HPΔ*relA*Δ*spoT* was stained with Coomassie dye. The protein band of interest was isolated at the Indiana University School of Medicine Proteomics Core Facility. The excised band was subjected to liquid

chromatography followed by tandem mass spectrometry. Analysis showed that the protein band contained peptides mapping to multiple proteins. Only proteins with high peptide confidence levels (over 90%) were reported. Identified proteins with at least 2 unique peptide matches were considered for further analysis.

***De novo* (p)ppGpp synthesis assay.** For detection of (p)ppGpp synthesis in *H. ducreyi,* we modified two published assays (145, 146). Briefly, *H. ducreyi* strains were grown in GC broth. At different phases of growth, the bacteria were harvested by centrifugation, washed in phosphate-limited RPMI (US Biological Life Sciences) and suspended (1 x 10^5 cells/ml) in phosphate-limited RPMI. Pilot experiments showed that there was no reduction in bacterial viability for up to 4 hours in this media. For the labeling experiments, the bacteria were suspended in phosphate-limited RPMI media supplemented with 5% FBS and $KH_2{}^{32}PO_4$ (specific activity, 900-1100 mCi/mmol; Perkin Elmer) at 100 µCi/ml. The bacteria were incubated for 3 hours, washed, and incubated for an additional 15 mins in phosphate-limited RPMI. For extraction of (p)ppGpp, cells were treated with 40 mg/ml lysozyme in 10 mM Tris HCl (pH 8.0) for 20 mins and lysed on ice using 1% SDS (w/v) for 20 mins. Finally, an equal volume of 13 M formic acid was added to the lysate, which was incubated on ice for 15 mins. Cell debris was removed by centrifugation. A sample of the supernatant containing the extracted (p)ppGpp was spotted onto PEI TLC plates (Sigma Aldrich). (p)ppGpp was separated in 1.5 M H_3PO_4 (pH 3.4) buffer and detected using autoradiography. The film was then exposed at -80°C in an x-ray film cassette. CTP, ATP, and GTP standards (Sigma Aldrich) were detected using iodine staining.

Adherence assays. 24-well tissue culture plates (Costar) were seeded with 10^5 HFF cells and allowed to reach confluence in HFF medium [500 ml RPMI with L-glutamine (GIBCO), 1 mM Sodium Pyruvate (GIBCO), 10% (w/v) heat inactivated FBS (Hyclone)]. The bacteria were serially diluted in HFF medium to determine the inoculum. 100 μl of the 10^{-1} dilution was added to each well of HFF cells (MOI 10:1). The plates were centrifuged at 1500 rpm for 5 mins then incubated at 33°C for 2 hours. After incubation, the wells were washed 3 times with sterile PBS. To collect bacteria, trypsin-EDTA was added then the contents of each well was collected and plated for quantitative culture. Percent adherence of *H. ducreyi* to HFF cells was determined by calculating the ratio of HFF-adhered bacteria to initial CFU.

Phagocytosis assays. Human peripheral blood mononuclear cells (PBMC) were isolated from leukopacks obtained from anonymous donors from the Central Indiana Regional Blood Center or from blood obtained from normal healthy volunteers. Informed consent was obtained in accordance with an IRB-approved protocol. PBMCs were isolated by Ficoll-Pacque Plus purification, and CD14+ cells were isolated (Miltenyi Biotech). The CD14+ cells were differentiated into MDMs in X-vivo 15 medium (Lonza) supplemented with 1% human AB serum (Invitrogen) for 5 days. The MDMs were harvested by centrifugation and seeded into 24 well tissue culture plates at 4×10^5 cells per well and grown for 24 hours. Bacteria were grown to mid-log and stationary phases and opsonized in 100% complement replete normal human serum for 20 mins at room temperature. After washing with Hank's balanced salt solution (HBSS), the MDM were infected with bacteria at a multiplicity of infection (MOI) of 10:1. The plates were centrifuged at 1800

x *g* for 5 mins to synchronize infection and were incubated for 30 mins at 35°C in 5% CO_2. To kill extracellular bacteria, gentamicin (100 μg/ml) was added and incubated for 30 mins and washed with HBSS. The MDMs were lysed with 0.2% saponin at room temperature for 10 mins, and the lysates were quantitatively cultured. The percentage of bacterial uptake was calculated as the ratio of bacteria within the lysed MDMs compared to the initial CFU. To determine intracellular bacterial survival, the co-cultures were incubated in antibiotic-free medium containing 10% fetal bovine serum for an additional 5 hours and quantitatively cultured. Survival was determined by calculating the ratio of recoverable bacteria of co-culture compared to the initial uptake.

Oxidative stress assays. Bacteria were treated with either hydrogen peroxide (H_2O_2) to mimic extracellular oxidative stress or paraquat (Sigma Aldrich) and pyrogallol (Sigma Aldrich) to mimic intracellular oxidative stress. Bacteria were exposed to known concentrations of each chemical at 33°C in PBS for 1 hour without shaking and quantitatively cultured. For assays using complemented strains, bacterial cells were grown to mid-log phase in broth without antibiotics, collected and exposed to oxidative stress as described above. Percent survival was calculated as the ratio of recovered bacteria to the input CFU.

Heat shock assays. Bacteria were incubated at 37°C for 1 hour in PBS and quantitatively cultured. Percent survival was calculated as the ratio of recovered bacteria to the input CFU. An untreated control was utilized as a measure of viability for each bacterial strain.

Serum bactericidal assay. Bacteria were cultivated for 24 hours on chocolate plates and suspended in PBS to an OD of 0.2 (about 10^8 CFU/ml). Serum from one donor was utilized with half being heat inactivated for 35 mins at 56°C. Equal volumes of the bacterial suspension and serum were mixed in 96 well plate and the plates were incubated for 45 mins at 33°C. Bacterial survival (% survival) was calculated as the ratio between surviving bacteria in control wells containing heat-inactivated serum compared to the number of surviving bacteria in the complement-replete serum multiplied by 100.

mRNA enrichment. The removal of 23S, 16S, and 5S rRNA from total RNA was performed with the Ribo-Zero Magnetic kit for Gram-negative bacteria (Epicentre Biotechnologies) by following the manufacturer's instructions. The Agilent 2100 Bioanalyzer confirmed removal of rRNA from total RNA.

Preparation of RNA-seq libraries and sequencing. The TruSeq Stranded mRNA sample preparation kit (Illumina) was used to prepare stranded RNA-Seq libraries by following the manufacturer's instructions. Approximately 400 ng of the enriched mRNA was fragmented and randomly primed for first-strand cDNA synthesis. Second-strand synthesis incorporated dUTP in place of dTTP, which prevents second strand synthesis during subsequent amplification and results in a stranded library. The cDNA was end repaired, adenylated, and ligated to adapters. The adapter-ligated cDNA library was then PCR-enriched. Finally, the enriched RNA-Seq library was validated with the Agilent 2100 Bioanalyzer and qRT-PCR. Clusters were generated on the cBOT automated cluster-generating system with the TruSeq PE Cluster kit (Illumina). Libraries were

sequenced with the Illumina HiSeq 2500 sequencer with the TruSeq SBS kit (Illumina) for single end sequencing with read lengths of 100 bp in the Biomedical Genomics Core facility at Nationwide Children's Hospital (Columbus, OH). Image analysis and base calling were performed with the HiSeq Control software and the Real Time Analysis software. Demultiplexing was performed with the Illumina CASAVA software.

Sequence mapping and quantification of transcript levels. The sequenced reads were mapped to the *H. ducreyi* 35000HP genome (GenBank accession no. AE017143) with the Burrows-Wheeler Alignment tool (147) allowing up to two base mismatches. Reads that failed to map to any gene in the chromosome and reads that mapped to multiple locations in the genome were removed before quantifying the transcript levels. The total number of reads corresponding to the coding region of each gene was determined with the NGSUtils suite (148).

Identification of differentially expressed genes. Differential expression of genes across all 3 strains and growth phases was determined with edgeR software, a Bioconductor package (93). To favor true identification of differentially expressed genes of biological significance, we used a pre-specified false-discovery rate of ≤ 0.1 and a 2-fold change as a threshold. The differentially expressed genes were functionally classified using the annotations and pathway information from the sequenced *H. ducreyi* genome (Munson 2004, unpublished), and KEGG (149). We also determined if any biological pathways were enriched among the genes differentially expressed in the Δ*relA*Δ*spoT* and Δ*dksA* mutants compared to 35000HP by using pathway annotations from BioCyc (150). We

44

used the functional annotation-clustering algorithm of the DAVID (Database for Annotation, Visualization, and Integrated Discovery) bioinformatics resources (http://david.abcc.ncifcrf.gov/) to identify the biological pathways enriched in the Δ*relA*Δ*spoT* and Δ*dksA* mutants relative to 35000HP (151). A pathway was considered enriched if the Fisher's exact *P* value for the cluster was < 0.05, the enrichment score for the cluster was greater than 2, and the cluster involved greater than 5% of the total list of genes submitted for query (152).

RNA-seq data accession number. The data from these RNA-seq experiments were deposited at the NCBI Gene Expression Omnibus (GEO) database (http://www.ncbi.nlm.nih.gov/geo/) under accession number GSE67202.

Statistical analysis. All data are expressed as means ± standard deviations. An adjusted, two-sided *p* value of ≤ 0.05 was considered statistically significant. Stress, bactericidal, and macrophage uptake data were analyzed using a mixed-model ANOVA followed by Tukey's honestly significant difference test. qRT-PCR and densitometry data were analyzed using Student's t-test followed by Tukey's adjustment. For growth curve analysis, the data were log-transformed before analysis to correct for the large amount of skewness in the distribution. They were then analyzed using a repeated measures (mixed model) ANOVA followed by pairwise analysis of the strains at each time point.

Chapter III:

Ability to synthesize (p)ppGpp is required for

Haemophilus ducreyi **pathogenesis**

Given the fastidious nature of *H. ducreyi*, inducing the stringent response *in vitro* poses several challenges. Stringent response studies in other bacteria take advantage of minimal medium; however, no minimal medium exists for *H. ducreyi*. Alternatively, drug treatments that induce nutrient limiting conditions, such as serine hydroxamate,which mimics amino acid starvation, have been used in non-minimal media to activate the stringent response in some species. However, it is unclear how *H. ducreyi* would respond to treatment with serine hydroxamate. Moreover, use of drug treatments to induce the stringent response in *H. ducreyi* might prove lethal. Therefore, because chemical induction of the stringent response in wild-type *H. ducreyi* may introduce confounding factors, we used a genetic approach to characterize the stringent response in *H. ducreyi*.

Conservation of the *relA* and *spoT* genes in *H. ducreyi* clinical strains. We conducted a limited strain survey to determine if *relA* and *spoT* were conserved across multiple clinical isolates. Using primers constructed for detection of the 35000HP *relA* and *spoT* genes (P3/P4; P5/P6), PCR was performed using DNA isolated from two representative strains for each of the 3 groups of *H. ducreyi*. The representative strains were as follows: Class HD183, 82-029362 and I; Class II, 33921 and CIP542; CUD, NZS3 and NZS4. Specific details regarding these strains are contained in Table 1.

35000HP was included for reference. Amplicons of both *relA* and *spoT* were detected in all the representative strains indicating that these genes are conserved across multiple classes of *H. ducreyi* (Figure 5).
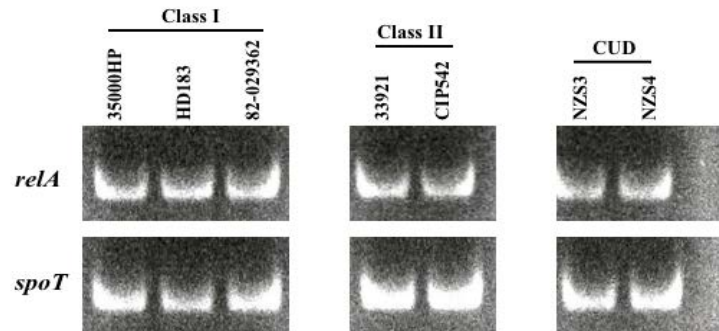
Figure 5. Survey of *H. ducreyi* clinical isolates – *relA* and *spoT*. PCR products of *relA* and *spoT* in clinical *H. ducreyi* isolates to determine conservation of genes across multiple classes.

Characterization of the *relA* and *spoT* genomic locus in 35000HP. The *H. ducreyi* homolog of *relA* (HD1185) is in the same orientation and 77 bp upstream of the *dxr* coding region, which is predicted to encode a DXP reductoisomerase (Figure 6A). To examine if *relA* and *dxr* were in an operon, we conducted RT-PCR on the intergenic regions between *relA* and *dxr*. Although RT-PCR confirmed that both *relA* and *dxr* transcripts were present in the cDNA utilized for analysis (data not shown), the data suggested that *relA* was not co-transcribed with *dxr* (Figure 6B). The *H. ducreyi spoT* homolog (HD1924) is in a putative operon with the gene order *recG* → *rpoZ* → *spoT* → *menB* (Figure 6C). The genes *recG, rpoZ,* and *menB* are predicted to encode an ATP-

dependent DNA helicase, RNA polymerase omega chain, and dihydroxynaphthoic acid synthase, respectively. RT-PCR suggested that *spoT* is co-transcribed with *rpoZ*, *menB,* and *recG* (Figure 6D).
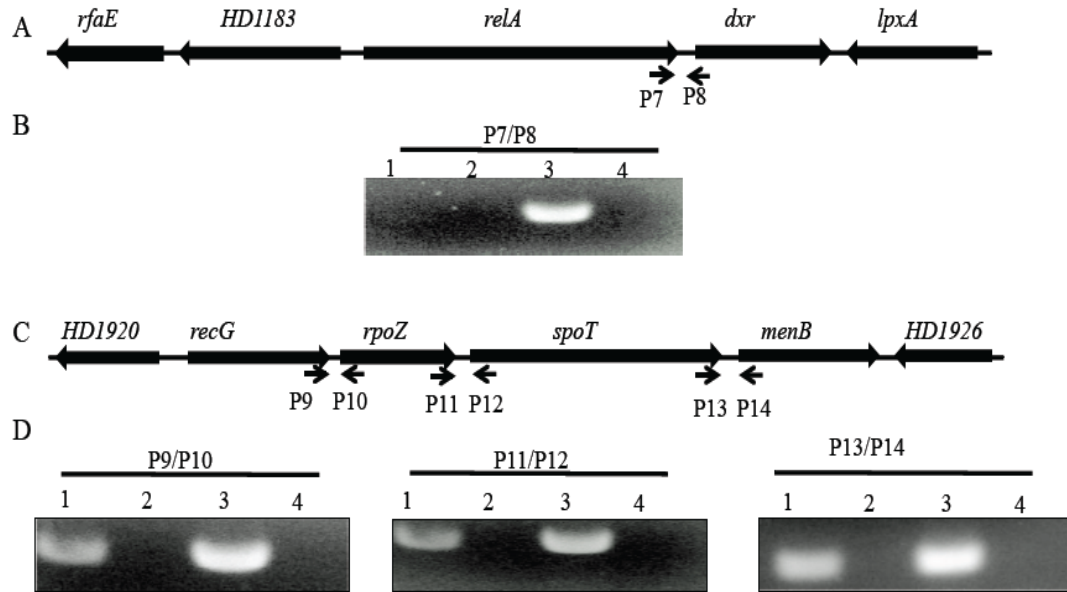
Figure 6. Chromosomal loci containing *relA* and *spoT* in *H. ducreyi*. (A) Genomic organization of *relA* locus in *H. ducreyi*. The small arrows indicate locations of intergenic primers used for RT-PCR analysis. (B) Agarose gel electrophoresis of *relA–dxr* intergenic region amplified by RT-PCR. Lane 1, RNA sample with reverse transcriptase; Lane 2, RNA sample without reverse transcriptase control; Lane 3, genomic DNA control; and Lane 4, no template control. (C) Genomic organization of *spoT* locus in *H. ducreyi*. (D) Agarose gel electrophoresis of products amplified by RT-PCR. The intergenic regions of *recG-rpoZ*, *rpoZ-spoT*, and *spoT-menB* were examined. Lanes are as in (B). Products were of the expected sizes: P7/P8: *relA–dxr* (515 bp), P9/P10: *recG-rpoZ* (541 bp), P11/P12: *rpoZ-spoT* (497 bp), and P13/P14: *spoT-menB* (222 bp)**.**

Construction of *relA* and *relA spoT* deletion mutants. To understand the role of (p)ppGpp in *H. ducreyi* pathogenesis, we constructed an unmarked, in-frame *relA* deletion mutant and an unmarked, in-frame *relA spoT* double deletion mutant. To

construct a *relA* deletion mutant, primers P15/P16 were used to amplify the *spec* cassette

flanked by FRT sites from pRSM2832. The coding region of *relA* was amplified using

primers P17/P18 and cloned into pCR-XL-TOPO®. The construct, designated pCH1 was

then electroporated into *E. coli* DY380. Following induction of the recombinase, the *relA*

gene was replaced with the *spec* cassette with the exception of the start codon and the last

21 bp of the *relA* gene. PCR and sequence analyses confirmed the replacement of the

relA gene with the *spec* cassette. The strain was then electroporated with pRSM2975.

PCR and sequence analyses were used to confirm removal of the *spec* cassette. The final

mutant was designated 35000HPΔ*relA*.

Using these methods, a *spoT* mutant could not be recovered. In other organisms,

expression of (p)ppGpp synthase in the absence of hydrolase leads to growth arrest and

cell death; as a result, for many species, *spoT* is considered an essential gene (138, 153).

Similar to what has been shown in other species, *spoT* is likely essential in *H. ducreyi*

(138). Therefore, using the *relA* deletion mutant background, we constructed a *relA spoT*

double deletion mutant using the methods described above that primers P19/P20 were

used to amplify the *spec* cassette and primers P21/P22 were used to amplify the *spoT*

coding and flanking regions, resulting in pCH11 (Table 3). After allele exchange and

excision of the *spec* cassette (Figure 7), PCR and sequence analysis confirmed deletion of

the *spoT* gene. The double mutant was designated 35000HPΔ*relA*Δ*spoT*. PCR (Figure 7)

and sequence analyses confirmed that both *relA* and *spoT* genes were deleted in

35000HPΔ*relA*Δ*spoT* with the exception of the start codon and the last 21 bp of the *relA*

ORF and the *spoT* ORF.
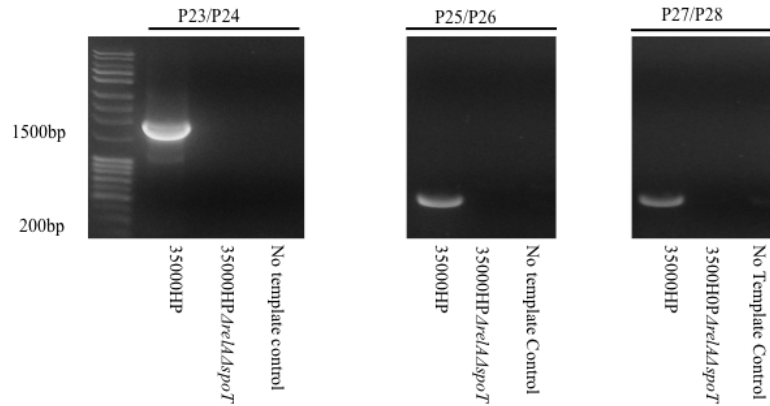
Figure 7. Confirmation of deletion of *relA* and *spoT*. PCR products using primers inside the *spoT* gene. Primers that recognize the *spec* cassette were utilized to confirm that the mutant is unmarked. Products were of the expected sizes: P23/24: *spec* int, P25/P26: *relA* int, and P27/P28: *spoT* int.

To determine if deletion of *relA* or *spoT* affected the expression of their downstream genes *dxr* and *menB*, qRT-PCR was performed using primers P29/P30; P31/P32. Deletion of *relA* and *spoT* did not affect transcription of their downstream genes (data not shown).

Deletion of *relA* and *spoT* affects the growth and survival of *H. ducreyi*. Given that (p)ppGpp mutants are often growth impaired, we next compared *in vitro* growth of the mutants. In our medium, neither the 35000HPΔ*relA* nor the 35000HPΔ*relA*Δ*spoT* mutant exhibited any growth inhibition. In fact, analysis showed that the Δ*relA* and Δ*relA*Δ*spoT* mutants survived better in stationary phase than the parent strain (Figure 8).
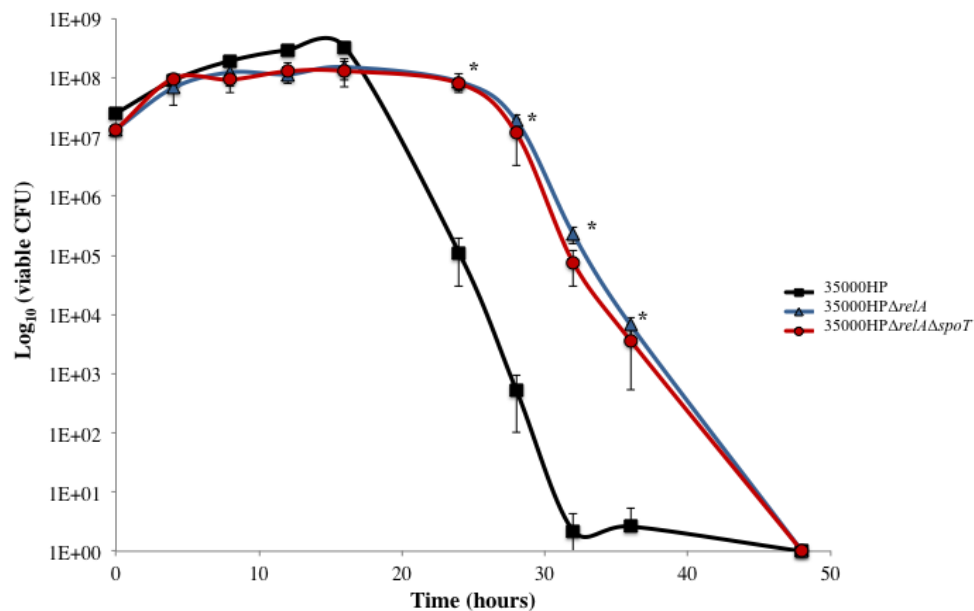
Figure 8. Growth of 35000HP, 35000HPΔ*relA,* and 35000HPΔ*relA*Δ*spoT*. Measured by CFU over 48 hours. The CFU data are geometric means ± SD from three independent experiments. *, $P \leq 0.05$.

Identification of a labeling medium for *de novo* (p)ppGpp synthesis assay. We

wanted to determine if deletion of *relA* and *spoT* would prevent *H. ducreyi* from being

able to synthesize (p)ppGpp. One method for detecting (p)ppGpp in bacteria is incubation

of the bacteria in nutrient limited media with radioactive phosphate as the only phosphate

source. Given that there is no defined media for *H. ducreyi*, we chose to use a modified

tissue culture medium for our labeling experiments. We first compared the ability of

35000HP to survive for 2 and 4 hours in the rich media RPMI, DMEM and HBSS, in

which we could limit the phosphate concentrations. We compared survival of *H. ducreyi*

to controls incubated in GC broth and dH$_2$O. We found that *H. ducreyi* survived at least

as well in RPMI medium as in GC broth for 4 hours (Figure 9A). We tested growth in

decreasing concentrations of phosphate in RPMI to determine the lowest concentration of

sodium phosphate needed to support *H. ducreyi* growth. We found that at 2 hours, no

51

survival defect could be detected in 0.0563 mM, 100-fold less phosphate than the RPMI

standard concentration (Figure 9B).
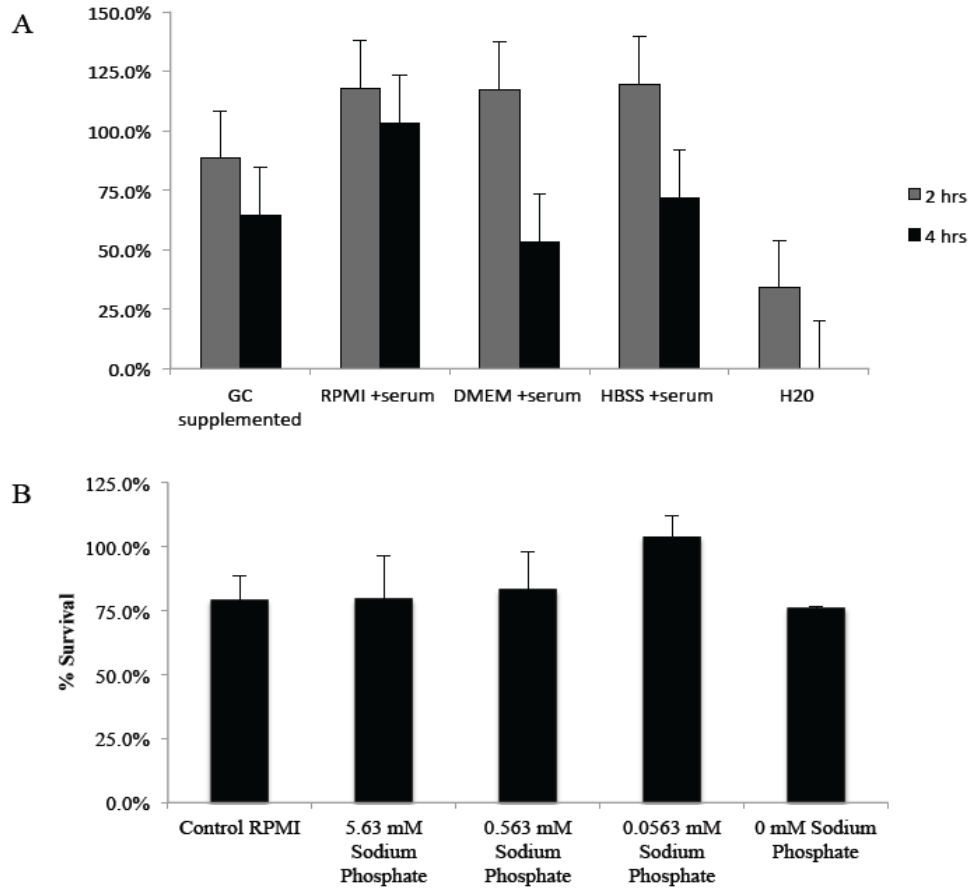
Figure 9. Identification of a ^{32}P labeling medium for *H. ducreyi.* (A) Survival of 35000HP in media after 2 and 4 hours culture. (B) Survival of 35000HP in RPMI with varying amounts of phosphate. All media contain serum.

H. ducreyi synthesizes (p)ppGpp and deletion of *relA* and *spoT* results in a

loss of (p)ppGpp synthesis. To determine if *H. ducreyi* synthesizes (p)ppGpp, 35000HP,

35000HPΔ*relA* and 35000HPΔ*relA*Δ*spoT* were grown to the mid-log, transition and

stationary phases, collected, and labeled with $KH_2{}^{32}PO_4$. *De novo* (p)ppGpp synthesis

was detected using autoradiography. (p)ppGpp synthesis was detected in 35000HP grown

to the mid-log and transition phases. Maximal synthesis of (p)ppGpp was detected in cells harvested from the transition phase (Figure 10). *De novo* synthesis of (p)ppGpp was only variably detected in 35000HP harvested from the stationary phase (data not shown). We detected a single species of the alarmone, indicated by the presence of only one spot on the TLC plate. We were unable to distinguish between pppGpp and ppGpp species in this assay. In both 35000HP∆*relA* and 35000HP∆*relA*∆*spoT* collected from all phases of growth, synthesis of (p)ppGpp was not detected. Thus, deletion of *relA* and deletion of *relA* and *spoT* resulted in a (p)ppGpp° phenotype in our assay.
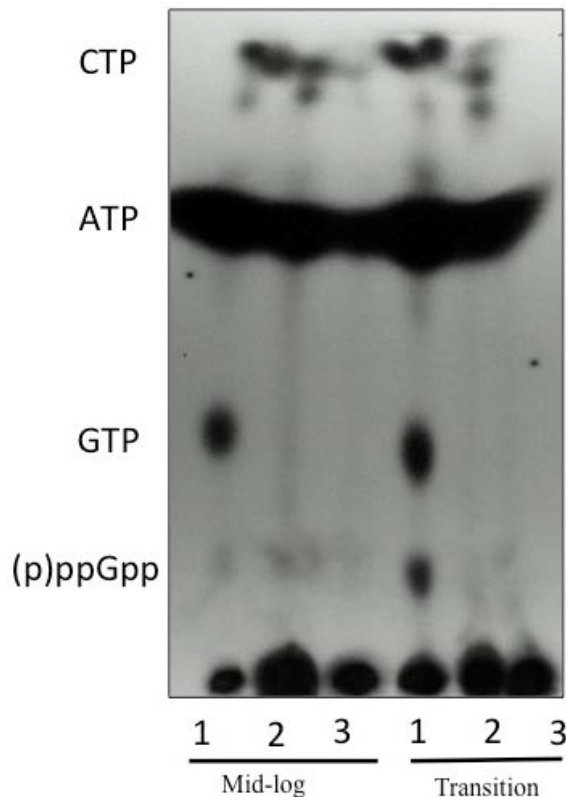
Figure 10. *De novo* synthesis of (p)ppGpp in *H. ducreyi*. Bacteria were labeled with $KH_2{}^{32}PO_4$ in phosphate-limited RPMI plus 5% FBS. (p)ppGpp was extracted and detected by polyethylenimine cellulose thin layer chromatography and autoradiography. Synthesis of (p)ppGpp was detected in cells harvested from mid-log and transition phases of growth. Lane 1, 35000HP; Lane 2, 35000HP∆*relA*; and Lane 3, 35000HP∆*relA*∆*spoT*. Blot is representative of three independent experiments.

Given the inability of the 35000HPΔ*relA* and 35000HPΔ*relA*Δ*spoT* mutants to synthesize (p)ppGpp, we wanted to confirm that the decreased synthesis resulted from loss of the enzyme machinery. To this end, we constructed complementation plasmids using Gibson Assembly. Fragments containing the *cat* promoter (P33/P34), the *spoT* RBS and ORF (P35/P36), and the *relA* RBS and ORF (P37/P38) were included with BamHI cut pACYC177 for assembly of the complementation plasmids. Given that unchecked synthesis of (p)ppGpp in the absence of *spoT* is often lethal, in this construct, *spoT* was placed immediately behind the *cat* promoter to ensure transcription of *spoT* (Figure 11A). Native transcription terminators of the *relA* gene and putative RBS for each gene were also included. The final construct, which contained both the *relA* and *spoT* ORF under control of the *cat* promoter, was named pCH30. We also constructed a plasmid which only expressed *relA,* pCH4, by removing *spoT* from pCH30. Strains containing pCH4 were slightly growth impaired as they do not express SpoT and thus cannot breakdown (p)ppGpp (Figure 11B). qRT-PCR indicated that in the pCH30 complemented strain, expression of both *relA* and *spoT* was equivalent to wild type levels (Figure 12).
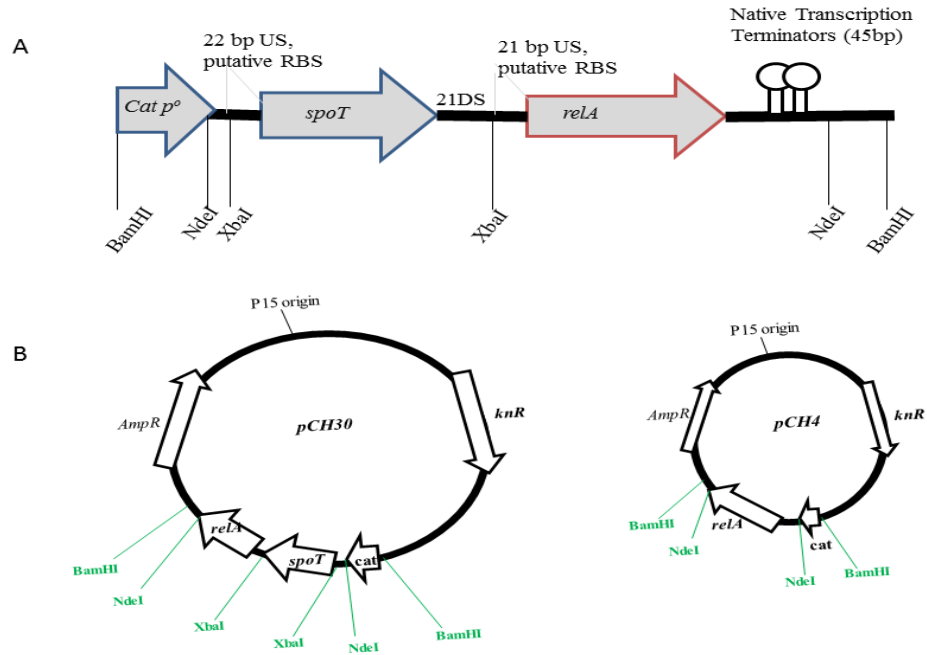
Figure 11. Complementation strategy for 35000HPΔ*relA*Δ*spoT*. (A) Schematic of gene organization in plasmid (B) Plasmid maps for constructs pCH4 and pCH30. US, native upstream region of target gene.
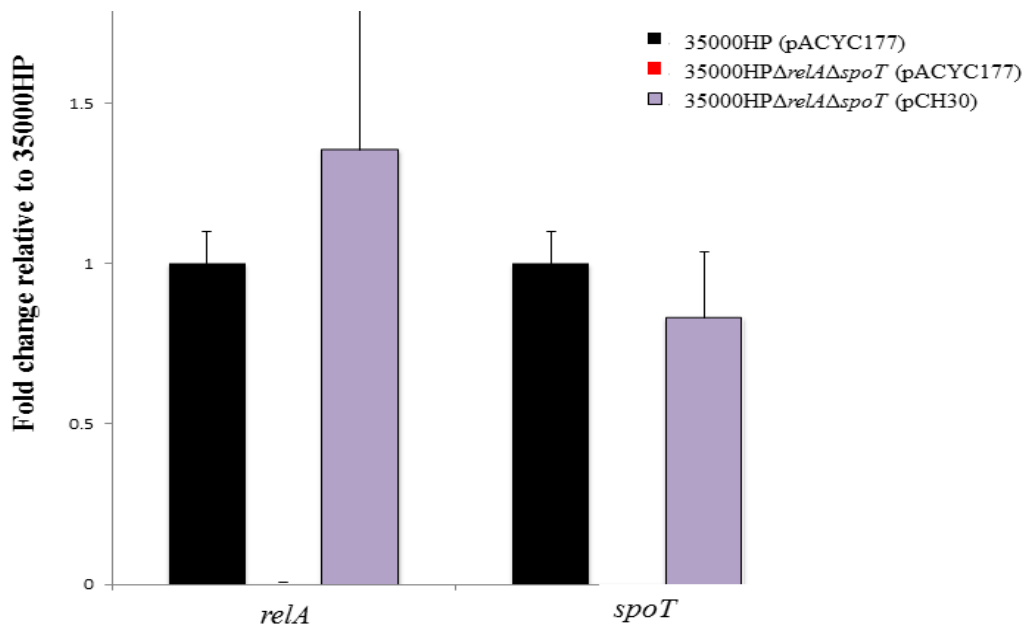
Figure 12. Complementation of the *relA spoT* mutant by pCH30. qRT-PCR of *relA* and *spoT* in 35000HP (pACYC177), 35000HPΔ*relA*Δ*spoT* (pACYC177), and the complemented strain 35000HPΔ*relA*Δ*spoT* (pCH30).

As shown in Figure 10, 35000HP synthesized (p)ppGpp readily in transition phase but not the 35000HPΔ*relA* nor the 35000HPΔ*relA*Δ*spoT* mutants. Therefore, we next determined if we could complement the loss of (p)ppGpp synthesis in the null mutants. 35000HP(pACYC177) and 35000HPΔ*relA*Δ*spoT*(pACYC177) recapitulated the phenotypes of the non-plasmid containing strains (Figure 13). When the Δ*relA*Δ*spoT* mutant was complemented with only *relA* (pCH4), (p)ppGpp synthesis was restored (Figure 13). Thus, pCH4 can complement for loss of (p)ppGpp in 35000HPΔ*relA*Δ*spoT*. However, complementation with pCH30, which contained both genes did not show a spot correlating with (p)ppGpp. We thought that in the double complemented mutant, (p)ppGpp is likely being rapidly synthesized by RelA and degraded as rapidly by SpoT into the breakdown products depicted in Figure 1. As neither *relA* nor *spoT* were regulated by their native promoters, the stoichiochemistry of the two enzymes likely does not reflect natural conditions. Still, taken together, this showed that pCH30 restores expression levels of *relA* and *spoT* to wild type levels and suggests that SpoT is functional *in vitro*.
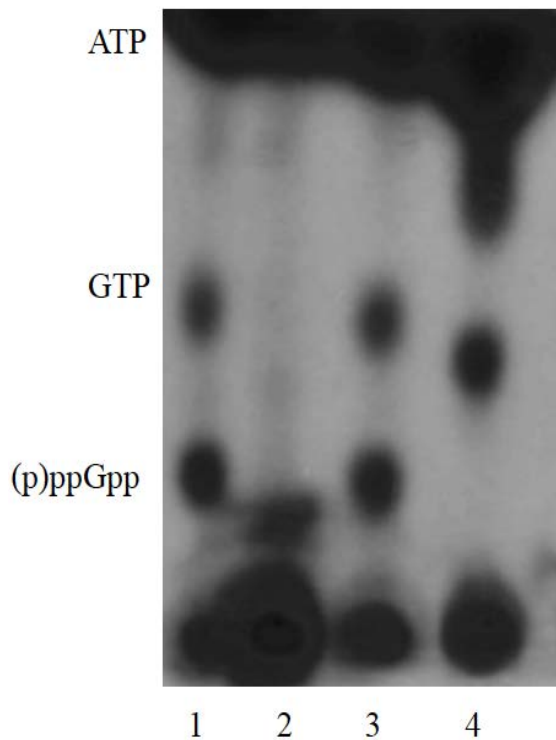
Figure 13. De novo synthesis of (p)ppGpp with complemented strains. Bacteria were labeled with $KH_2^{32}PO_4$ in phosphate-limited RPMI plus 5% FBS. (p)ppGpp was extracted and detected by polyethylenimine cellulose thin layer chromatography and autoradiography. Synthesis of (p)ppGpp was detected in cells harvested from mid-log and transition phases of growth. Lane 1, 35000HP(pACYC177); Lane 2, 35000HPΔ*relA*Δ*spoT*(pACYC177); Lane 3, 35000HPΔ*relA*Δ*spoT*(pCH4); and Lane 4, 35000HPΔ*relA*Δ*spoT* (pCH30). Blot is representative of three independent experiments.

***relA* and *spoT* contribute to *H. ducreyi* virulence in human volunteers.** To determine if RelA and SpoT contribute to virulence in humans, we inoculated four groups of volunteers with 35000HP and with the 35000HPΔ*relA*Δ*spoT* mutant. In the first iteration, one volunteer was inoculated at three sites with an EDD of 157 CFU of 35000HP and three sites with an EDD of 24, 48, and 96 CFU of 35000HPΔ*relA*Δ*spoT*. In the second iteration, three volunteers were each inoculated at three sites with an EDD of 74 CFU of 35000HP and with Δ*relA*Δ*spoT* at three sites with EDDs of 33, 66, and 132 CFU. In the third iteration, one volunteer was inoculated with an EDD of 49 CFU of 35000HP at three sites and at EDDs of 21, 41, and 81 CFU of Δ*relA*Δ*spoT* at three sites. In the final iteration, one volunteer was inoculated with an EDD of 81 CFU of 35000HP at three sites and at three sites with EDDs of 35, 71, and 141 of Δ*relA*Δ*spoT*. Overall,

papules formed at 94% (95% CI, 84.5 - 99.9%) of the parent-inoculated sites and at 94% (95% CI, 84.5 - 99.9%) of the mutant inoculated sites (P = 1.0) (Table 5). After 24 hours of infection, the mean surface area of the papules was 23.7 ± 24.4 mm^2 at parent sites and 18.2 ± 22.4 mm^2 at mutant sites (P = 0.36). Pustules formed at 72.2% (95% CI, 48.3 – 96.2%) of parent sites and 27.8% (95% CI, 0.1-56.2%) of mutant sites (P = <0.0001). Thus, the *relA spoT* mutant was partially attenuated for pustule formation in humans.

At least one positive surface culture for *H. ducreyi* was obtained during follow-up visits from 39.9% of the parent inoculation sites and 16.7% of the mutant inoculation sites. All colonies recovered from the surface cultures of the parent sites (n = 280) and mutant sites (n = 32) were tested for the presence of *relA, spoT,* and *dnaE* sequences by colony hybridization. The *dnaE* probe hybridized to colonies from both parent and mutant sites, while the *relA* and *spoT* probes only bound to colonies from the parent sites. All 3 biopsy specimens from parent sites yielded *H. ducreyi*, and all 3 biopsy specimens from mutant sites yielded *H. ducreyi*. The *dnaE* probe hybridized to both parent (n = 108) and mutant (n = 101) colonies obtained from the biopsies. When the inocula were tested, the *dnaE* probe hybridized to all the colonies tested from both parent (n = 144) and mutant (n = 140) colonies, while the *relA* and *spoT* probes only hybridized to the parent inoculated colonies. There was no evidence of cross-contamination between the mutant and parent inoculation sites.

Table 4. Response to inoculation of live *H. ducreyi* strains – parent vs. Δ*relA*Δ*spoT*

Volunteer (gender)[a]	Observation period (days)	Strain[b]	Dose (CFU)[c]	No. of initial papules	Final outcome of papules	
					No. resolved	No. of pustules
433 (F)	7	P	157	3	2	1
		M	24-96	3	3	0
436 (F)	8	P	74	3		3
		M	33-132	3	2	1
437 (F)	7	P	74	3		3
		M	33-132	2	1	1
438 (M)	7	P	74	3		3
		M	33-132	3		3
439 (M)	7	P	49	3	1	2
		M	21-81	3	3	0
440 (M)	9	P	81	2	1	1
		M	35-141	3	2	0

[a]Volunteer 433 was inoculated in the first iteration. Volunteers 436, 437, and 438 were inoculated in the second iteration. Volunteer 440 was inoculated in the third iteration. Volunteer 439 was inoculated in the fourth iteration. M, male; F, female.
[b]P, Parent strain 35000HP; M, mutant strain 35000HPΔ*relA*Δ*spoT*.
[c]Doses inoculated at 3 sites, except 24-96, one dose each of 24, 48, and 96 CFU; 33-132, one dose each of 33, 66 and 132 CFU; 21-81, one dose each of 21, 41, and 81 CFU; 35-141, one dose each of 35, 71, and 141 CFU.

Three volunteers (436, 437, and 438) developed pustules at both mutant and parent sites. For each subject, one parent site and one mutant site were biopsied and stained with hematoxylin-eosin and anti-CD3 antibodies as previously described (154). All samples contained micropustules in the epidermis and dermal CD3 cells (data not shown). Histopathologically, pustules formed at mutant sites were indistinguishable from pustules formed at parent sites.

Deletion of *relA* alters the OMP profile of *H. ducreyi*. We investigated if deletion of *relA* and *spoT* affected expression of outer membrane components of *H ducreyi*. OMP and LOS were prepared from 35000HP, 35000HPΔ*relA* and 35000HPΔ*relAΔspoT* harvested from mid-log phase. 35000HP, 35000HPΔ*relA,* and 35000HPΔ*relAΔspoT* had identical LOS profiles (Figure 14).
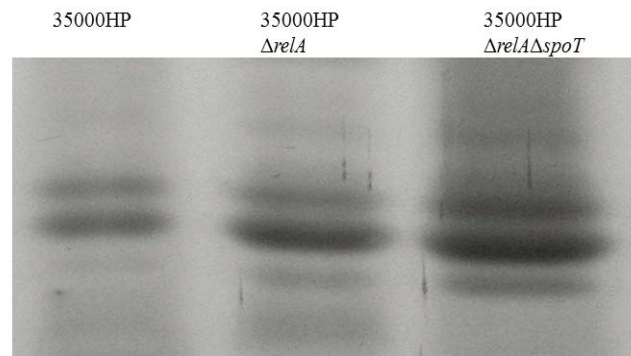
Figure 14: LOS Profile of 35000HP, 35000HPΔ*relA* and 35000HPΔ*relAΔspoT*.

Analysis of OMP showed increased expression of a band that migrates between 40 - 45 kDa in both 35000HPΔ*relA* (data not shown) and 35000HPΔ*relA*Δ*spoT* compared to the parent strain (Figure 15A). Tandem mass spectrometry experiments performed on the excised band identified 19 potential proteins, with predicted molecular weights between 41-49 kDa (Table 6). The protein with the highest overall score was OmpP2B, a putative porin previously described in *H. ducreyi* (155). Western blot analysis with an OmpP2B-specific antibody confirmed that the *relA spoT* mutant expressed more OmpP2B than the parent strain (Figure 15B).
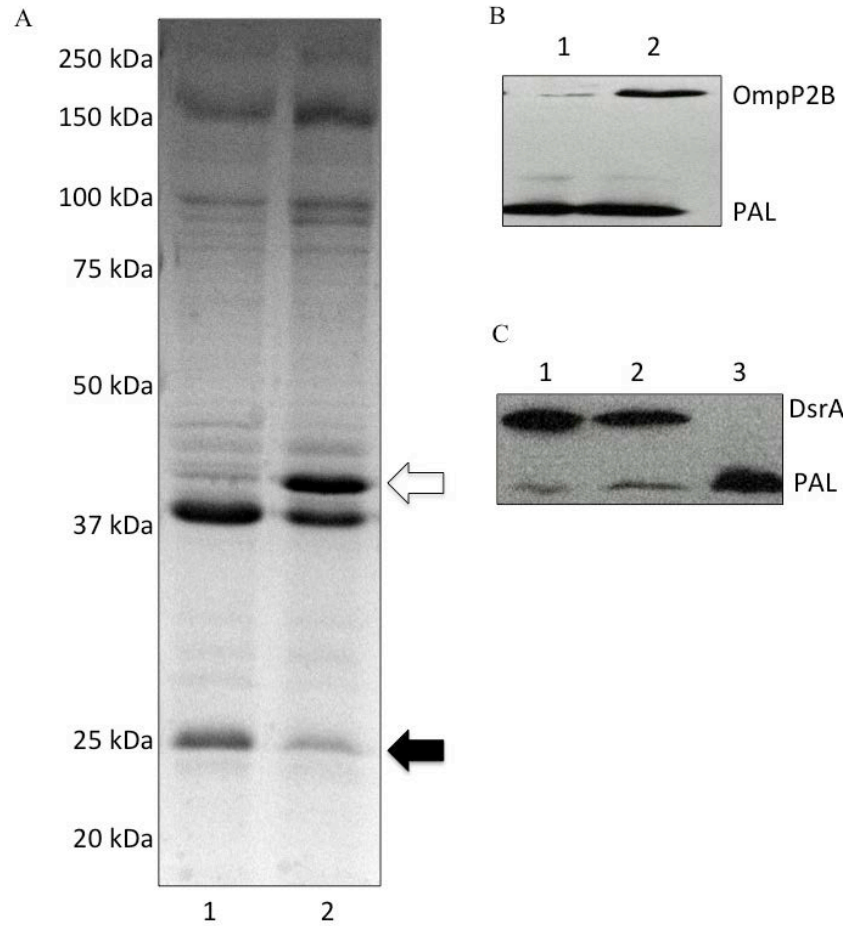
Figure 15: OMP expression of 35000HP and 35000HPΔ*relA*Δ*spoT* harvested from mid-log phase (A) Purified outer membranes were analyzed by SDS-PAGE and Coomassie staining. Arrows indicate protein bands selected for further analysis; open arrow, OmpP2B; filled arrow, DsrA. Lane 1, 35000HP; and Lane 2, 35000HPΔ*relA*Δ*spoT*. *(B)* Western blot analysis of purified outer membrane proteins of 35000HP and 35000HPΔ*relA*Δ*spoT*. Lysates were probed with OmpP2B specific antibody. (C) Western blot analysis of purified outer membrane proteins of 35000HP, 35000HPΔ*relA*Δ*spoT* and the *dsrA* mutant, FX517. Lysates were probed with DsrA specific antibody. Anti-PAL MAb 3B9 was used to verify equivalent loading. Lane 1, 2 as in (B); Lane 3, FX517.

Table 5. *Haemophilus ducreyi* proteins identified by tandem mass spectrometry

Protein annotation	Accession no.	Matching unique peptides, no.	Protein Coverage	Predicted MW, kDa[b]	Theoretical pI[b]	Predicted cellular location	Protein score[c]
OmpP2B	Q7VLJ6	25	63.98	44.6	9.05	outer	336.46
L-lactate dehydrogenase (cytochrome)	Q7VPI9	11	48.82	41.7	8.38	cytoplasm	181.79
Acetate kinase	Q7VLI5	14	65.75	43.8	5.26	cytoplasm	134.43
Cysteine desulfurase	Q7VMA9	13	41.87	45.6	6.04	cytoplasm	102.8
Elongation factor Tu	Q7TTF9	10	39.85	43.4	5.24	cytoplasm	98.11
protein TolB	Q7VKU3	10	33.1	45.6	7.79	periplasm	87.92
Momp	G1UB86	7	36.48	44.1	9.22	outer	84.86
Histidine tRNA ligase	Q7VME1	7	30.73	47.5	5.85	cytoplasm	76.7
L-lactate dehydrogenase (cytochrome)	B0BTC7[a]	1	15.22	41.7	6.68	cytoplasm	74.91
putative RND efflux membrane fusion	Q7VLE4	10	32.42	47.3	9.32	membrane	56.49
Cell division protein ftsA	Q7VMY4	5	23	45.6	5.69	cytoplasm	43.37
Na(+) translocating NADH-quinone	Q7VNU4	7	25.18	45.6	5.01	inner	40.75
OmpA2	G1UB72	4	27.03	44.7	9.40	outer	40.11
Histidine tRNA ligase	Q0I2E8[a]	1	10.12	48.1	5.61	cytoplasm	30.42
Penicillin-binding protein 5	Q7VKA7	3	12.47	43.2	8.41	inner	28.88
Spermidine/putrescine import ATP-binding	Q7VNG4	3	13.21	41.9	5.12	inner	23.17
Adenylosuccinate synthetase	Q7VKR5	3	8.8	47.2	5.56	cytoplasm	16.34
putative secreted protease	Q7VMW6	1	5.41	39.1	9.26	plasma	12.19
Riboflavin biosynthesis protein RibBA	Q7VM45	3	9.98	44.1	5.65	cytoplasm	11.67

Note: MW, molecular weight.

[a]Peptides matched to a protein that was not *H. ducreyi* specific.

[b]Predicted based on amino acid sequence of protein by Uniprot.

[c]Sum of the scores of the individual peptides matching to each protein.

Analysis of OMP profiles showed that a band that migrates at the apparent molecular weight of DsrA, the major determinant of serum resistance, appeared to be decreased in both 35000HPΔ*relA* (data not shown) and 35000HPΔ*relAΔspoT* relative to 35000HP (Figure 15A). By Western blot, the level of expression of DsrA between in 35000HPΔ*relAΔspoT* was somewhat reduced compared to 35000HP (Figure 15C).
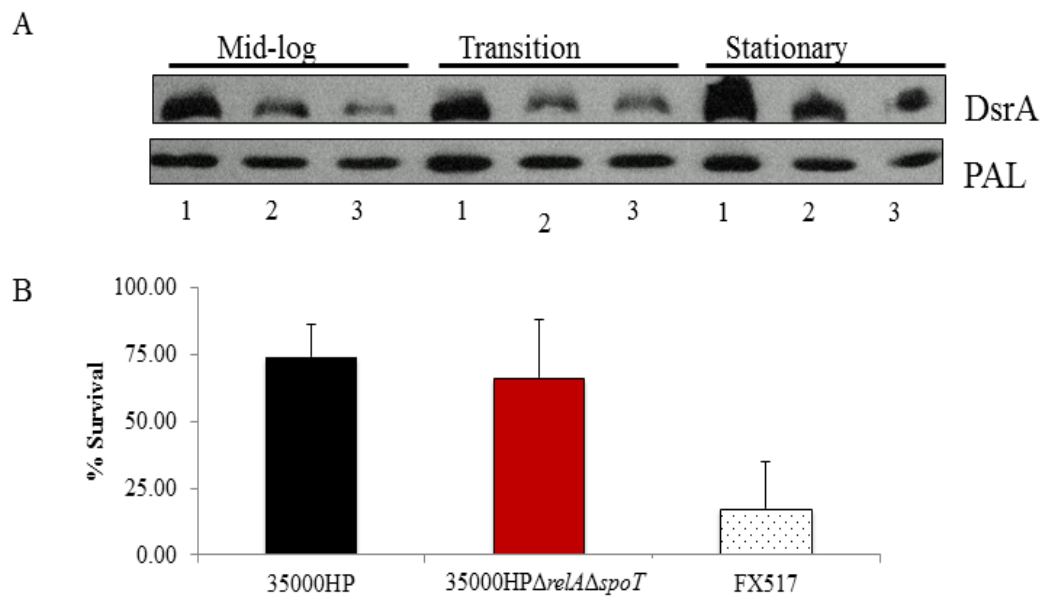
Figure 16: Effect of *relA* and *spoT* deletion on the expression of DsrA. (A*)* Western blot analysis of whole cell lysates of 35000HP, 35000HPΔ*relA*, and 35000HPΔ*relAΔspoT* harvested from mid-log, transition and stationary phases of growth. Lysates were probed with DsrA antibody. Lane 1*,* 35000HP*;* Lane 2*,* 35000HP*ΔrelA*; and Lane 3*,* 35000HP*ΔrelAΔspoT.* Blot is representative of three independent experiments. (B) *H. ducreyi* sensitivity to complement-replete human serum. Percent survival of 35000HP, 35000HPΔ*relAΔspoT*, and *dsrA* mutant strain FX517 in normal human serum (NHS). Survival was calculated as [(geometric mean CFU in NHS/geometric mean CFU in heat-inactivated NHS) × 100]. Data are means ± SD of three independent experiments. All strains were compared to 35000HP.

We harvested cells from the 3 strains collected at the mid-log, transition and stationary phases of growth; Western blot and densitometry analysis showed that expression of DsrA was significantly reduced in both the single ($P = 0.05$) and double mutants ($P = 0.043$) compared to the parent in cells collected at mid-log phase but not in cells collected in the transition or stationary phases (all P values > 0.24) (Figure 16A). In bactericidal assays using 50% normal human serum and colonies harvested from chocolate agar plates, 35000HP$\Delta relA\Delta spoT$ was as resistant to killing as the parent strain (Figure 16B). Thus, the reduction in DsrA expression in the mutant during mid-log phase may not be biologically significant.

RelA and SpoT do not contribute to heat stress resistance. In other organisms, (p)ppGpp induces expression of genes critical for responses to heat shock such as *rpoH* (156-158). *H. ducreyi* 35000HP grows optimally at 33°C (13). To determine if *relA* and *spoT* had a role in regulating responses to heat shock, we compared the survival of 35000HP$\Delta relA$ and 35000HP$\Delta relA\Delta spoT$ relative to 35000HP after incubation at 37°C for 1 hour. Percent survival rates were not significantly different among the strains (Figure 17). Thus, RelA and SpoT did not contribute to *H. ducreyi* survival following heat shock.
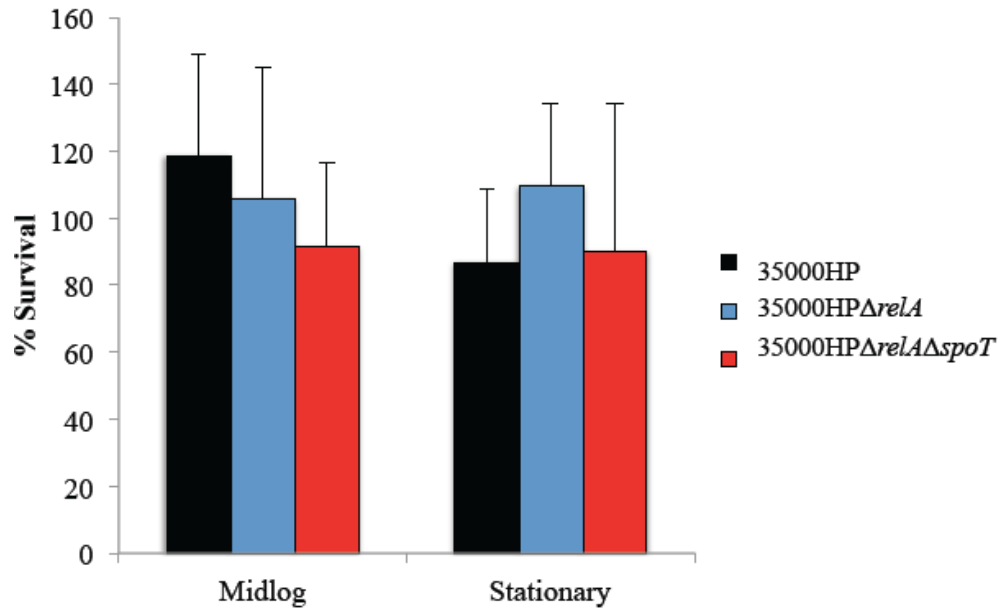
Figure 17: Response of 35000HPΔ*relA* and 35000HPΔ*relA*Δ*spoT* to heat stress at 37°C. Data are means ± SD of three independent experiments. All strains we compared to survival at 33°C.

Loss of (p)ppGpp decreased phagocytic uptake of mid-log phase grown *H. ducreyi*. During both natural and experimental infection, *H. ducreyi* associates with neutrophils and macrophages but remains extracellular (50, 159). LspB is required for the secretion of LspA1 and LspA2, which are responsible for resistance to phagocytosis (61, 62). *lspB* and *lspA2* are co-transcribed; LspB is maximally expressed and LspA1 and LspA2 are maximally secreted during stationary phase. To determine the role of (p)ppGpp in resistance to phagocytosis, we compared the uptake of 35000HP, 35000HPΔ*relA* and 35000HPΔ*relA*Δ*spoT* cells grown to mid-log and stationary phase by primary human macrophages. No differences were found for the uptake of cells harvested at stationary phase (Figure 18A). However, compared to the parent, a significant

reduction in the uptake of the $\Delta relA\Delta spoT$ mutant ($P = 0.0076$) and trended towards reduction in the uptake of the $\Delta relA$ mutant ($P = 0.052$) was shown for cells harvested at mid-log phase.
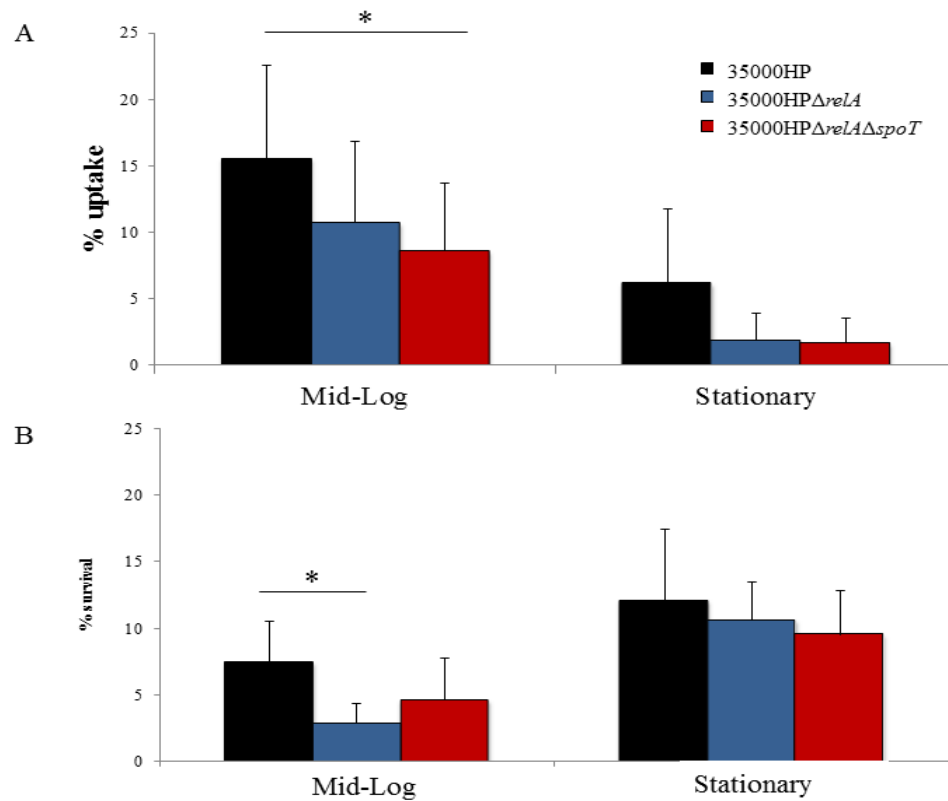
Figure 18: Uptake by and survival in macrophages. (A) Percent uptake of 35000HP, 35000HP$\Delta relA$, and 35000HP$\Delta relA\Delta spoT$ by human macrophages. MDM were infected with opsonized *H. ducreyi* at an MOI of 10:1. After 30 minutes of incubation, gentamicin was added to kill extracellular bacteria. The percent uptake was calculated as [(geometric mean CFU of gentamicin-protected bacteria at 1 hour/ geometric mean CFU of input bacteria) x 100]. Data are mean ± SD from five independent donors. (B) Survival was calculated as [(geometric mean CFU of after 6 hours co-culture/ geometric mean CFU of gentamicin-protected bacteria at 1 hour) x 100].

RelA and SpoT are important for resistance to oxidative stress. (p)ppGpp expression is often critical for survival of bacteria during oxidative stress (160-162). We compared the survival of 35000HP, 35000HPΔ*relA,* and 35000HPΔ*relA*Δ*spoT* after incubation with hydrogen peroxide. When mid-log or stationary phase bacteria were incubated with 0.2 mM or 2 mM H_2O_2, both the *relA* and *relA spoT* mutants survived at significantly lower levels than the parent strain (Figure 19A). Complementation of the *relA spoT* mutant restored resistance to both 0.2 mM and 2 mM H_2O_2 (Figure 19B).
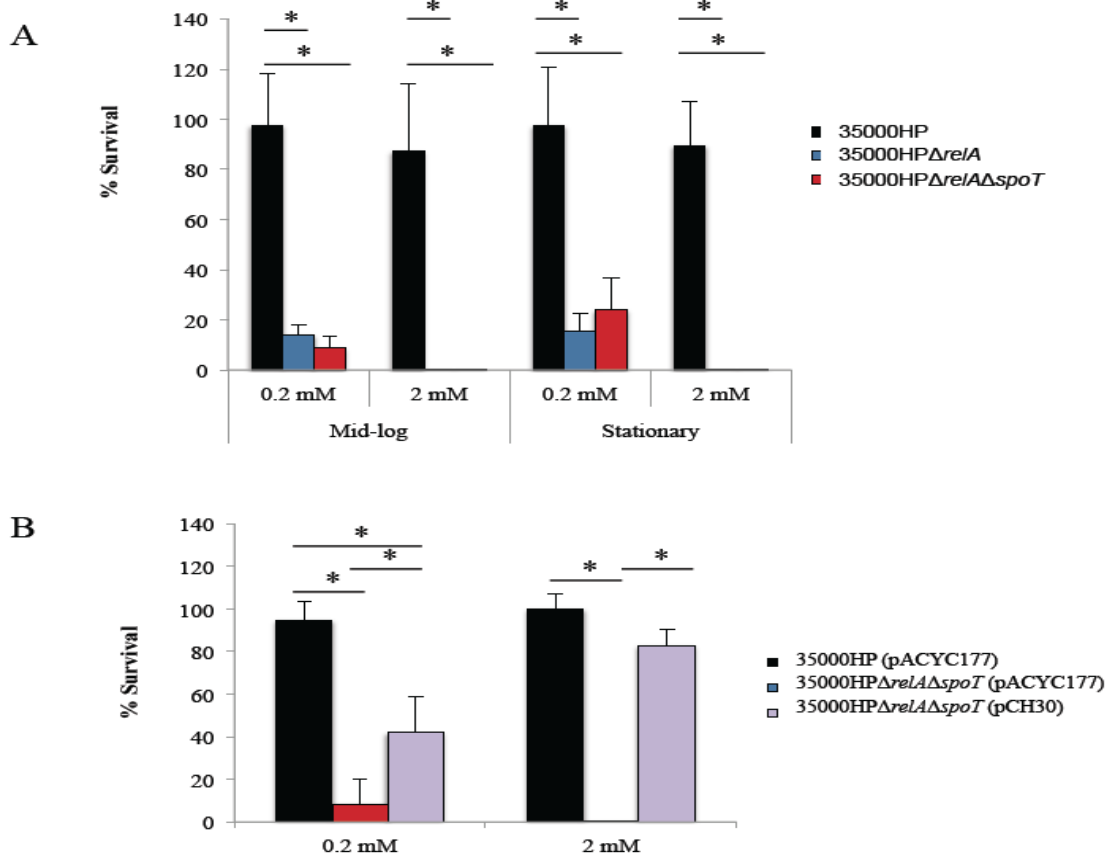
Figure 19: *H. ducreyi* survival after oxidative stress at mid-log and stationary phase. (A) Percent survival of 35000HP, 35000HPΔ*relA,* and 35000HPΔ*relA*Δ*spoT* following incubation with 0.2 mM or 2 mM H_2O_2 for 1 hour. (B) Percent survival of mid-log phase 35000HP (pACYC177), 35000HPΔ*relA*Δ*spoT* (pACYC177)*,* and the complemented strain 35000HPΔ*relA*Δ*spoT* (pCH30) following incubation with 0.2 mM or 2 mM H_2O_2 for 1 hour.

When bacteria in either mid-log or stationary phase were incubated with 0.2 mM or 2 mM paraquat, the *relA* and *relA spoT* mutants survived at significantly lower levels than the parent strain (Figure 20A). Complementation with *relA spoT* was able to restore statistically significant resistance to 2 mM paraquat (Figure 20B). Therefore, RelA and SpoT contribute to *H. ducreyi* survival to oxidative stress generated by paraquat.
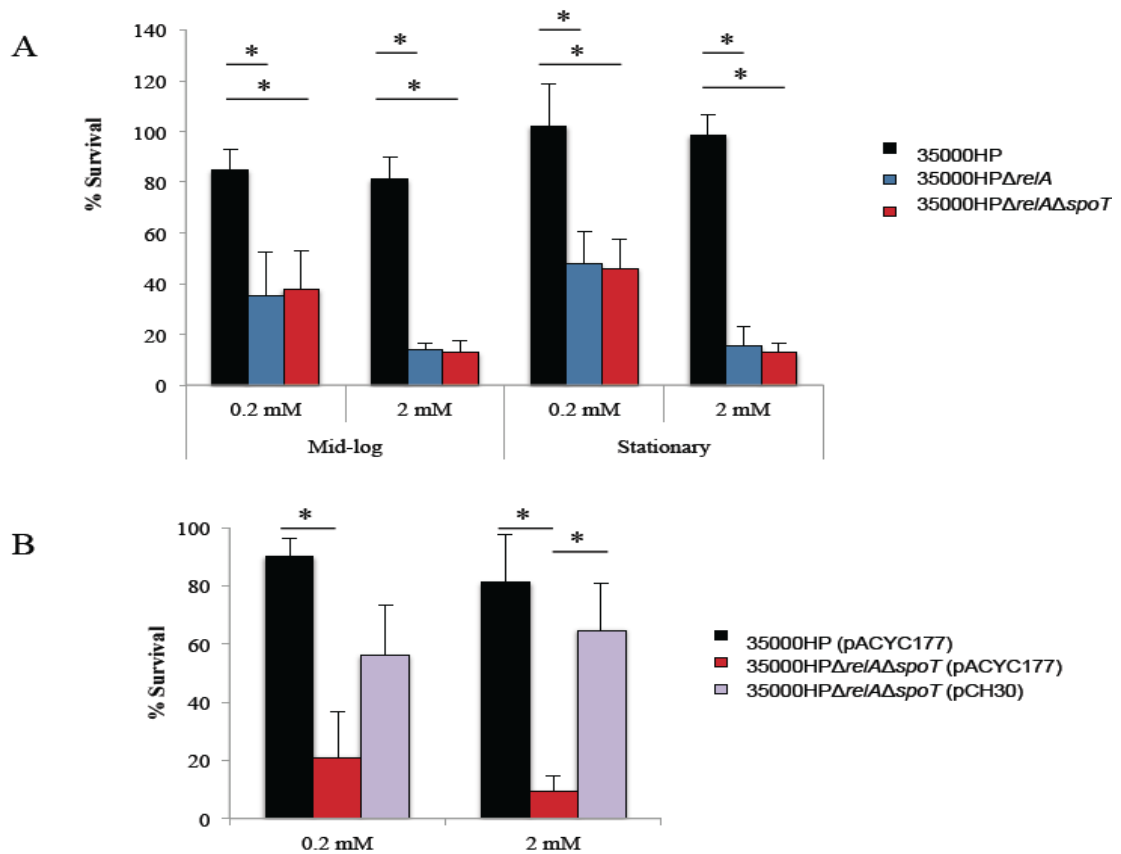
Figure 20: Survival in paraquat-induced oxidative stress. (A) Percent survival of 35000HP, 35000HPΔ*relA,* and 35000HPΔ*relA*Δ*spoT* following 1 hour incubation with 0.2 mM or 2 mM paraquat. (B) Percent survival of mid-log phase 35000HP (pACYC177), 35000HPΔ*relA*Δ*spoT* (pACYC177)*,* and 35000HPΔ*relA*Δ*spoT* (pCH30) following incubation with 0.2 mM or 2 mM paraquat for 1 hour. All percent survivals were calculated as [(geometric mean CFU after treatment/ geometric mean before treatment) x 100]. The data are mean ± SD from four independent experiments. *, $P \leq 0.05$.

Given that the *relA spoT* mutant was more sensitive to oxidative stress, we investigated if (p)ppGpp regulated the expression of genes that encode putative oxidative stress responsive proteins. The genes *oxyR* and *sodC* encode the hydrogen peroxide-inducible gene activator and periplasmic Cu-Zn superoxide dismutase, respectively. Compared to the parent, transcript levels of both *oxyR* and *sodC* were unchanged in the 35000HPΔ*relA*Δ*spoT* mutant (data not shown). Thus, the mechanism of (p)ppGpp-mediated resistance to oxidative stress is unclear.

Deletion of *relA* and *spoT* affects expression of *dksA*. DksA is an important cofactor of (p)ppGpp that helps stabilize the interaction of (p)ppGpp with RNA polymerase (106). As overexpression of *dksA* has been shown to compensate for the loss of (p)ppGpp in other bacteria, we determined if loss of (p)ppGpp affected transcript levels of *dksA*. qRT-PCR showed that compared to wild type strain results, *dksA* was significantly upregulated in the 35000HPΔ*relA*Δ*spoT* mutant harvested from the mid-log phase (4.31 ± 0.87, $P = 0.0025$) and the transition phase (5.33 ± 2.01, $P = 0.03$) of growth. No difference in the levels of *dksA* expression was found between the 35000HPΔ*relA*Δ*spoT* and 35000HP strains grown to the stationary phase (1.69 ±1.16). Thus, loss of *relA* and *spoT* may be in part compensated by upregulation of *dksA*.

DksA may compensate for loss of (p)ppGpp in resistance to oxidative stress. In *E. coli, dksA* overexpression can compensate for loss of (p)ppGpp (134, 163). We therefore tested whether overexpression of *dksA* could compensate for loss of (p)ppGpp. To this end, we generated 35000HPΔ*relA*Δ*spoT*(pCH24), which overexpresses *dksA* but

does not synthesize (p)ppGpp. We used strain 35000HPΔ*relA*Δ*spoT*(pCH30), the

Δ*relA*Δ*spoT* complemented strain, as a control for the assay (164). Sensitivity of

35000HPΔ*relA*Δ*spoT*(pACYC177) to 2 mM hydrogen peroxide was significantly

restored in both 35000HPΔ*relA*Δ*spoT*(pCH30) (*P*= 0.0002) and

35000HPΔ*relA*Δ*spoT*(pCH24) (*P*= 0.0029) (Figure 21). Therefore, DksA overexpression

may partially compensate for the loss of (p)ppGpp in resistance to oxidative stress *in*

vitro.
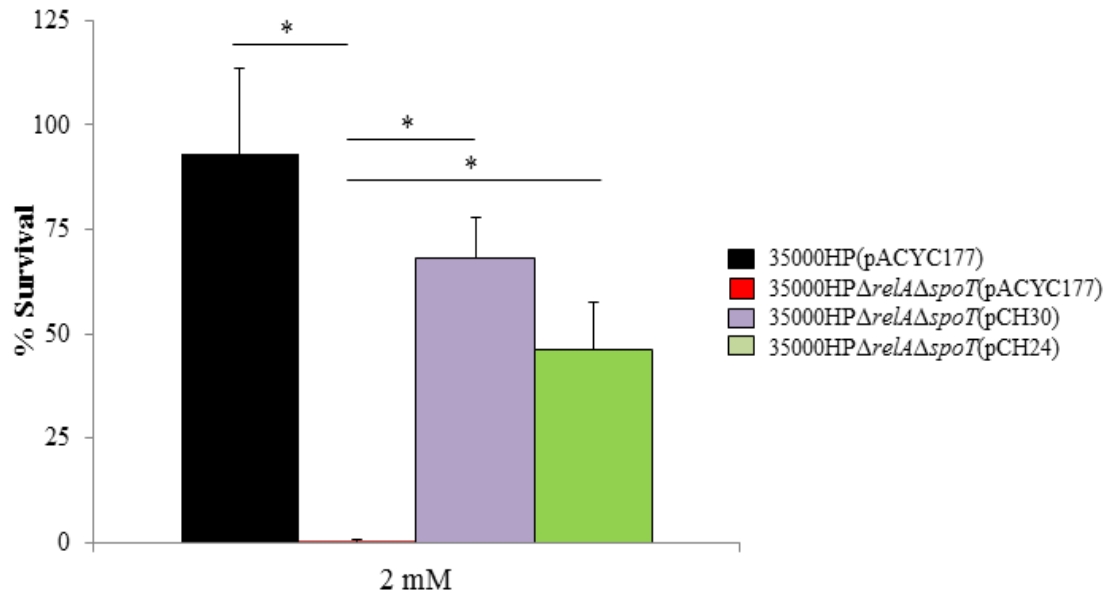
Figure 21. Complementation of the Δ*relA*Δ*spoT* mutant in oxidative stress. Percent survival of mid-log phase 35000HP (pACYC177), 35000HPΔ*relA*Δ*spoT* (pACYC177)*,* and the complementation strains 35000HPΔ*relA*Δ*spoT* (pCH30) and 35000HPΔ*relA*Δ*spoT* (pCH24) following incubation with 0.2 mM or 2 mM H_2O_2 for 1 hour. All percent survivals were calculated as [(geometric mean CFU after treatment/ geometric mean before treatment) x 100]. The data are mean ± SD from five independent experiments. *, $P \leq 0.05$.

In summary, our findings suggest an important role for (p)ppGpp in *H. ducreyi* virulence in humans. Our findings also highlight the underappreciated roles of (p)ppGpp in regulating phenotypes associated with exponential growth. Given that upregulation of *dksA* may partially compensate for the loss of ppGpp *in vivo*, we next determined the role of DksA in *H. ducreyi* pathogenesis.

Chapter IV:

A DksA mutant is partially attenuated in humans due to alteration

of multiple virulence-associated phenotypes

Given that overproduction of DksA is known to phenotypically compensate for lack of (p)ppGpp in *E. coli* and may compensate for loss of (p)ppGpp in *H. ducreyi*, we next characterized a *dksA* deletion mutant (134).

Characterization of the *dksA* genomic locus. The *H. ducreyi* homolog of *dksA* (HD0603) is in a putative operon with the gene order *tbpA* → *dksA* → *pcnB* → *folK* (Figure 22A). The genes *tbpA, pcnB,* and *folK* are predicted to encode a thiamin ABC transporter, poly (A) polymerase, and 7,8-dihydro-6-hydroxymethylpterin-pyrophosphokinase, respectively. RT-PCR analysis indicated that *dksA* is co-transcribed with *tpbA, pcnB,* and *folk* (Figure 22B)
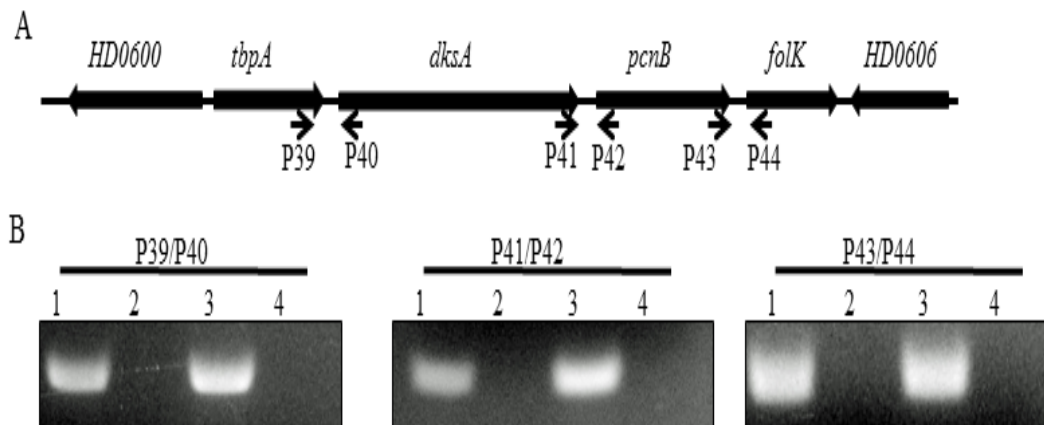
Figure 22. Chromosomal locus containing *dksA* in *H. ducreyi*. (A) Genomic organization of *dksA* locus in *H. ducreyi*. The small arrows indicate locations of intergenic primers used for RT-PCR analysis. (B) Agarose gel electrophoresis of products amplified by RT-PCR. The intergenic regions of *tbpA-dksA*, *dksA-pcnB*, and *pcnB-folK* were examined. Lane 1, RNA sample with reverse transcriptase; Lane 2, RNA sample without reverse transcriptase control; Lane 3, genomic DNA control; and Lane 4, no template control. Products were of the expected sizes: *tbpA-dksA* (197 bp), *dksA-pcnB* (332 bp), and *pcnB-folK* (371 bp).

Conservation of the *dksA* gene in *H. ducreyi* clinical strains. We conducted a limited strain survey to determine if *dksA* was conserved across clinical isolates of *H. ducreyi*. Using primers constructed for detection of the 35000HP *dksA* gene (P45/P46), PCR was performed on two representative strains from each of the 3 classes. The representative strains were the following: Class HD183, 82-029362 and I; Class II, 33921 and CIP542; CUD, NZS3 and NZS4. Specific details regarding these strains are contained in Table 1. Analysis indicated that the *dksA* gene is detected in all the representative strains indicating that this gene is are conserved in *H. ducreyi* (Figure 23).
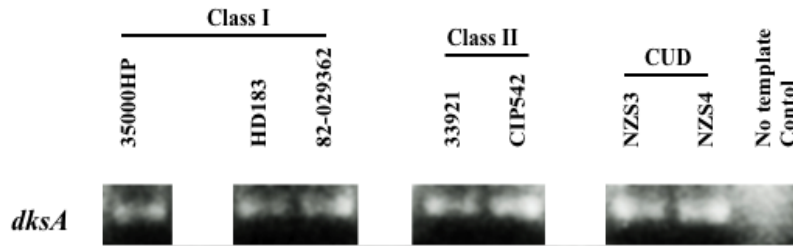
Figure 23. Strain survey of *H. ducreyi* clinical isolates - *dksA*. PCR products of *dksA* in clinical *H. ducreyi* isolates to determine conservation of genes across multiple classes.

dksA contributes to H. ducreyi virulence in human volunteers. To determine if DksA contributes to virulence in humans, we constructed an unmarked, in-frame *dksA* deletion mutant. The mutant was constructed as previously described except that primers P47/P48 were used to amplify the *spec* cassette and the *dksA* ORF was amplified using primers P49/P50. The final mutant was designated 35000HPΔ*dksA*.

We next confirmed that 35000HPΔ*dksA* was in fact a *dksA* deletion mutant using PCR (Figure 24). PCR confirmed a size shift indicating that the *dksA* gene has been removed. PCR using primers interior to the *dksA* gene confirmed that *dksA* has been deleted in the mutant (Figure 24). Sequencing confirmed that the mutant was correct.
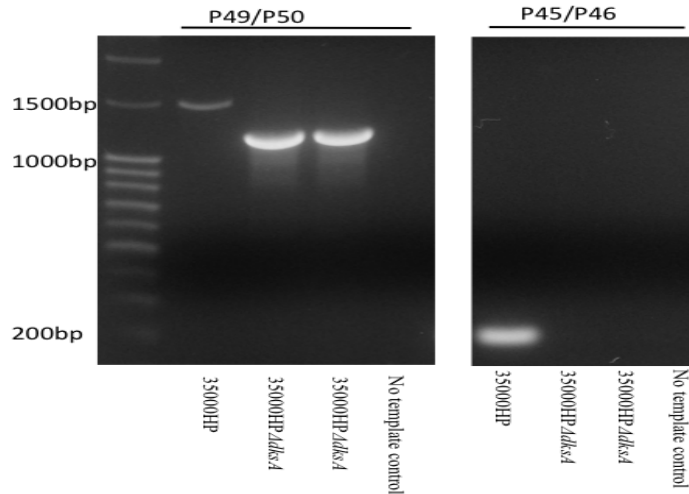
Figure 24. Confirmation of deletion of *dksA*. PCR products using primers both outside and inside the *dksA* gene. Products were of the expected sizes: P49/50, exterior *dskA* and P45/P46, *dksA* int.

Deletion of *dksA* does not alter OMP or LOS profiles of *H. ducreyi*. We investigated if deletion of *dksA* affected expression of outer membrane components of *H ducreyi*. OMPs and LOS were prepared from 35000HP and 35000HPΔ*dksA* harvested from mid-log phase. 35000HP and 35000HPΔ*dksA* had identical LOS profiles indicating that no qualitative differences in LOS exist between the mutant and the wild type strain (Figure 25).
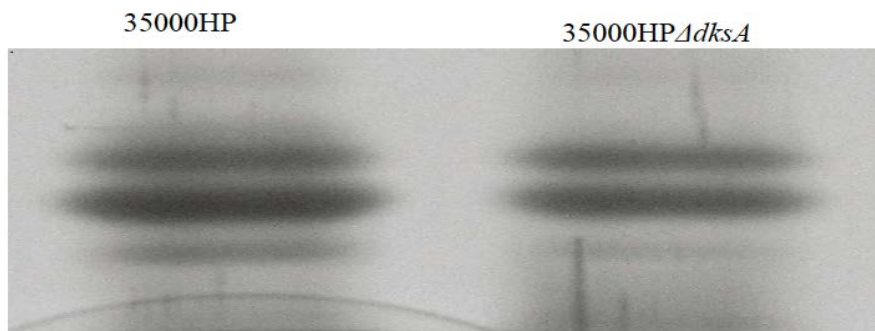
Figure 25. LOS Profile of 35000HP and 35000HPΔ*dksA*.

76

As expected, the *dksA* mutant has no qualitative differences in protein expression in the outer membrane (Figure 26). Analysis of the OMP indicated that 35000HPΔ*dksA* expresses DsrA at similar levels to 35000HP.
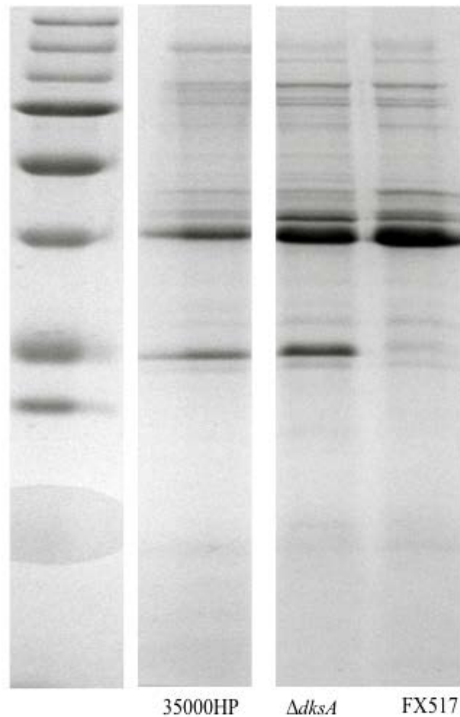
Figure 26: OMP expression of 35000HP and 35000HPΔ*dksA*. Purified outer membranes were analyzed by SDS-PAGE and Coomassie staining.

35000HP   Δ*dksA*   FX517

Human challenge with 35000HPΔ*dksA*. We inoculated volunteers in three iterations with 35000HP and with 35000HPΔ*dksA*. In the first iteration, three volunteers were inoculated at three sites with an EDD of 82 CFU of 35000HP and at 1 site each with an EDD of 52, 104, and 207 CFU of 35000HPΔ*dksA*. In the second iteration, two volunteers were each inoculated at three sites with an EDD of 150 CFU of 35000HP and with Δ*dksA* at three sites with EDDs of 87, 174, and 348 CFU. In the third iteration, two volunteers were inoculated with an EDD of 77 CFU of 35000HP at three sites and an

EDD of 137 CFU of $\Delta dksA$ at three sites. Overall, papules formed at 90.5% (95% CI, 79.3 - 99.9%) of the parent-inoculated sites and at 81.0% (95% CI, 63.0 - 98.9%) of the mutant inoculated sites ($P = .094$) (Table 6). After 24 hours of infection, the mean surface area of the papules was $9.1 \pm 9.2 \text{ mm}^2$ at parent sites and $4.6 \pm 6.9 \text{ mm}^2$ at mutant sites ($P = 0.012$). Pustules formed at 42.9% (95% CI, 14.2 – 71.5%) of parent sites and 14.3% (95% CI, 2.1-26.5%) of mutant sites ($P = 0.043$). Thus, the $\Delta dksA$ mutant was partially attenuated for pustule formation in humans.

Three volunteers (455, 457, and 459) developed pustules at both mutant and parent sites. For each subject, one parent site and one mutant site were biopsied, divided in half and semi-quantitatively cultured or stained with hematoxylin-eosin and anti-CD3 antibodies as previously described (154). All samples contained micropustules in the epidermis and dermal CD3 cells (data not shown). Histopathologically, pustules formed at mutant sites were indistinguishable from pustules formed at parent sites.

Table 6. Response to inoculation of live *H. ducreyi* strains – parent vs. Δ*dksA*

Volunteer (gender)[a]	Observation period (days)	Strain[b]	Dose (CFU)[c]	No. of initial papules	Final outcome of papules	
					No. of pustules	Resolved
454 (F)	7	P	82	2	0	2
		M	52-207	2	0	2
455 (M)	9	P	82	3	1	2
		M	52-207	3	1	2
456 (F)	5	P	82	3	0	3
		M	52-207	2	0	2
457 (F)	7	P	150	3	3	0
		M	87-348	3	1	2
458 (F)	5	P	150	2	0	2
		M	87-348	1	0	1
459 (M)	8	P	77	3	1	2
		M	137	3	1	2
460 (F)	12	P	77	3	3	0
		M	137	3	0	3

[a]Volunteers 454, 455, and 456 were inoculated in the first iteration. Volunteers 457 and 458 were inoculated in the second iteration. Volunteers 459 and 460 were inoculated in the third iteration; M, male; F, female
[b]P, Parent strain 35000HP; M, mutant strain 35000HPΔ*dksA*.
[c]Doses inoculated at 3 sites, except 52-207, one dose each of 52, 104, and 207 CFU; 87-348, one dose each of 87, 174 and 348 CFU.

All colonies recovered from the inocula, surface cultures and biopsies were tested for the presence of *dksA* and *dnaE* sequences by colony hybridization. The *dnaE* probe hybridized to all the colonies tested from both parent (n = 108) and mutant (n = 107) inocula, while the *dksA* probe only hybridized to colonies from the parent inocula. At least one positive surface culture for *H. ducreyi* was obtained during follow-up visits from 19.5% of the parent inoculation sites and 4.8% of the mutant inoculation sites. The *dnaE* probe hybridized to colonies from both parent (n = 106) and mutant (n = 29) inoculated sites, while the *dksA* probe only bound to colonies from the parent sites. All 3 paired biopsies of mutant and parent pustules yielded *H. ducreyi*. The *dnaE* probe hybridized to all of both parent (n = 107) and mutant (n = 69) colonies obtained from the biopsies, while the *dksA* probe only hybridized to colonies obtained from the parent biopsies. There was no evidence of cross-contamination between the inocula and mutant and parent inoculation sites.

In vitro characterization of the *dksA* mutant. The virulence of *H. ducreyi* has been correlated with resistance to serum-mediated killing, phagocytosis, and oxidative stress as well as adherence to human foreskin fibroblasts. *H. ducreyi* mutants with defects in the above *in vitro* phenotypes are partially or fully attenuated in the human challenge model. The level of expression of DsrA, the major determinant of serum resistance, in 35000HPΔ*dksA* was no different than that of 35000HP (Figure 26). To determine if the *dksA* mutant was sensitive to serum-mediated killing, a bactericidal assay was performed. 35000HPΔ*dksA* was as resistant to 50% normal human serum as the parent strain (Figure

27); both the parent and the *dksA* mutant were significantly more resistant to serum killing than the serum sensitive *dsrA* mutant, FX517 (Figure 27).
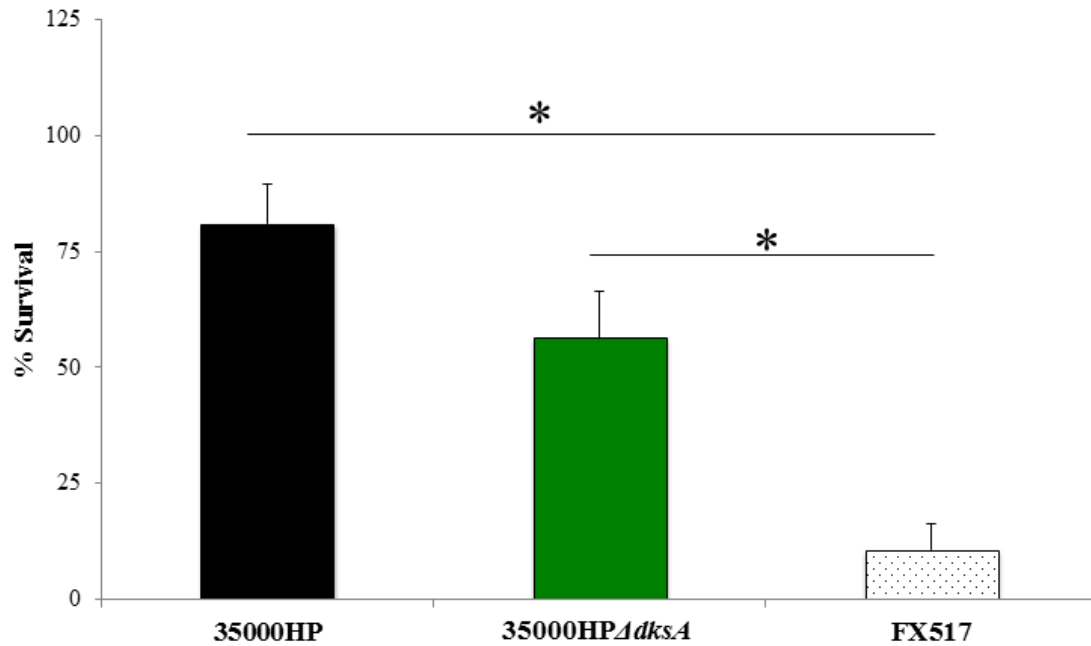
Figure 27. *H. ducreyi* sensitivity to complement-replete human serum. Percent survival of 35000HP, 35000HPΔ*dksA*, and *dsrA* mutant strain FX517 in normal human serum (NHS). Survival was calculated as [(geometric mean CFU in NHS/geometric mean CFU in heat-inactivated NHS) × 100]. Data are means ± SD of five independent experiments. All strains were compared to 35000HP. *, $P \leq 0.05$.

To determine the role of DksA in resistance to phagocytosis, we compared the uptake and intracellular survival of cells collected at mid-log and stationary phase by primary human macrophages. No differences were found in the uptake of the *dksA* mutant harvested at mid-log phase compared to the parent (Figure 28A). However, there was a trend for the *dksA* mutant to be taken up at a higher rate than the parent when the bacteria were harvested at stationary phase ($P = 0.055$).
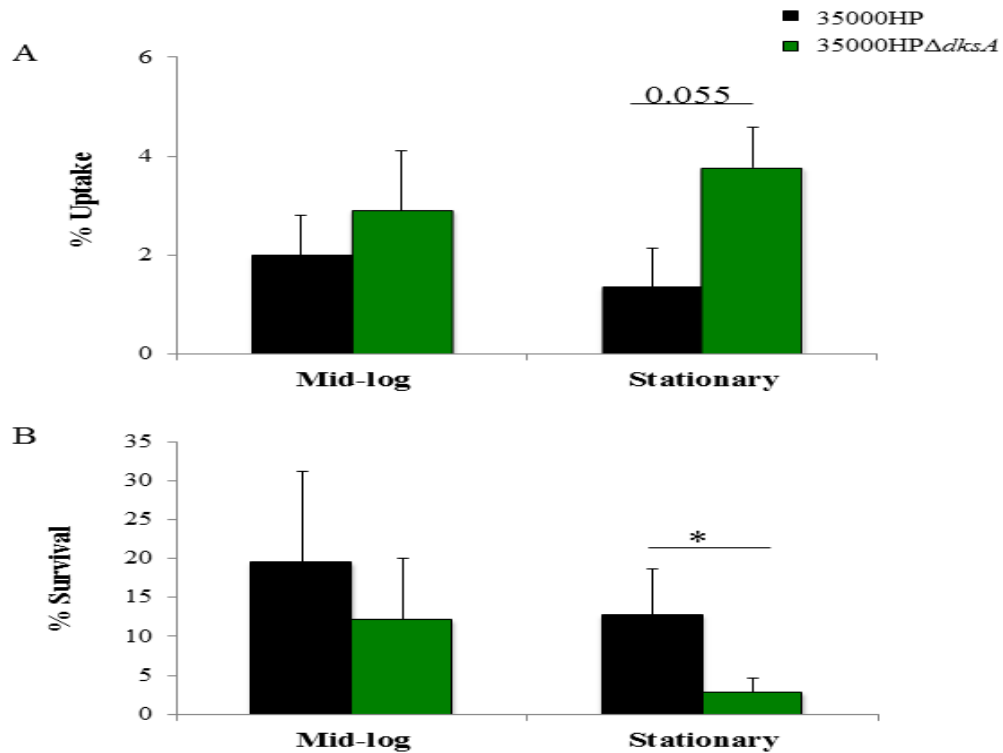
Figure 28. Uptake of *H. ducreyi* by and survival within human macrophages. (A) Percent uptake of 35000HP and 35000HPΔ*dksA* by human macrophages. Primary human CD14+ cells were differentiated into monocyte-derived macrophages (MDM). MDM were infected with opsonized *H. ducreyi* at an MOI of 10:1. After 30 minutes of incubation, gentamicin was added to kill extracellular bacteria. The percent uptake was calculated as [(geometric mean CFU of gentamicin-protected bacteria at 1 hour/ geometric mean CFU of input bacteria) x 100]. Data are mean ± SD from five independent donors. *, P ≤ 0.05. To determine survival, MDMs were incubated an additional 6 hours and bacteria were collected. Survival after uptake was calculated as [(geometric mean CFU of bacteria collected after 6 hours / geometric mean CFU of gentamicin- protected bacteria at 1 hour) x 100]. Data are mean ± SD from 5 independent donors.

No differences were found for the intracellular survival of the mutant compare to the parent harvested at mid-log phase (Figure 28B). However, a significant reduction in the intracellular survival of the *dksA* mutant (*P* = 0.023) was shown for cells harvested at stationary phase. Thus, DksA plays a role in resistance to phagocytosis and intracellular survival for stationary phase cells.
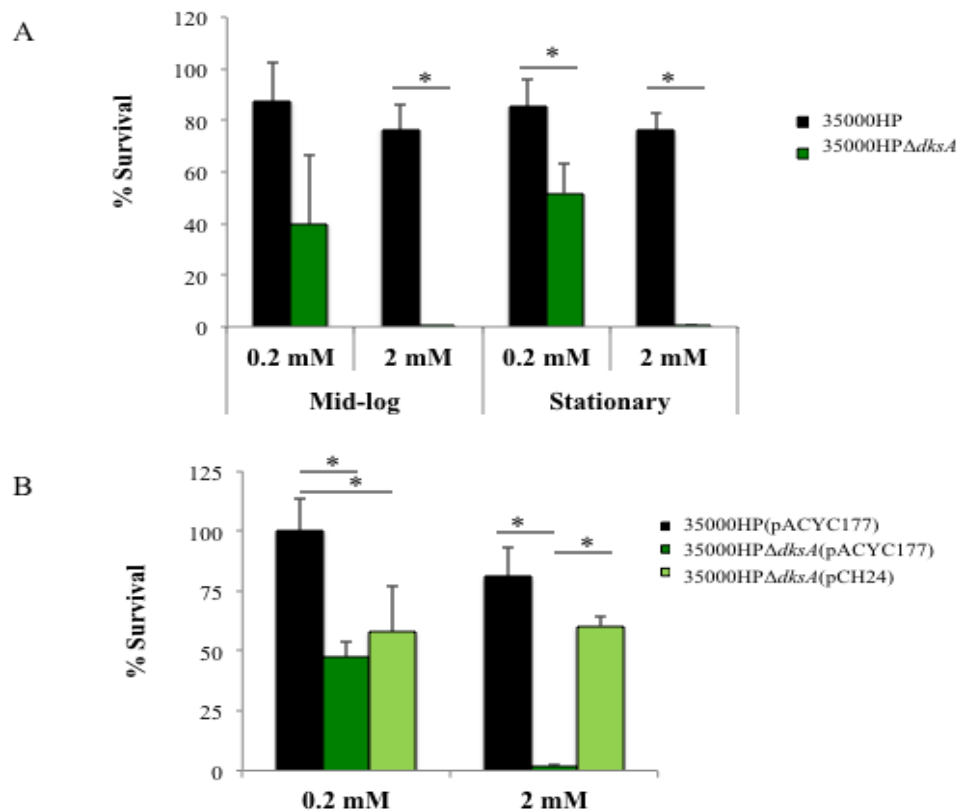
Figure 29. Survival of the *dksA* mutant after oxidative stress. (A) Percent survival of 35000HP and 35000HPΔ*dksA* following incubation with 0.2 mM or 2 mM H₂O₂ for 1 hour. (B) Percent survival of 35000HP (pACYC177), 35000HPΔ*dksA* (pACYC177), and the complemented strain 35000HPΔ*dksA* (pCH24) following incubation with 0.2 mM or 2 mM H₂O₂ for 1 hour. All percent survivals were calculated as [(geometric mean CFU after treatment/ geometric mean before treatment) x 100]. The data are mean ± SD from five independent experiments. *, $P \leq$ 0.05.

The reduced survival of *H. ducreyi* within macrophages is linked to increased sensitivity to oxidative stress (94, 164). We thus compared the survival of 35000HP and 35000HPΔ*dksA* after incubation with hydrogen peroxide. When stationary phase bacteria were incubated with 0.2 mM or 2 mM H₂O₂, the *dksA* mutant survived significantly less than the parent strain (*P*= 0.023 and *P*= 0.0002, respectively) (Figure 29A). For cells

grown to mid-log phase, the *dksA* mutant survived significantly less than the parent at 2 mM H_2O_2 ($P= 0.0005$) with a trend towards significance at 0.2 mM ($P= 0.052$).

To confirm that the increased sensitivity to H_2O_2 seen in the Δ*dksA* mutant was due to deletion of *dksA*, we constructed the *dksA* complement plasmid pCH24. Primers P51/P52 were used to amplify the *dksA* ORF. The fragment was ligated into plasmid pCH31, a plasmid containing a *cat* promoter with NdeI sites for gene insertion. Expression of pCH24 in the *dksA* mutant restored wild type levels of *dksA* (Figure 30). However, as the gene is under control of a constitutive promoter and not its native promoter, any expression that occurs in the complemented strain will be independent of native regulation.
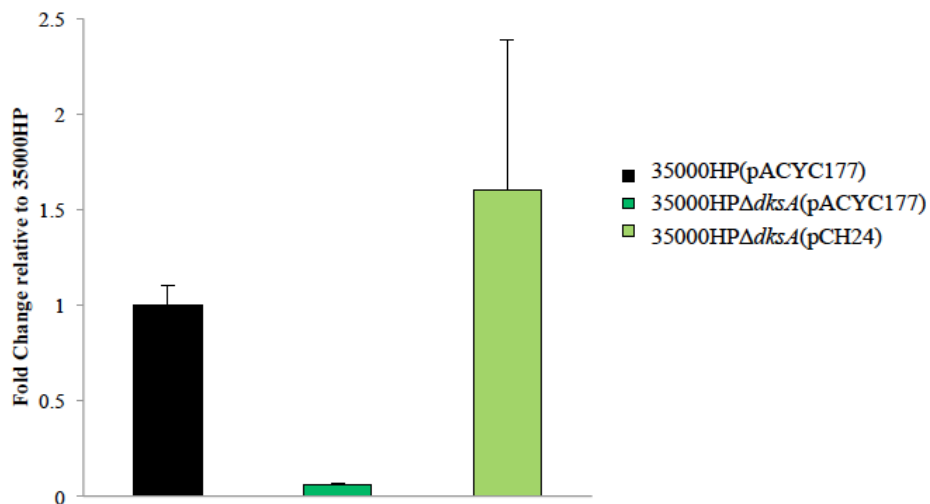
Figure 30. Complementation of the *dksA* mutant by pCH24. qRT-PCR of *dksA* in 35000HP (pACYC177), 35000HPΔ*dksA* (pACYC177), and the complemented strain 35000HPΔ*dksA* (pCH24).

We next used the complemented *dksA* strain in our oxidative sensitivity assay. In cells harvested at mid-log phase, 35000HPΔ*dksA* (pACYC177) survived significantly less well than 35000HP (pACYC177) at both 0.2 ($P = 0.044$) and 2 mM ($P < 0.0001$) (Figure 29B). Complementation of the *dksA* mutant *in trans* with plasmid pCH24 restored resistance to 2 mM H_2O_2 ($P = <0.0001$) but not 0.2 mM (Figure 29B). Therefore, DksA contributes to *H. ducreyi* survival after exposure to H_2O_2.

Adherence to human foreskin fibroblasts mediated by the Flp-Tad operon is associated with virulence in the human challenge model (70, 72). Similarly, a UPEC *dksA* mutant is impaired in its ability to adhere to eukaryotic cells, perhaps due to downregulation of Type 1 fimbriae expression (134). Other studies in *E. coli* and EHEC also indicate that *dksA* mutants tend to have decreased attachment as well as decreased expression of genes involved in the regulation of attachment (163, 165). Therefore, we compared the adherence of 35000HP, 35000HPΔ*dksA*, and 35000HPΔ*flp1-3* to HFF cells at both mid-log and stationary phase. For cells harvested at mid-log phase, the Δ*dksA* mutant attached to HFF cells at significantly lower levels (46.9 ± 9.6 %) than did the parent (116.6 ± 25.2 %) ($P = 0.0004$) but tended to attach to HFF cells better than the Δ*flp1-3* mutant (17.6 ± 10.7 %) ($P= 0.052$) (Figure 31). In cells harvested from stationary phase, both the Δ*dksA* mutant (15.6 ± 8.5 %) and the Δ*flp1-3* mutant (10.7 ± 4.3 %) exhibited significantly reduced attachment compared to the parent strain (95.9 ± 10.2 %) ($P = <0.0001$) (Figure 31).
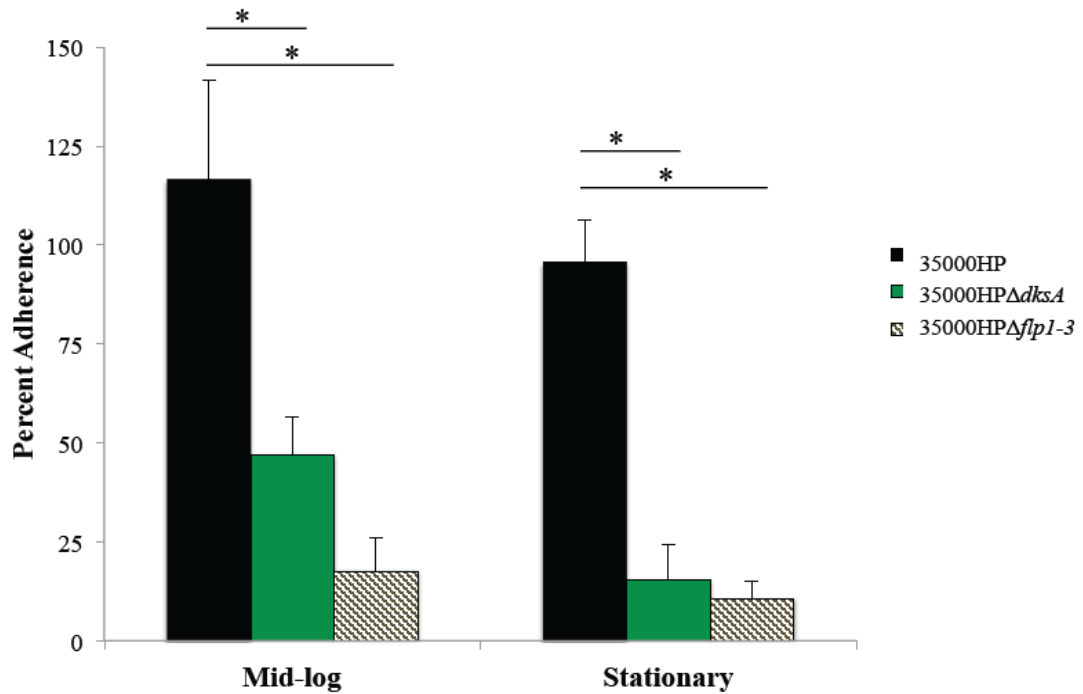
Figure 31. Adherence of the *dksA* mutant to HFF cells. Percent adherence of 35000HP, 35000HPΔ*dksA and* 35000HPΔ*flp1-3* to HFF cells calculated as follows: (geometric mean CFU of HFF-adherent bacteria/geometric mean CFU of initial bacteria added per well) × 100. The data represent the means ± SD from 5 independent experiments. *, $P ≤$ 0.05.

The decreased attachment of the *dksA* mutant could have resulted from decreased secretion of the Flps by the Flp-Tad secretion system, decreased expression of the Flp proteins, or decreased expression of co-factor(s) required for Flp-dependent adherence. Compared to the parent, the transcript levels of *flp1* and *tadA* were unchanged in the *dksA* mutant (data not shown). To determine if the decreased adherence of the *dksA* mutant harvested at stationary phase was a result of decreased expression or altered localization of the Flp proteins, we examined the expression of Flp1/2 in whole cell lysates and outer membranes by Western blot. The *tadA* mutant (35000HP.400) and the *Δflp1-3* mutant were used as controls for the assay. While the *Δflp1-3* mutant expressed no Flp proteins,

the *tadA* mutant expressed the Flps but did not secrete the proteins to the outer membrane. Flp expression in whole cells and outer membranes were comparable between wild type and the *dksA* mutant (Figure 32). Thus, the adherence defect in the *dksA* mutant cannot be attributed to decreased expression or lack of localization of the Flp proteins to the outer membrane, suggesting that DksA regulates the expression of co-factor(s) that are required for Flp-mediated adherence.
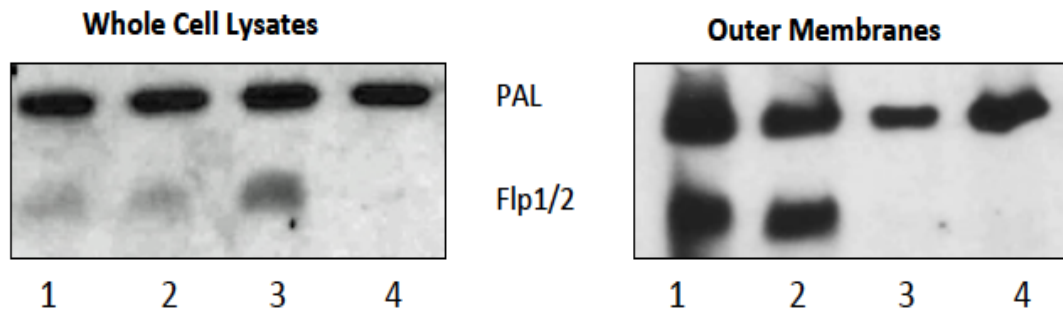
Figure 32. Expression of the Flp1/2 protein in *dksA* mutant OMP and WCL. Lane 1, 35000HP*;* Lane 2, 35000HPΔ*dksA;* Lane 3, 35000HP.400*,* the *tad* mutant; and Lane 4, 35000HPΔ*flp1-3*, the *flp* mutant. Samples were probed with Flp1/2 antibody. MAb 3B9 was used to verify equivalent loading. Data is representative of 4 independent experiments.

Overall, in this chapter we showed that in addition to (p)ppGpp, DksA contributes to the virulence of *Haemophilus ducreyi* in humans and plays an important role in pathogenesis. This study, when taken together with the (p)ppGpp mutant data, underscores the potentially distinct roles DksA and (p)ppGpp play in regulation of *H. ducreyi* virulence. Given the similarities of the two mutants, comparison of the two regulons would help to elucidate the overlapping and independent functions of (p)ppGpp and DksA in *H. ducreyi*. Therefore, we next analyzed the transcriptomes to better understand the intersecting and diverging roles of the two regulators in *H. ducreyi* virulence.

Chapter V:

Loss of (p)ppGpp or DksA dysregulates multiple virulence

determinants as identified by RNA-seq

Loss of *dksA* and (p)ppGpp can have unique, overlapping, and pleiotropic effects on transcription. To better understand their respective contributions to pathogenesis, we next determined the effect of DksA and (p)ppGpp deficiency on gene expression.

DksA and (p)ppGpp deficient transcriptomes significantly overlap at stationary phase. We compared the transcriptomes of 35000HP, 35000HPΔ*dksA* and 35000HPΔ*relA*Δ*spoT*, which is (p)ppGpp°. Four biological replicates were included for each strain harvested at the mid-log, transition, and stationary phases of growth (Figure 33), summing a total of 36 samples.

The percentage of total reads aligned with the reference genome from all strains, growth phase, and replicates range from 82.89- 95.87% (Table 7). We calculated the fold change in the expression of genes in 35000HPΔ*dksA* or 35000HPΔ*relA*Δ*spoT* compared to 35000HP. As described previously, we used a false-discovery rate (FDR) of ≤ 0.1 and a 2-fold change as criteria for differential transcript expression (166). A positive fold change indicates that expression of the gene is higher in the mutant strain while a negative fold change signifies that the expression is higher in the parent strain. All differentially expressed genes identified in this study are listed in Appendix III.
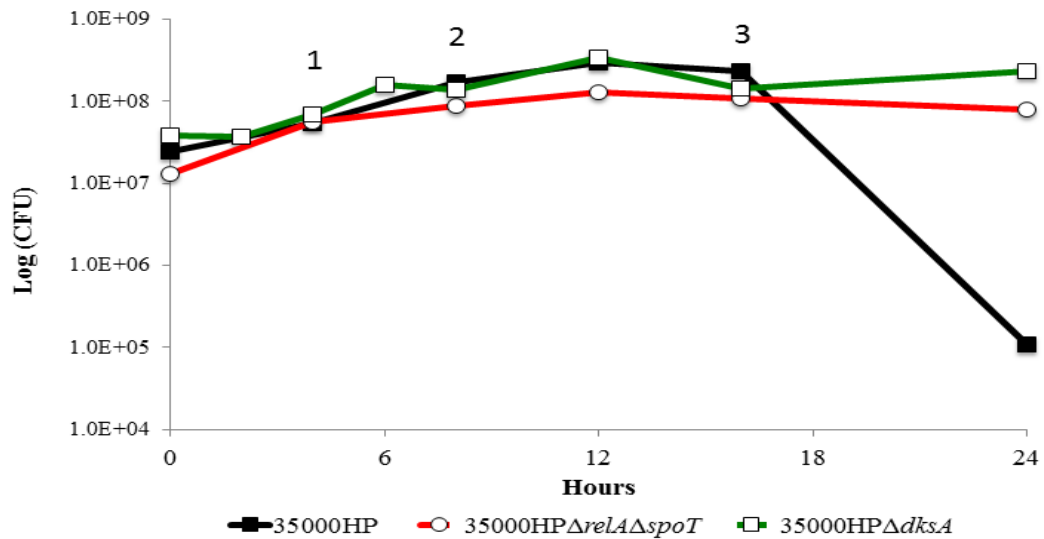
Figure 33. Growth kinetics of 35000HP, 35000HPΔ*relA*Δ*spoT*, and 35000HPΔ*dksA* used for RNA-seq. Growth kinetics determined by measuring the CFU at different time points following inoculation from overnight cultures. 1, 2, and 3 indicate the time points at which bacteria were harvested for transcriptome analysis in the mid-log, transition, and stationary growth phases, respectively.

The *H. ducreyi* genome is comprised of 1758 genes. Comparison of the transcriptomes of the (p)ppGpp° mutant to the parent in mid-log, transition, and stationary phase yielded 149, 107 and 494 differentially expressed genes, respectively; approximately equal numbers of genes were up- and downregulated (Figure 34A). Comparison of the transcriptomes of the *dksA* mutant to the parent in mid-log, transition, and stationary phase yielded 58, 184, and 304 differentially expressed genes, respectively; the majority of genes were upregulated (Figure 34B).

Table 7. Summary of the RNA-seq read statistics

Bacterial Strain	Growth Phase	Biological Replicate	Total Reads	Aligned Reads	% Aligned Reads	% Unaligned Reads
35000HP	Mid-Log	R1	10,301,365	9,429,934	91.54%	8.46%
		R2	8,402,713	7,676,013	91.35%	8.65%
		R3	10,090,817	9,247,646	91.64%	8.36%
		R4	10,093,183	8,918,683	88.36%	11.64%
	Transition	R1	17,841,534	14,788,825	82.89%	17.11%
		R2	12,594,439	11,279,753	89.56%	10.44%
		R3	14,468,362	13,087,351	90.45%	9.55%
		R4	12,585,911	11,724,490	93.16%	6.84%
	Stationary	R1	12,250,624	10,667,706	87.08%	12.92%
		R2	13,022,098	11,743,715	90.18%	9.82%
		R3	11,638,354	10,314,179	88.62%	11.38%
		R4	11,745,737	10,479,877	89.22%	10.78%
35000HP $\Delta relA\Delta spoT$	Mid-Log	R1	10,222,017	9,800,254	95.87%	4.13%
		R2	9,464,896	8,611,107	90.98%	9.02%
		R3	10,980,962	9,854,192	89.74%	10.26%
		R4	10,483,047	9,585,534	91.44%	8.56%
	Transition	R1	15,068,994	13,809,711	91.64%	8.36%
		R2	10,800,119	9,994,775	92.54%	7.46%
		R3	12,098,519	10,852,532	89.70%	10.30%
		R4	10,443,013	9,406,044	90.07%	9.93%
	Stationary	R1	15,008,374	13,617,319	90.73%	9.27%
		R2	10,355,069	9,240,150	89.23%	10.77%
		R3	11,335,796	10,479,164	92.44%	7.56%
		R4	8,205,523	7,542,286	91.92%	8.08%
35000HP $\Delta dksA$	Mid-Log	R1	13,075,344	11,631,470	88.96%	11.04%
		R2	11,369,827	10,089,573	88.74%	11.26%
		R3	15,429,356	14,230,161	92.23%	7.77%
		R4	15,350,792	13,965,504	90.98%	9.02%
	Transition	R1	13,698,233	12,967,727	94.67%	5.33%
		R2	12,114,949	11,048,993	91.20%	8.80%
		R3	10,500,995	9,431,736	89.82%	10.18%
		R4	11,307,711	10,317,164	91.24%	8.76%
	Stationary	R1	13,934,290	12,469,947	89.49%	10.51%
		R2	13,181,478	12,347,374	93.67%	6.33%
		R3	12,793,798	11,909,717	93.09%	6.91%
		R4	13,875,693	12,545,996	90.42%	9.58%
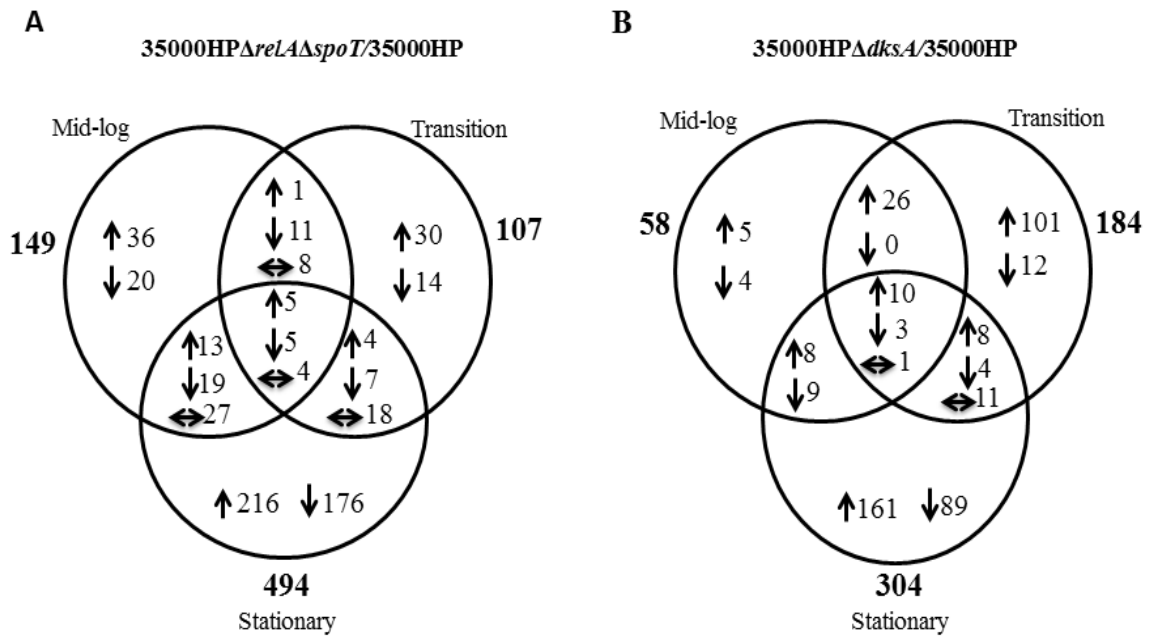
Figure 34. Venn diagram showing the number of genes differentially regulated by (p)ppGpp or DksA deficiency at different phases of growth. (A) 35000HPΔ*relA*Δ*spoT* compared to 35000HP; and (B) 35000HPΔ*dksA* compared to 35000HP. The total number of genes or operons differentially regulated in different phases of growth is indicated in bold outside the Venn diagram. Up (↑) and Down (↓) regulated genes; contra- regulated (←→) in different growth phases.

Comparison of the genes differently regulated by loss of DksA to those differentially regulated by loss of (p)ppGpp in cells harvested from mid-log, transition, and stationary phase yielded 11, 11, and 222 overlapping genes, respectively (Figure 35).
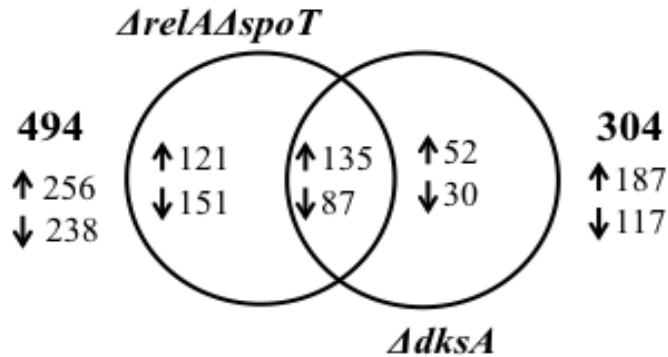
Figure 35. Venn diagram showing the number of differentially regulated genes that overlap between (p)ppGpp and DksA deficiency at stationary phase. 35000HPΔ*relA*Δ*spoT* compared to 35000HP versus 35000HPΔ*dksA* compared to 35000HP. The total number of genes or operons differentially regulated in different phases of growth is indicated in bold outside the Venn diagram. Up (↑) and Down (↓) regulated genes; contra- regulated (←→) in different growth phases.

To identify the overlap of the genes that were differentially regulated by the loss of (p)ppGpp or DksA, we plotted the $\log_{10}$-transformed fold changes in 35000HPΔ*relA*Δ*spoT*/35000HP against 35000HPΔ*dksA*/35000HP. At mid-log and transition phase, (p)ppGpp and *dksA* deficiency primarily altered unique sets of genes while at stationary phase the differentially expressed genes significantly overlapped and were coordinately regulated (Chi-Square = 367.1903; $P < 0.001$) (Figure 35; Figure 36). These data showed that, in stationary phase, (p)ppGpp and DksA deficiency primarily alters expression of similar targets. As (p)ppGpp and DksA primarily respond to nutrient stress, we focused the remainder of our analysis on the stationary phase transcriptomes.
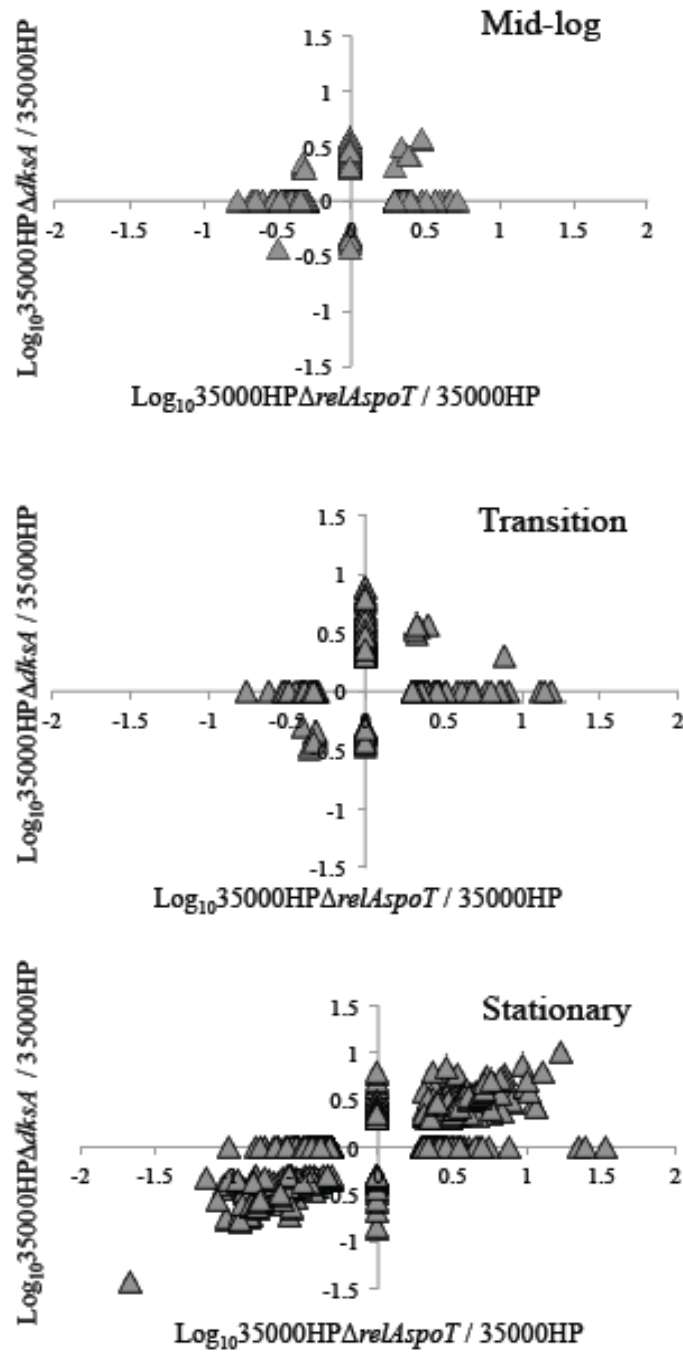
Figure 36. Scatter plots showing fold changes in the expression of genes differentially expressed in 35000HPΔ*relA*Δ*spoT* and 35000HPΔ*dksA* compared to 35000HP. The scatter plots were generated by plotting the $\log_{10}$-transformed fold changes in 35000HPΔ*relA*Δ*spoT* versus 35000HP against 35000HPΔ*dksA* versus 35000HP at different growth phases. Each triangle in the graph indicates a single gene.

We validated selected differentially regulated genes using qRT-PCR. We focused on the (p)ppGpp° mutant transcriptome as it had the largest number of differentially expressed genes. The genes were grouped into 3 categories based on their expression levels (low, medium, and high), grouped into up- and downregulated targets, and further sub-grouped based on their fold change ranges (2.0-fold to 5.0-fold, 5.1-fold to 10.0-fold, and 10.1-fold to 50.0-fold). Representative genes were selected from each category; a total of 15 genes were selected for qRT-PCR validation using primer pairs P59-P94 (Table 2). qRT-PCR analysis confirmed the differential expression of 14/15 genes identified by RNA-Seq (Figure 37A). However, *hfq* expression was 11.67 upregulated by RNA-seq but unchanged (0.97) by qRT-PCR (Figure 37B); the reason for this discrepancy is unclear. In general, the fold changes derived from RNA-Seq were in good agreement with those measured by qRT-PCR ($R^2 = 0.902$).

There were 3 contra-regulated genes, *HD0097, HD0098,* and *HD0931*, identified between the DksA and (p)ppGpp deficient sets of differentially regulated genes at mid-log phase (Figure 35). No other growth phase showed any contra-regulation of genes. To confirm that our RNA-seq method could reliably identify contra-regulated genes, we performed qRT-PCR using primers P95-P98 and P31/P32. We compared fold change of *HD0098* in the (p)ppGpp° and *dksA* mutants. For comparison we also calculated the fold changes of a gene not identified as differentially expressed by (p)ppGpp or DksA deficiency, *menB*, and a gene identified to be downregulated by both regulators, *ompP2A*. qRT-PCR validated the contra-regulation of *HD0098* (Figure 38).

Figure 37. qRT-PCR validation of the RNA-Seq data. (A) Fold change in the expression of target genes in 35000HPΔ*relA*Δ*spoT* relative to 35000HP in stationary phase. The criteria used for selecting the targets for qRT-PCR validation are outlined in the figure. The expression levels of target genes were normalized to that of *dnaE*. The data represent the means ± SD from four independent experiments. (B) Correlation between the fold changes derived from qRT-PCR and RNA-Seq.
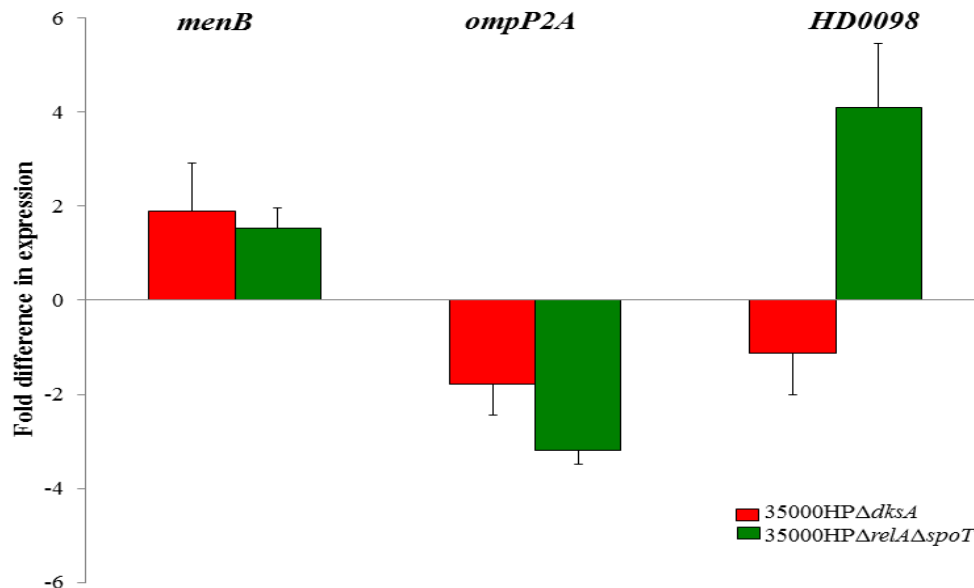
Figure 38. Relative expression levels of selected *H. ducreyi* genes in 35000HPΔ*relA*Δ*spoT* and 35000HPΔ*dksA*. The mid-log phase expression levels of *menB (*unchanged)*, ompP2A* (downregulated)*,* and *HD0098* (contraregulated) were normalized to that of *dnaE*. The data represent the means ± SD of the results of four independent experiments.

Functional classification of genes altered by deficiency of (p)ppGpp° or *dksA*.

Using annotations and pathway information from the sequenced 35000HP genome (Munson, unpublished) and KEGG, the identified differentially expressed genes were classified into multiple functional categories including energy metabolism, biosynthesis, transcription, translation, cell membrane and binding (Table 9). In both mutants, pathway enrichment analysis with annotations from both Biocyc and DAVID bioinformatics resources showed that genes encoding proteins involved in pilus formation, ion transport, oxidative reduction/phosphorylation, carbohydrate transport, and cytochrome complex assembly were enriched (data not shown). The (p)ppGpp° mutant also showed enrichment in genes encoding proteins involved in regulation of transcription and translation.

Table 8. Functional classification of genes differentially regulated by (p)ppGpp or DksA in stationary phase *H. ducreyi*

Parameter	35000HPΔ*relA*Δ*spoT* / 35000HP[a]		35000HPΔ*dksA* / 35000HP[b]	
	Stationary		Stationary	
% Downregulated Genes	52		62	
% Upregulated Genes	48		38	
	Regulation		Regulation	
Functional Categories[c]	Up	Down	Up	Down
Amino acid biosynthesis	2	4	5	1
Amino acid Transport and metabolism	6	6	5	2
Amino Sugar and nucleotide metabolism	4	12	2	7
Cellular carbohydrate biosynthetic process	7	5	3	1
Carbohydrate metabolism	1	2	3	0
Cell division	2	5	1	2
Cell membrane	11	15	9	7
Cellular homeostasis	4	2	2	1
Cellular response to stress	0	2	3	0
DNA binding	3	1	4	2
DNA metabolic process	8	4	8	1
Fatty acid biosynthesis and metabolism	7	3	4	2
Intracellular trafficking and secretion	1	11	1	5
Ion transport	3	7	2	4
Iron sulfur cluster binding	2	6	0	3
Lipid biosynthesis and metabolism	3	4	5	2
Metal ion binding	10	8	7	5
Nucleotide binding	8	19	4	11
Protein fate	7	9	5	5
RNA binding	4	0	1	0
RNA processing	9	8	5	3
Transcription	10	9	2	3
Translation	15	27	12	6
Transport of proteins and carbohydrates	7	11	2	6
Uncharacterized conserved protein	6	10	7	1
Hypothetical proteins	75	89	30	92

[a]Genes differentially expressed in 35000HPΔ*relA*Δ*spoT* versus 35000HP at stationary phase.
[b]Genes differentially expressed in 35000HPΔ*dksA* versus 35000HP at stationary phase.

(p)ppGpp° and *dksA* deficiency leads to dysregulation of virulence determinants required for human infection. Since both the *dksA* and (p)ppGpp° mutants were partially attenuated in humans, we determined the effect their deficiency on the expression of genes required for human infection. (p)ppGpp deficiency in 35000HP resulted in decreased expression of genes in the *flp-tad* operon, the *lspB-lspA2* operon, *lspA1*, *hgbA*, and *csrA*, which are all required for pustule formation in humans (Table 9) (47, 70, 94). Loss of (p)ppGpp increased the expression of *fgbA*, which is required for virulence (47). These data are consistent with the partial attenuation and some phenotypes of the (p)ppGpp° mutant reported previously (164). Deletion of (p)ppGpp downregulated expression of *cdtC* and upregulated expression of *OmpP2B, sodC, momp, lst, ftpA, neuA, pea,* and *cpxR,* all of which are dispensable for human infection (Table 9). The upregulation of expression of *ompP2B* is consistent with our previous findings that deletion of *relA spoT* resulted in increased expression of the OmpP2B protein in purified outer membranes (164).

DksA deficiency resulted in decreased expression of *flp3, hgbA,* and *lspB*, which would favor decreased virulence (Table 9, Appendix III) (47). The *dksA* mutant also had increased expression of *hfq, dltA*, and *spoT,* which would favor increased virulence (70, 93, 164). Additionally, deletion of DksA altered expression of genes not required for virulence. Genes encoding membrane proteins *ompP2B, momp, and ompP4,* as well as *cdtC, ftpA, cpxR* and a phosphoethanoloamine transferase are all differentially expression in the deletion mutant. These results suggest that the partial attenuation of the *dksA* mutant might also be due to conflicting phenotypes.

Table 9. Expression of genes tested for virulence in humans altered by deficiency of (p)ppGpp or DksA

Gene(s)[a]	Function	35000HP/ 35000HPΔ*relA*Δ*spoT*[bc]	35000HP/ 35000HPΔ*dksA*[bd]
Fully attenuated			
flp1-flp2-flp3	Adherence and microcolony formation	-8.91	-2.33
dsrA	Major role in serum resistance	–[e]	–
lspA1, *lspA2*	Escape from phagocytosis	-5.07	–
ncaA	Collagen binding	–	–
tadA	Adherence and microcolony	-6.86	–
hgbA	Heme and/or iron uptake	-2.54	-2.37
pal	Outer membrane stability	–	–
hfq	RNA binding chaperone	11.67	2.64
sapB-sapC	Resistance to antimicrobial peptides	–	–
cpxA	Two component sensor kinase	–	–
Partially			
dltA	Partial role in serum resistance	–	4.98
wecA	Initiates synthesis of putative glycoconjugate	–	–
luxS	Quorum Sensing	–	–
fgbA	Fibrinogen binding	2.04	–
sapA	Resistance to antimicrobial peptides	–	–
csrA	Posttranscriptional regulation	-2.34	–
dksA	DnaK repressor; (p)ppGpp co-factor	–	NA
relA,spoT	(p)ppGpp synthetase and hydrolase; stringent response	NA	2.09
Virulent			
hhdB[f]	Lysis of fibroblasts	–	–
ompP2A, *ompP2B*	Encode classical trimeric porins	10.28	3.93
sodC	Detoxifies ROS[g]	2.40	–
momp	OmpA homolog; minor role in fibronectin binding	2.81	2.43
losB	Extends LOS[h] beyond KDO[i]-triheptose-glucose	–	–
lst	Adds sialic acid to LOS	2.83	–
cdtC[f]	Toxic for T cells, epithelial cells, and fibroblasts	-2.93	-2.47
ftpA	Pilus	7.79	3.03
tdX/tdhA	Heme uptake	–	–
glu	Adds glucose to KDO-triheptose	–	–
ompP4	Outer membrane lipoprotein	–	2.32
cpxR	Two Component Response	7.19	5.89
neuA	Enables sialic acid addition to LOS	2.74	–
pea	Phosphoethanolamine transferases	2.98	2.04

[a]Strains with mutated genes that have been tested in human volunteers and classified as attenuated, partially attenuated, or virulent.

[b]Fold change of first gene is shown for multi-gene mutants

[c]Fold change on 35000HPΔ*relA*Δ*spoT* relative to 35000HP in

[d]Fold change on 35000HPΔ*dksA* relative to 35000HP in stationary

[e]–, no change in expression.

[f]*hhdB cdtC* double mutant is also virulent in humans.

[g]ROS, reactive oxygen species.

[h]LOS, lipooligosaccharide.

[i]KDO, 2-keto-3-deoyoctulosonic acid.

The set of transcripts altered by (p)ppGpp deficiency significantly overlaps with the sets of transcripts controlled by Hfq and CpxRA. Hfq is a major regulator of *H. ducreyi* stationary phase gene expression and contributes to the positive regulation of virulence determinants such as LspB, DsrA, and Flp1 (93). Given that both mutants upregulated *hfq* (Table 9) and given the discrepancy in the *hfq* expression levels determined by different methods for the (p)ppGpp° mutant, we determined if the transcriptomes of the (p)ppGpp° and DksA mutants significantly overlapped with that of the *hfq* mutant (93). The transcriptomes of the (p)ppGpp° and the *hfq* mutants were negatively correlated and overlapped significantly (Chi-Square = 38.172; *P* < 0.001), while that of the *dksA* mutant did not. Thus, it is likely that (p)ppGpp deficiency results in upregulation of *hfq* transcription.

(p)ppGpp and DksA deficiency resulted in 7.19- and 5.89-fold upregulation of *cpxR*, respectively (Table 9). We therefore compared the effects of *dksA* and (p)ppGpp deficiencies on transcription to those produced by activation of CpxRA, defined as the transcription effects of a CpxR activating mutant compared to a *cpxR* deficient mutant in stationary phase (166). The differentially expressed genes in *dksA* mutant did not overlap with those of CpxRA. The effects of (p)ppGpp deficiency positively correlated and significantly overlapped with effects of activation of CpxRA (Chi-Square = 17.070; *P* < 0.001). Since activation of the CpxRA system is associated with loss of virulence, these results were consistent with the partial attenuation of the (p)ppGpp° mutant (164).

Differential Expression of *H. ducreyi* putative small RNAs. In *E. coli* and other bacteria, Hfq is crucial for function of small RNAs (sRNAs) (167). sRNAs are non-protein coding RNAs involved in cell regulatory functions. sRNAs integrate environmental stress signals and regulate a plethora of stress responses. *Trans*-encoded regulatory RNAs usually require Hfq as a cofactor to facilitate the interaction between sRNAs and their target mRNAs (168, 169). RelA was shown to increase Hfq binding to low affinity small RNA targets in *E. coli* (122). In *Salmonella enterica* serovar Typhimurium*,* (p)ppGpp is required for expression of 100 known and putative sRNAs (170). In *Rhizobium etli,* activation of the stringent response was implicated in the expression of 33 sRNAs (171). We previously identified ten putative *H. ducreyi* small RNAs potentially regulated by Hfq ((93); unpublished). Given the significant overlap between the (p)ppGpp regulated genes and Hfq targets, we further analyzed to determine if loss of (p)ppGpp or DksA affected expression of these small RNAs.

At stationary phase, we found that (p)ppGpp deficiency altered expression of 9 of the 10 putative small RNAs while DksA deficiency altered expression of 2 of the small RNAs (Table 10). These results correlate with the regulon overlap data. The significant overlap of the (p)ppGpp regulon with the Hfq regulon as well as the highly upregulated levels of *hfq* in the 35000HPΔ*relA*Δ*spoT* mutant hint at an interplay of Hfq and (p)ppGpp in *H. ducreyi.*

Table 10. Putative *H. ducreyi* small regulatory RNAs differentially expressed by (p)ppGpp or DksA deficiency

ID	Length (nt)	Flanking Gene Left	Flanking Gene Right	Rfam Annotation	Family description or	35000HP/ 35000HPΔ*relA*Δ*spoT* Mid-Log	Transit-ion	Stationary	35000HP/ 35000HPΔ*dksA* Mid-Log	Transit-ion	Stationary
HDsRNA01	359	*HD0084*	*HD0085*	RF00023	tmRNA/SsrA			-6.28			
HDsRNA02	139	*HD0953*	*HD0954*		Unique to *H. ducreyi*		-2.48	-7.08			-4.01
HDsRNA03	165	*HD1000*	*HD1001*	RF00013	6S RNA/SsrS			-6.78			
HDsRNA04	174	*HD1027*	*HD1028*	RF00022	GcvB	-3.33	-4.17	-12.04		-2.77	
HDsRNA05	134	*glpC*	*ribD*	RF00050	FMN riboswitch						
HDsRNA06	223	*HD1171*	*HD1172*		Unique to *H. ducreyi*			3.52			
HDsRNA07	194	*HD1226*	*HD1227*	RF00168	Lysine riboswitch			7.96			3.92
HDsRNA08	97	*hhdA*	*HD1328*	RF00169	Bacterial small RNA SRP/Ffs			2.26		-2.29	
HDsRNA09	410	*HD1622*	*HD1623*	RF00010	RnpB			-11.16			
HDsRNA10	183	*HD1765*	*HD1766*		Unique to *H. ducreyi*			3.47		-2.66	

103

The (p)ppGpp and DksA mutants are defective in adherence to human fibroblasts by different mechanisms. The *flp-tad* operon is composed of a Tad secretion system that secretes the fimbria-like proteins Flp1-3, which mediate the adherence of the bacterium to HFF cells and are associated with virulence (69). The *flp-tad* operon was downregulated approximately 12-fold in the (p)ppGpp° mutant; only *flp3* was downregulated 2-fold in the *dksA* mutant (Table 9; Appendix III). We compared the adherence of 35000HP, 35000HP*ΔdksA*, 35000HP*ΔrelAΔspoT* and 35000HP*Δflp1-3* collected at stationary phase to HFF cells. The *Δflp1-3* mutant served as a negative control for the assay. As expected, both the (p)ppGpp° (66.7 ± 9.5 %) and *Δflp1-3* mutant (4.6 ± 1.6 %) mutant exhibited reduced attachment compared to the parent (115.8 ± 21.5 %) (*P*= 0.0002 and *P*= < 0.0001, respectively) (Figure 39A). Surprisingly, the *dksA* mutant attached to HFF cells at significantly lower levels (15.9 ± 5.2 %) than the parent *P* = <0.0001) and the *ΔrelAΔspoT* mutant (P= .019 and at levels that were not significantly different than the *Δflp1-3* mutant (Figure 39A). Thus, the *dksA* mutant was more impaired than the (p)ppGpp° mutant in attachment to HFF cells.

The decreased attachment of the (p)ppGpp° mutant likely resulted from decreased expression of the Flp proteins. We probed whole cell lysates of the (p)ppGpp° and *dksA* mutants with a Flp1/2 antisera by Western blot. The *tadA* and *dksA* mutants and the *Δflp1-3* mutant were used as controls for the assay. As expected, the *tadA* mutant expressed the Flp proteins in whole cell lysates while the *Δflp1-3* mutant did not (Figure 39B). Unlike the *dksA* mutant, compared to the wild type, the (p)ppGpp° mutant expressed reduced levels of the Flp proteins (Figure 39B). Thus, the adherence defect in the (p)ppGpp° mutant could be attributed to decreased expression of the Flp proteins. As

is shown in Figure 32B, the *dksA* mutant expressed wild type levels of the Flp proteins in both whole cell lysates and outer membranes; the adherence defect of the *dksA* mutant could not be attributed to decreased expression or altered localization of the Flp proteins. These data suggest that the adherence defect of the mutants resulted from different mechanisms.
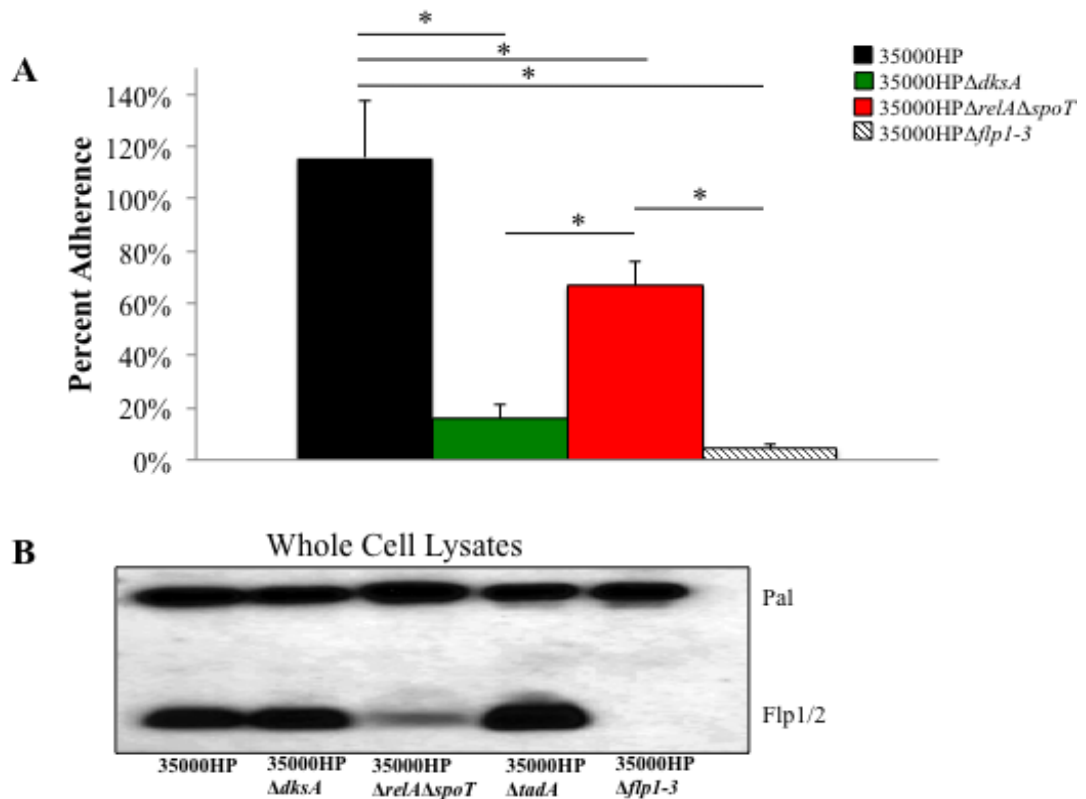
Figure 39. Adherence of the *dksA* and *relA spoT* mutants to HFF cells and Flp protein expression. (A) Percent adherence of 35000HP, 35000HPΔ*dksA*, 35000HPΔr*elA*Δ*spoT* and 35000HPΔ*flp1-3* to HFF cells calculated as follows: (geometric mean CFU of HFF-adherent bacteria/geometric mean CFU of initial bacteria added per well) × 100. The data represent the means ± SD from 5 independent experiments. *, P ≤ 0.05. (B) Western blot analysis of whole cell lysates analyzed by SDS-PAGE. Samples were probed with Flp1/2 antibody. The anti-PAL MAb 3B9 was used to verify equivalent loading. Data are representative of 4 independent experiments.

Here, we defined genes whose expression is altered by (p)ppGpp and DksA deficiency in *H. ducreyi*. In summary, we provided evidence that in *H. ducreyi*, (p)ppGpp and DksA primarily coordinate regulation of gene expression in stationary phase. We also demonstrated that (p)ppGpp and DksA control some unique targets highlighting their independent functions in bacterial gene regulation.

Chapter VI:

Discussion

Here we showed that *H. ducreyi* Δ*relA*Δ*spoT* and Δ*dksA* mutant were partially attenuated for virulence in human volunteers, indicating that the stringent response plays an important role in *H. ducreyi* pathogenesis. A summary of phenotypes regulated by (p)ppGpp or DksA are depicted in Figure 40. We provided evidence that (p)ppGpp and DksA likely contribute to regulation of gene expression in stationary phase. Taken together, our study suggests an important role for (p)ppGpp and DksA in controlling *H. ducreyi* stationary phase and virulence gene expression.

For those bacterial species that contain stringent response homologs, insight into the *in vivo* significance of the stringent response has been pursued by conducting studies in small mammals and extrapolating findings to human infection. We have the ability to determine the *in vivo* significance of bacterial pathogen in humans. Our study offers the unique opportunity to examine the effect of the stringent response in bacterial virulence within the human host. To our knowledge, this was the first study that evaluated (p)ppGpp and DksA in the context of a human infection.

Contribution of (p)ppGpp to *H. ducreyi* virulence

We constructed a *relA* deletion mutant and a *relA spoT* double mutant in *H. ducreyi* but were unable to recover a *spoT* deletion mutant. In other organisms, expression of a (p)ppGpp synthase in the absence of a hydrolase leads to growth arrest and cell death; therefore, for many species, *spoT* is considered an essential gene (138, 153). In a radiolabeling-based *de novo* (p)ppGpp synthesis assay, both the *H. ducreyi* *relA* and *relA spoT* mutants were unable to synthesize (p)ppGpp. As there is no defined media available for *H. ducreyi,* one limitation of our study data is that we did not evaluate (p)ppGpp synthesis in response to nutrient stress. Nutrient limitation is usually used to enhance the synthetase activity of these enzymes. Given that deletion of *relA* alone was sufficient to abolish the ability of *H. ducreyi* to synthesize (p)ppGpp and that we were not able to construct a *spoT* mutant in the presence of *relA*, these data suggest that RelA is likely the primary (p)ppGpp synthetase and that SpoT is likely the primary (p)ppGpp hydrolase in *H. ducreyi*.
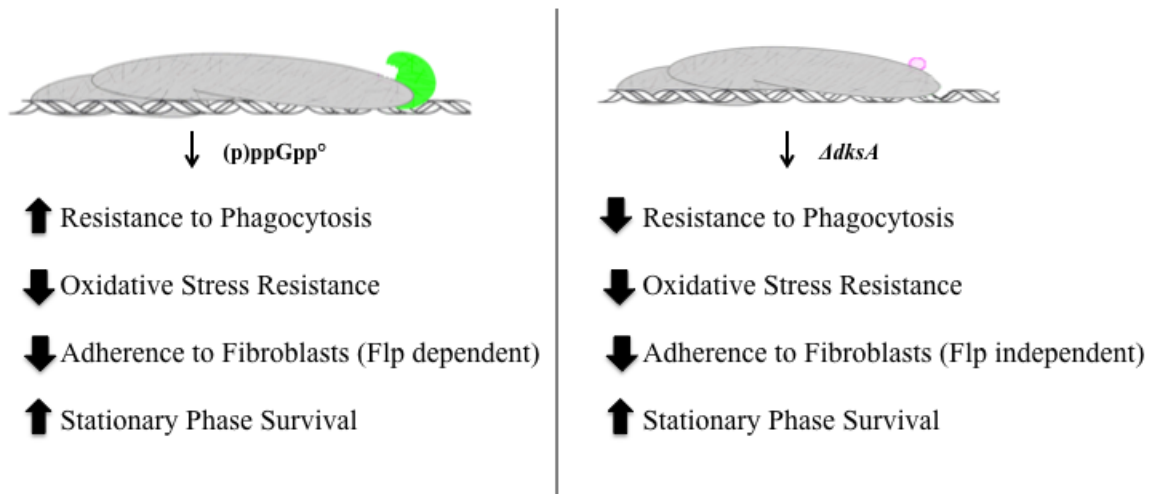
Figure 40. Model of phenotypes altered by (p)ppGpp or DksA deficiency. Top: Diagram of the stringent response system. (p)ppGpp is synthesized by two parallel pathways. After synthesis, (p)ppGpp then interacts with DksA and RNAP to drive transcription in favor or survival. Bottom: Phenotypes associated with either (p)ppGpp deficiency (left) or DksA deficiency (right). Adapted from Figure 1.

Human volunteers formed pustules at a significantly lower rate in response to the *relA spoT* double mutant compared to the parent strain; therefore, the double mutant met the criteria for partial attenuation in the model (47). Since OmpP2B is not required for pustule formation in humans (172), the increased expression of OmpP2B by the mutant likely had no effect on its virulence. The increased sensitivity to oxidative stress and growth phase dependent reduction in the expression of DsrA favor attenuation of the mutant. However, the decreased uptake by macrophages and the increased longevity of the mutant in stationary phase favor virulence. DksA overexpression may phenotypically compensate for the loss of (p)ppGpp in a (p)ppGpp^0 mutant in *E. coli* (134). Thus, increased *dksA* expression may have partially compensated for the loss of (p)ppGpp in the mutant and contributed to the partial attenuation of the mutant *in vivo.*

Contribution of DksA to virulence

In *E. coli*, DksA is a transcription factor that acts by binding directly to the RNAP and amplifies the effects of (p)ppGpp to enhance the stringent response. In addition to its critical role in the stringent response, DksA can interact with RNAP and regulate gene transcription independently of (p)ppGpp expression. The rate of pustule formation in response to the *dksA* mutant was significantly lower than to he isogenic parent strain in human volunteers; the *dksA* mutant met the criteria for partial attenuation in the model (47). Similarly, a *dksA* deletion mutant of *Salmonella enterica* serovar Typhimurium is attenuated in both chick and murine models of infection (133, 173, 174).

The ability of *H. ducreyi* to attach to human foreskin fibroblasts has also been correlated with virulence, and the *dksA* mutant showed decreased attachment to HFF cells compared to the parent. Similarly, studies in pathogenic and nonpathogenic bacteria show that *dksA* mutants tend to have decreased attachment to eukaryotic cells as well as decreased expression of genes involved in the regulation of attachment (134, 163, 165). We found no evidence for decreased expression or altered localization of the Flp proteins in the *dksA* mutant. Taken together, these data suggest that DksA affects adherence to HFF cells through another mechanism, such as regulating one or more yet-to-be defined co-factors that are required for Flp-mediated adherence.

Regulation of *H. ducreyi* genes by stringent response mediators

In cells harvested from stationary phase, loss of (p)ppGpp and *dksA* led to differential expression of 28% and 17% of the *H. ducreyi* open reading frames, respectively. We found that many of the differentially regulated genes identified in our study have been previously associated with the stringent response (158, 163). (p)ppGpp and DksA deficiency in *H. ducreyi* resulted in altered expression of genes involved in transcription, translation, biosynthesis of macromolecules, and energy metabolism. Functional pathways enriched in the differentially expressed genes are depicted in Figure 41. This is consistent with findings in *E. coli* that the (p)ppGpp/DksA system regulates genes necessary for adaptation to nutritional stress (134, 158, 163). Comparison of the sets of genes differentially expressed by the (p)ppGpp° and *dksA* mutants in stationary phase showed a significant overlap. This data indicated that, in stationary phase, the genes affected by lack of (p)ppGpp and DksA in *H. ducreyi* are highly co-regulated. As the majority of genes altered by (p)ppGpp and DksA deficiency were identified in stationary phase, this data also indicates that these two regulators may play roles in stationary phase gene regulation.

(p)ppGpp deficiency	DksA deficiency
Functional Pathways Altered	**Functional Pathways Altered**
Pilus formation	Pilus formation
Ion transport	Ion transport
Oxidative reduction/phosphorylation	Oxidative reduction/phosphorylation
Carbohydrate transport	Carbohydrate transport
Cytochrome complex assembly	Cytochrome complex assembly
Regulation of transcription	Iron Sulfur Clusters
Regulation of translation	

Figure 41. Model of functional pathways altered by (p)ppGpp or DksA deficiency. Enriched Pathways associated with either (p)ppGpp deficiency (left) or DksA deficiency (right). Adapted from Figure 1.

Regulation of stringent response is one of the well-established roles of (p)ppGpp and DksA. In response to nutrient stress, (p)ppGpp controls stringent response by a trade-off wherein the RNAP is redistributed from replicating activities to maintenance and repair (175, 176). An alternative theory argues that (p)ppGpp and DksA induce programmed cell death upon growth arrest by regulating a chromosomally located toxin-antitoxin locus (176, 177). Despite entering stationary phase earlier, both the (p)ppGpp and DksA mutants survived longer than the wild-type strain in stationary phase. To our knowledge, this is the first study reporting the increased longevity of a bacterial pathogen upon deletion of (p)ppGpp and DksA. These data suggest that (p)ppGpp and DksA deficiency could fail to trigger programmed cell death during stationary phase in *H. ducreyi.*

Summary

Both the *dksA* mutant and (p)ppGpp° mutant were partially attenuated for pustule formation in human volunteers. While inoculation with the (p)ppGpp° mutant resulted in papules whose sizes were not significantly different than the parent, the *dksA* mutant caused significantly smaller papules than the parent. Although we have not compared the two mutants directly in human volunteers, the data suggest that the DksA and (p)ppGpp might have different effects on virulence. The *dksA* mutant was taken up more readily than the parent by macrophages while the (p)ppGpp° mutant was phagocytized less readily than the parent. Both the *dksA* mutant and the (p)ppGpp° mutant exhibited increased sensitivity to oxidative stress. This increased sensitivity could be linked to decreased survival within macrophages seen in both the *dksA* and (p)ppGpp° mutants. Both the *dksA* mutant and the (p)ppGpp° mutant exhibited decreased attachment to HFF cells; however, the decreased attachment likely resulted from different mechanisms. Taken together, the data suggest that DksA and (p)ppGpp have both distinct and overlapping functions.

There is a strong possibility that (p)ppGpp and DksA mutually compensate for one another *in vivo*. As depicted in Figure 40, absence of (p)ppGpp does not preclude interaction of DksA with RNAP; the reverse is also true. Additionally, (p)ppGpp and DksA deficiency result in alteration of similar genes and functional pathways (Figure 41). It is therefore difficult to ascertain the primary cause of a particular phenotype: deletion of the mediator or compensation by its partner.

One limitation of our study is that we only examined the mutants for a limited number of phenotypes that are usually associated with the virulence of *H. ducreyi* in

human volunteers. Given the pleiotropic effects of (p)ppGpp and DksA deficiencies on gene transcription, it is likely that other factors played a role in the attenuation of the mutants. Nevertheless, our findings suggest important role for (p)ppGpp and DksA in *H. ducreyi* virulence in humans. Our findings also highlight the underappreciated roles of (p)ppGpp and DksA in regulating phenotypes associated with stationary phase.

Another limitation of our study is that we did not define the (p)ppGpp transcriptome in response to nutrient stress. Recent studies, however, have demonstrated the importance of basal levels of (p)ppGpp in regulation of genes and metabolic processes in absence of a stringent response (178-180). Therefore, despite lack of induction of a stringent response, our study is highly relevant to defining the effect of (p)ppGpp deficiency on virulence of *H. ducreyi*. As DksA functions independently of (p)ppGpp and is not known to respond to any defined stresses, defining the DksA deficient transcriptome is a valid method of identifying DksA-dependent differentially regulated genes.

Based on our *in vitro* and transcriptome data presented in this thesis, we have shown a potential role for the stringent response in *H ducreyi.* Using some extrapolations from both *H. ducreyi* and *E. coli* literature, we propose a stringent response model in *H. ducreyi* in Figure 42. In *H. ducreyi,* stringent response activation will lead to upregulation of genes involved in amino acid biosynthesis, proteolysis and nutrient transport. Upregulation of these particular functional categories will increase amino acid availability and external nutrient acquisition. Simultaneously, genes that code ribosomal proteins and elongation factors are downregulated along with genes involved in fatty

acid, lipid and protein synthesis. The ultimate goal is to inhibit cell division until nutrients become available.

In addition to genes directly involved in nutrient synthesis, the stringent response upregulates expression of stasis survival genes and universal stress proteins although it appears to downregulate the alternative sigma factor, *rpoE*. *rpoE* upregulates genes involved in envelope maintenance and repair as well as *rpoH*, which upregulates heat shock proteins and chaperones. By upregulating universal stress proteins, the stringent response is utilizing multiple mechanisms to address a potentially lethal condition. In *H. ducreyi*, *rpoE* upregulates CpxRA and Hfq. As stated previously, Hfq and CpxRA regulate virulence determinants such as LspA1 and DsrA; Hfq upregulates their expression, while CpxRA downregulates these targets. *cpxR* and *hfq* are upregulated in both the (p)ppGpp and DksA deficient mutants suggesting that they may be inhibited by the stringent response.

sRNAs can be used to regulate metabolic processes in bacteria. In *S. Typhimurium*, a large percentage of the (p)ppGpp-dependent sRNAs were directly involved in nutrient acquisition or synthesis. The stringent response in *H. ducreyi* may or may not directly regulate expression of putative sRNAs. It is possible that the altered regulation of sRNAs in the deficient mutants is indirect and mediated by Hfq.

Nutrient stress likely leads to translation blocks that may result in the synthesis of truncated or misfolded proteins. For this reason, the stringent response may be involved in an integrated stress response network in *H. ducreyi* that involves multiple systems. The final outcome of this interplay, as depicted in Figure 42, is unclear. It will be interesting

to continue determining how *H. ducreyi* utilizes this complicated network of stress components for virulence.

In summary, we show that DksA and (p)ppGpp likely serve as major contributors of virulence and stationary phase gene regulation in *H. ducreyi*. We also show that, despite similar gene expression patterns, the *dksA* and (p)ppGpp° mutants are phenotypically distinct. Future studies will focus on identifying (p)ppGpp and/or DksA-dependent proteins to better understand the unique intersecting and diverging roles the two regulators play in *H. ducreyi* virulence.
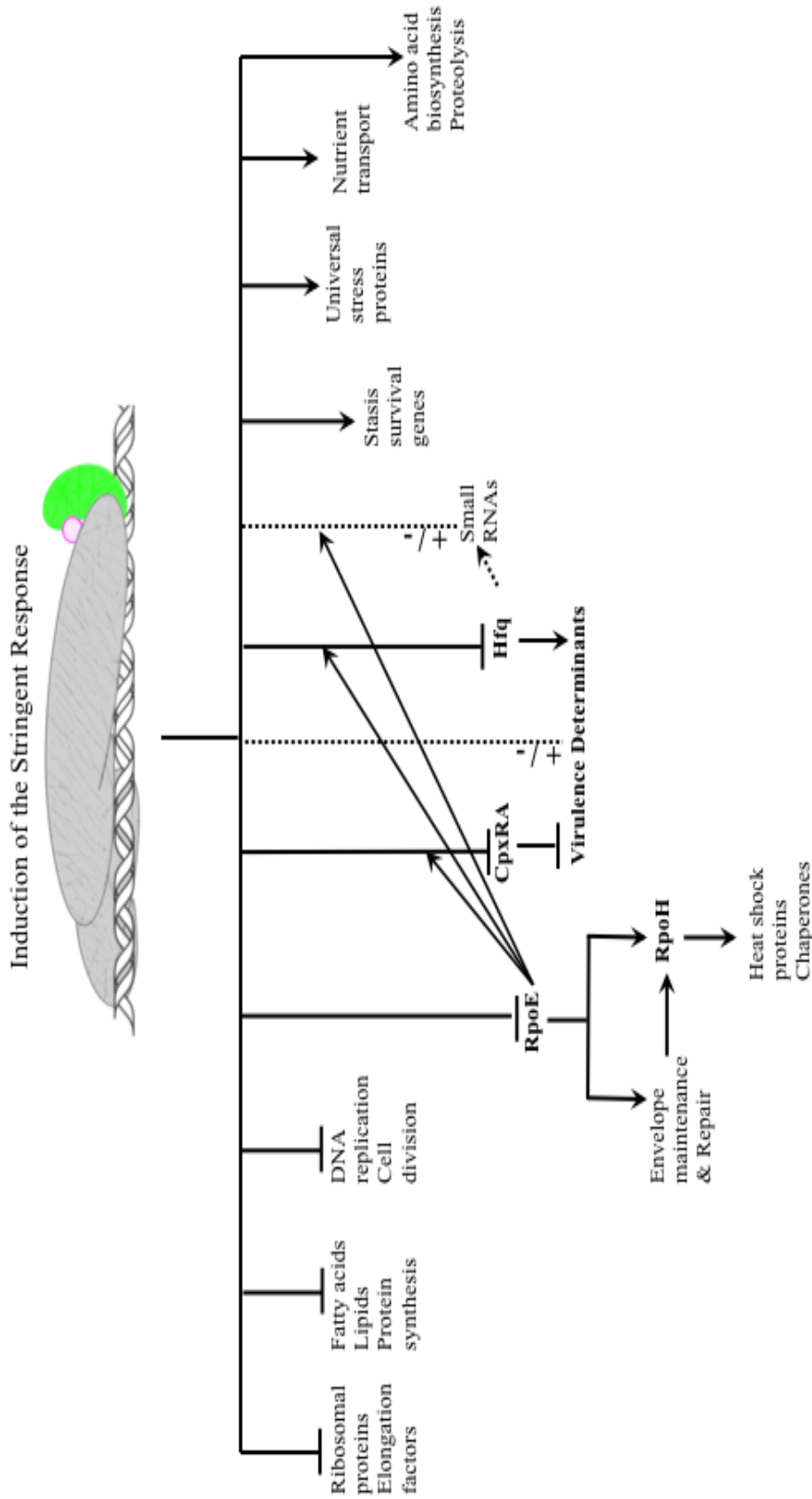
Figure 42. Proposed model of the stringent response in *H. ducreyi*. Through interactions with RNAP, (p)ppGpp (pink circle) and DksA (green) alter gene transcription (blunt ends indicate inhibition; arrows indicate stimulation;+/- denotes both inhibition and stimulation; dotted lines indicate unverified direct action). In addition to directly affecting several functional categories of genes, (p)ppGpp and DksA likely regulate other stress response regulators in *H. ducreyi*. Adapted from Figure 1.

Chapter VII:

Future Directions

The data presented in this thesis add a critical level of detail to the study of (p)ppGpp and DksA in direct virulence of a human pathogen, which was previously lacking in the field. Prior to this study, researchers had not examined the intricate role the stringent response plays in direct regulation of virulence genes required for human infection. By detailing the mechanisms by which (p)ppGpp and DksA affect virulence, we have added an important element to the bacterial pathogenesis field.

Identification of an *in vitro* trigger for stringent response in *H. ducreyi*

Although there has been a substantial body of work published detailing natural induction of the stringent response in other organisms, it is important to determine how the stringent response is induced in *H. ducreyi*. Traditionally, culturing bacteria in minimal media lacking one or more key nutrients such as serine induces the stringent response. The minimal media allows supplementation with nutrients in case species-specific auxotrophies are discovered. In the absence of minimal medium, many investigators utilize drug treatments to mimic nutrient deprivation.

To find a natural trigger of *H. ducreyi*, we will take advantage of chemical induction to identify stringent response triggers. Using one of the chemical mimics described below, we will first measure *de novo* synthesis of (p)ppGpp in wild type harvested from mid-log phase bacteria. We did not see large amount of *de novo* (p)ppGpp

production in mid-log phase 35000HP. Thus, we will use untreated mid-log phase 35000HP to establish basal (p)ppGpp production as a comparison to chemically induced synthesis. The Δ*relA* and Δ*relA*Δ*spoT* mutants will also be used in these assays to verify chemical induction.

Amino acid starvation is the primary inducer of the stringent response and induces RelA to synthesize (p)ppGpp. Serine hydroxamate is commonly used to mimic amino acid starvation by inhibiting charging of seryl-tRNA ribonucleic acid, reducing the synthesis of nucleic acids (181). 35000HP should produce (p)ppGpp if serine starvation is a stringent response trigger in *H. ducreyi*. In *E. coli,* RelA is the only stringent response enzyme that recognizes amino acid starvation. If the *H. ducreyi* RelA functions in a similar manner, both the Δ*relA* and Δ*relA*Δ*spoT* mutants would be incapable of producing (p)ppGpp in response to serine hydroxamate.

In contrast, SpoT responds to a variety of nutrient signals. SpoT synthesis of (p)ppGpp is triggered by fatty acid and carbon starvation. Cerulenin mimics fatty acid starvation through inhibition of β-keto-acyl-ACP synthase, permanently inhibiting the enzyme (182, 183). If *H. ducreyi* is sensitive to fatty acid limitation, 35000HP will synthesize (p)ppGpp after treatment with cerulenin. In *E. coli, relA* mutants are still capable of producing (p)ppGpp because SpoT is fully functional. If *H. ducreyi* SpoT has synthetic capacity and a similar trigger as *E. coli*, then a *H. ducreyi relA* mutant would synthesize (p)ppGpp in response to cerulenin.

Lastly, supplemented GC broth is carbon rich. α-methlyglucoside is a competitive inhibitor of glucose transport and can mimic carbon starvation in bacteria (184-186); treated cells transport significantly less glucose than untreated cells. This chemical would

result in less uptake of glucose, which might trigger a stringent response in *H. ducreyi*. As carbon starvation is a known SpoT- dependent synthesis trigger, the *relA* mutant will likely produce (p)ppGpp, (187, 188). However, it would be interesting to determine whether a *csrA* (carbon storage regulator) mutant responds to this method of carbon starvation. If CsrA induces accumulation of (p)ppGpp, the *csrA* mutant, which may not sense carbon stress, might not synthesize (p)ppGpp. If (p)ppGpp is not involved in CsrA response to carbon limitation, there should be basal levels of (p)ppGpp in the *csrA* mutant.

Nutrient deprivation is not the only known trigger of the stringent response. Induction of the stringent response has been shown to occur during anaerobic growth (111, 189). *H. ducreyi* is a facultative anaerobe. During infection, the abscess in which *H. ducreyi* resides can vary from an oxygen rich to an anaerobic environment. Thus, an anaerobic environment may be a more natural environment for *H. ducreyi*; anaerobic growth or an anaerobic shift may be a natural *in vivo* trigger for the stringent response. 35000HP may have evolved a dual sensory mechanism to stress; therefore it is possible that both RelA and SpoT sense anaerobic conditions. Thus, both the Δ*relA* and Δ*relA*Δ*spoT* mutants should be assayed for *de novo* (p)ppGpp synthesis during and after anaerobic growth.

Additionally, characterization of the transcriptional response to anaerobic conditions may also help elucidate genes that are more directly required for *in vivo* anaerobic growth and potentially identify the stringent response as an anaerobic response regulator in *H. ducreyi*.

Site directed mutagenesis of the *H. ducreyi* SpoT

As SpoT is the only (p)ppGpp hydrolase in *E. coli,* it is considered an essential gene. Without SpoT, the stringent response cannot be turned off. Given that the stringent response halts growth and inhibits synthesis of new macromolecules, a perpetual stringent response is toxic to bacteria. For this reason, there are no *E. coli spoT* deletion mutants. Similarly, we were unable to construct a *spoT* deletion mutant in *H. ducreyi* indicating that in *H. ducreyi*, SpoT is likely critical for hydrolysis of (p)ppGpp.

In *E. coli,* SpoT is capable of synthesizing (p)ppGpp in response to a plethora of triggers. *E. coli relA* mutants, when given the right stimulus, synthesize (p)ppGpp; without the correct stimuli, *E. coli relA* mutants do not accumulate (p)ppGpp. Our *relA* mutant did not synthesize (p)ppGpp *in vitro;* therefore, we have no evidence that *H. ducreyi* SpoT functions as a (p)ppGpp synthetase. However, it is possible that our *relA* mutants are simply lacking the proper stimulus for SpoT-dependent (p)ppGpp production in our system. The (p)ppGpp synthesis detected in our assay is likely RelA-dependent; this does not preclude the possibility that the *H. ducreyi* SpoT has synthetic capability.

To better elucidate the specific role of SpoT in *H. ducreyi,* we must first make a few assumptions. We will first assume that the *H. ducreyi* and *E. coli* SpoT proteins function similarly. If this first assumption is true, we will then assume that the *H. ducreyi* SpoT has both synthetase and hydrolase activity. The final assumption is that given the appropriate *in vitro* stimulus, the *H. ducreyi* SpoT will synthesize (p)ppGpp in our labeling assay. If these assumptions hold true, *spoT* point mutations in the hydrolase domain can be constructed on plasmids and ectopically expressed in the Δ*relA*Δ*spoT*

background. In these mutant strains, any (p)ppGpp synthesis that is detected is a direct result of SpoT synthetic activity.

Site-directed mutagenesis or overlapping primer extension could be utilized to construct the SpoT mutated genes. As illustrated in Figure 1, the active domains of the *H. ducreyi* and *E. coli* SpoT proteins are highly similar. Thus, we can begin constructing *H. ducreyi* SpoT mutant proteins by targeting amino acids deemed necessary for enzymatic activity of the *E. coli* SpoT protein.

In *E.* coli, SpoT a D73N mutation has been shown to prevent hydrolysis of (p)ppGpp (190). D73N containing strains have a constitutively active stringent response. It is possible that some of our difficulties visualizing (p)ppGpp in stationary phase were a result of rapid hydrolysis of (p)ppGpp by SpoT. The SpoT hydrolase mutants will accumulate (p)ppGpp, thus leading to their eventual lethality. This mutant could therefore be used to detect (p)ppGpp in a low induction condition or in stationary phase where there was minimal (p)ppGpp detection.

In addition to the hydrolase mutant above, we would also construct synthetase mutants. SpoT D259N and D293A mutations in *E. coli* result in bacterial strains that are incapable of synthesizing (p)ppGpp (190). These mutations would be useful in a *relA+* background. Both mutations would be useful for elucidating RelA-specific nutrient triggers, particularly if these are indistinguishable from SpoT nutrient triggers by other methods. In contrast to the SpoT D73N strain, any (p)ppGpp synthesis that is detected in the synthetase mutant strain could only be produced by RelA.

After identification of a trigger that induces (p)ppGpp in the wild type *H. ducreyi*, the mutated SpoT proteins can be utilized as tools to identify which enzyme, RelA or

SpoT, is the primary synthetic partner.. These SpoT mutations will result in monofunctional SpoT proteins that are incapable of either synthesizing or hydrolyzing (p)ppGpp. As stated previously, all of these amino acids are conserved in *H. ducreyi* SpoT and will likely result in similar phenotypic outcomes

Genes and mutants for further study

One major phenotype of both mutants is prolonged stationary phase survival. Both the *relA spoT* and *dksA* mutants had increased expression of survival genes *surE* and *surA*. These genes are associated with stationary phase survival of *E. coli* and *Thermotoga maritima* (115, 116, 118). If these genes are responsible for the increased stationary phase survival of the (p)ppGpp° and *dksA* mutants, then deletion of *surA*/*surE* in the *relA spoT* and dksA mutants should result in stationary phase survival to similar to wild type levels. The construction of isogenic mutants that eliminate one or both genes in 35000HP would also prove useful in ascertaining the role of the survival-associated genes in *H. ducreyi* virulence.

Finally, one of the most interesting questions to arise from this research is: what is the identity of the novel Flp-independent adhesin? We found no evidence for decreased expression or altered localization of the Flp proteins in the *dksA* mutant. Taken together, these data suggest that DksA affects adherence to HFF cells through another mechanism, such as regulating one or more yet to be defined co-factors that are required for Flp-mediated adherence. A UPEC *dksA* mutant is impaired in its ability to adhere to eukaryotic cells, perhaps due to downregulation of Type 1 fimbriae expression (134). Other studies in *E. coli* and EHEC also indicate that *dksA* mutants tend to have decreased

attachment as well as decreased expression of genes involved in the regulation of attachment (163, 165). For identification of the putative adhesin, we used the PSORTdb, a database of protein subcellular localization predictions for bacteria. We were able to narrow the potential co-factor to one gene, HD1123 or *pilA* (191).

In Gram-negative bacteria, PilA/PilE is the main constituent of the Type IV pilus. Type IV pili are multifunctional structures involved in adhesion to and invasion of host cells, formation of microcolonies and biofilms, DNA uptake and twitching motility (192). The *H. ducreyi* genome contains a *pilABCD* locus as well as homologs of other key components of the pilus: *pilF, pilM, pilN, pilO, pilT,* and *pilQ*. In *E. coli, pilC* encodes the tip-located adhesin while *pilD* encodes the prepilin peptidase responsible for cleaving prepilins and *N*-methylating the mature pilins (193). PilB/PilF and PilT are the ATPases that power pilus assembly and retraction respectively (193). PilM, PilN, and PilO assemble the Type IV pilus (193). The *pilQ-encoded* protein provides the channel for secretion of the pilus across the outer membrane (193). *H. ducreyi* lacks *pilG*, which is thought to function as a response regulator that is critical in other species for pilus assembly (194).

The *H. ducreyi pilABCD* locus is fully intact indicating that the pilin it can be formed. However, the *H. ducreyi pilM* and *pilN* are defective due to an internal stop codon and a frameshift mutation respectively (195). Therefore, only one of the three assembly proteins is intact in *H. ducreyi*. If this is the case, the *H. ducreyi pilABCD* locus may not be able to assemble a Type IV pilus structure, consistent with reports that another class of pili, not Type IV pili, are expressed by *H. ducreyi* (196-198). Nevertheless, in the *dksA* mutant, expression of *pilA* is downregulated (-4.76 fold) while

the (p)ppGpp mutant has no change in *pilA* expression. Importantly, *pilA* has been implicated as a key mediator of attachment and biofilm formation in several species including *Neisseria meningitidis, Burkholderia pseudomallei* and *Francisella tularensis* (199-203). We are currently characterizing a *pilA* mutant for its ability to attach to fibroblasts.

Appendix I:

Characterization of a 35000HPΔ*relA*Δ*spoT*Δ*dksA* triple deletion mutant

(p)ppGpp and DksA often work in concert to regulate key genes in many bacterial species. As we showed in this work, these two mediators have significantly overlapping targets *in vitro*. (p)ppGpp and DksA deficiencies result in pleiotropic effects that can overlap between mutants. Given this overlap, it is often difficult to delineate between the independent and collective roles that (p)ppGpp or DksA play in *in vitro* phenotypes and virulence. To discern effects due to compensation of one factor for the other, we decided to construct a mutant lacking all three genes.

Using the plasmid pCH21 discussed in Chapter 4, *dksA* was deleted in the (p)ppGpp° mutant background. All three gene deletions were confirmed by PCR and sequencing (Figure 43). Once the triple mutant was confirmed, we next conducted preliminary experiments to determine the usefulness of the triple mutant in our study.
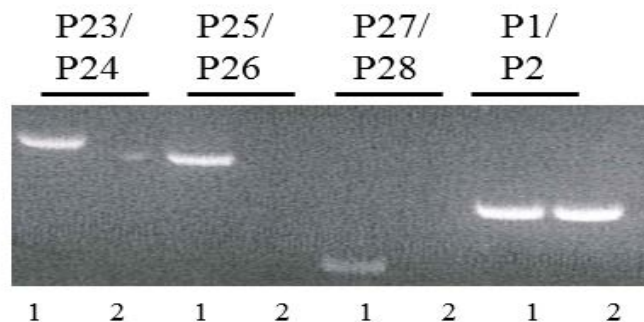
Figure 43: PCR confirmation of the 35000HPΔ*relA*Δ*spoT*Δ*dksA* triple deletion mutant. Lane 1, 35000HP and Lane 2, 35000HPΔ*relA*Δ*spoT*Δ*dksA*. Products were of the expected sizes: P23/24: *relA* int, P25/P26: *spoT* int, P27/P28: *dksA* int, and P1/P2: *dnaE* int.

Both the (p)ppGpp° and *dksA* mutants are sensitive to oxidative stress. However, only the (p)ppGpp° mutant exhibited decreased expression of *sodC* transcripts. Downregulation of *sodC*, a superoxide dismutase, would increase susceptibility to oxidative stress; *sodC* expression confers resistance to pyrogallol *in vitro* and a Δ*sodC* mutant was more sensitive to 2 mM pyrogallol than 35000HP. However, the survival rate for 35000HP was approximately 10%, indicating that even the wild type strain, exhibits low tolerance for this chemical. We therefore decided to perform a dose response with the *sodC* mutant to pinpoint a concentration of pyrogallol that inhibited survival of the *sodC* mutant but not the parent strain. We chose a cutoff of less than 80% survival as indicative of pyrogallol sensitivity. By this standard, the Δ*sodC* mutant showed sensitivity at 0.2 mM pyrogallol while the parent showed sensitivity at approximately 0.8 mM pyrogallol (Figure 44).
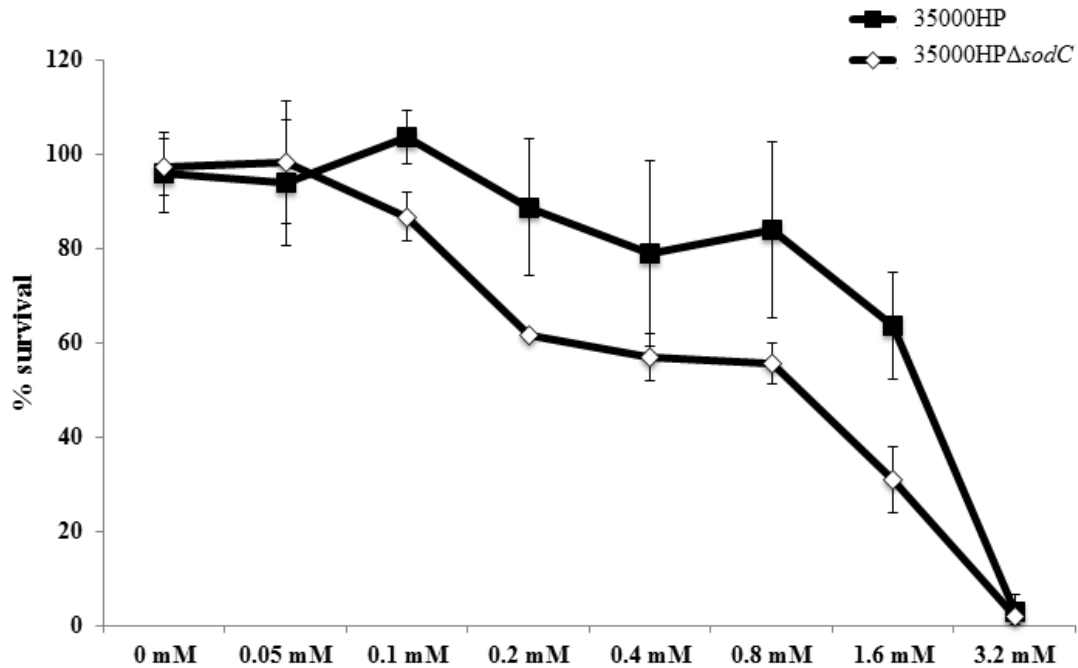
Figure 44: Validation of 35000HPΔ*sodC* mutant sensitivity to pyrogallol. 35000HP and 35000HPΔ*sodC* were incubated with increasing concentrations of Pyrogallol and assayed for virulence. Data are from 3 independent assays. No statistics were done for this assay.

As both the Δ*dksA* and Δ*relA*Δ*spoT* are sensitive to oxidative stress, we hypothesized that the Δ*relA*Δ*spoT*Δ*dksA* mutant would be more sensitive to pyrogallol than both the Δ*dksA* and Δ*relA*Δ*spoT* mutants. To this end, we treated 35000HP, 35000HPΔ*dksA,* 35000HPΔ*relA*Δ*spoT* and 35000HPΔ*relA*Δ*spoT*Δ*dksA* with 0.05, 0.1, and 0.2 mM pyrogallol. None of the deletion mutants were sensitive to 0.05mM pyrogallol. Further, the Δ*dksA* and Δ*relA*Δ*spoT* mutants were only sensitive to 0.2 mM pyrogallol (Figure 45). The triple mutant, however, is highly sensitive to 0.1 and 0.2 mM pyrogallol (Figure 45). Thus, this mutant was useful in showing synergistic effects of (p)ppGpp and DksA deficiency.
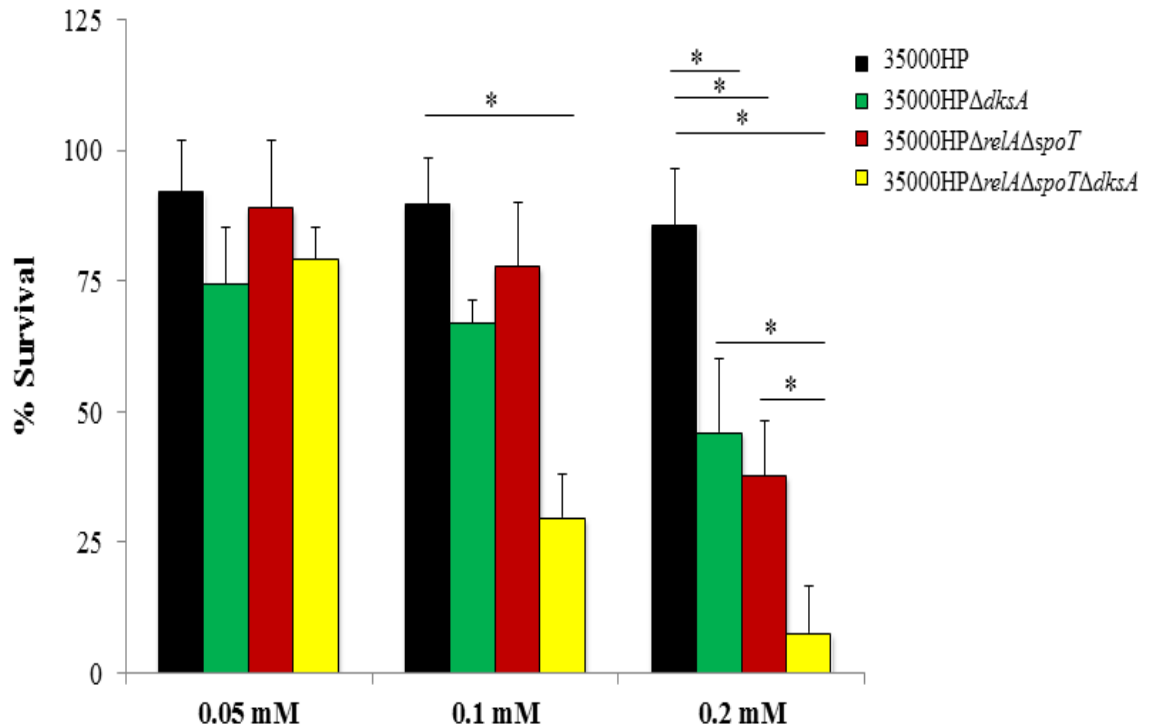
Figure 45. *H. ducreyi* survival after treatment with pyrogallol. Percent survival of 35000HP, 35000HP*ΔdksA*, 35000HP*ΔrelAΔspoT* and 35000HP*ΔrelAΔspoTΔdksA* following incubation with 0.05, 0.1 or 0.2 mM pyrogallol for 1 hour. All percent survivals were calculated as [(geometric mean CFU after treatment/ geometric mean before treatment) x 100]. The data are mean ± SD from five independent experiments. *, $P \le 0.05$.

(p)ppGpp and DksA deficiency resulted in a decreased ability to attach to HFF cells. The (p)ppGpp° mutant has reduced expression of the Flp proteins, which mediate attachment, while the DksA mutant expresses wild type levels of the Flps. It is possible that the increased expression of *dksA* in the (p)ppGpp° mutant allowed partial expression of *flp1-3*. Without *dksA* compensation, the triple mutant may express reduced levels of Flp proteins; thus, we next determined expression levels of the Flp1/2 proteins in the triple mutant. 35000HP*ΔrelAΔspoTΔdksA* expresses almost no Flp protein compared to the parent strain (Figure 46). The reduced expression of the Flp proteins suggested that

129

the triple mutant might be more impaired than either the Δ*relA*Δ*spoT* or Δ*dksA* mutants

in an adherence assay; we next performed an adherence assay with the triple mutant.
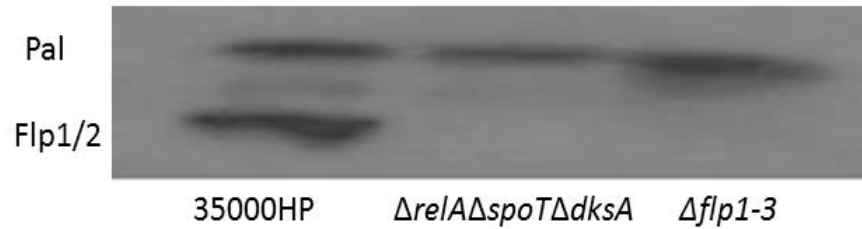
Figure 46. Expression of Flp protein in the 35000HPΔ*relA*Δ*spoT*Δ*dksA* mutant. Western blot analysis of whole cell lysates analyzed by SDS-PAGE.. Samples were probed with Flp1/2 antibody. The anti-PAL MAb 3B9 was used to verify equivalent loading. Data are representative of 2 independent experiments.

As expected, the triple mutant was defective in adherence to HFF cells (Figure 47). Both the (p)ppGpp° and the *dksA* mutants exhibit decreased adherence as has been shown previously in Figures 31 and 39. The adherence defect seen in the (p)ppGpp° mutant is Flp-dependent while the defect in the *dksA* mutant appears to be Flp-independent. The triple mutant was as defective in adherence as both the *dksA* and *flp1-3* mutants. Thus, deletion of *dksA* in the (p)ppGpp° mutant significantly reduced adherence of *H. ducreyi* to HFF cells. Taken together with the *dksA* mutant data, this confirms that DksA regulates an Flp-independent adhesin.
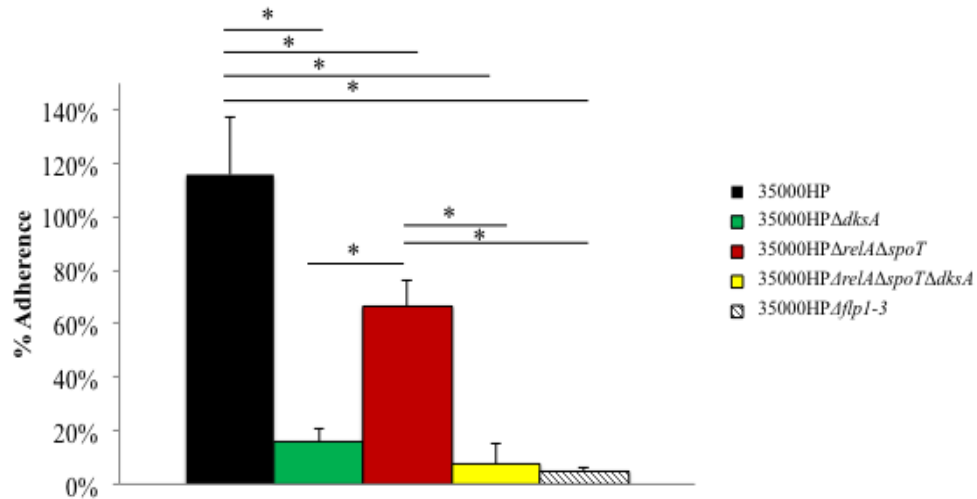
Figure 47. Adherence of the 35000HP$\Delta relA\Delta spoT\Delta dksA$ mutant to HFF cells. Percent adherence of 35000HP, 35000HP$\Delta dksA$, 35000HPΔr$elA\Delta spoT$, 35000HPΔr$elA\Delta spoT\Delta dksA$ and 35000HP$\Delta flp1-3$ to HFF cells calculated as follows: (geometric mean CFU of HFF-adherent bacteria/geometric mean CFU of initial bacteria added per well) $\times$ 100. The data represent the means $\pm$ SD from 5 independent experiments. *, P $\leq$ 0.05.

The (p)ppGpp° mutant exhibited reduced expression of DsrA at mid-log and stationary phase, yet plate grown organisms did not exhibit increased sensitivity to serum-mediated killing. The *dksA* mutant expressed wild type levels of DsrA at mid-log phase and was also not sensitive to serum killing. Surprisingly, when we examined expression levels of DsrA at mid-log phase, the triple mutant expressed no DsrA (Figure 48). The decreased expression of DsrA suggests that the triple deletion mutant would be more sensitive to serum-mediated killing than either the (p)ppGpp° and *dksA* mutants; thus, we decided to conduct a serum bactericidal assay with the triple mutant.

Figure 48: Expression of DsrA in the 35000HPΔ*relA*Δ*spoT*Δ*dksA* mutant. Western blot analysis of whole cell lysates analyzed by SDS-PAGE. Samples were probed with antibody against DsrA. The anti-PAL MAb 3B9 was used to verify equivalent loading. Data is representative of 2 independent experiments.

The triple mutant was significantly more sensitive to serum-mediated killing than the wild type (Figure 49). Neither the (p)ppGpp° nor the *dksA* mutants exhibit sensitivity to serum-mediated killing as has been shown previously in Figures 16 and 27. Although neither the (p)ppGpp° or *dksA* mutants show decreased transcript of *dsrA*, it is possible that the reduced level of DsrA in the triple mutant is due to posttranslational regulation. As we did not perform qRT-PCR for *dsrA* expression on the triple deletion mutant, we cannot exclude that reduced expression is due to decreased transcription.
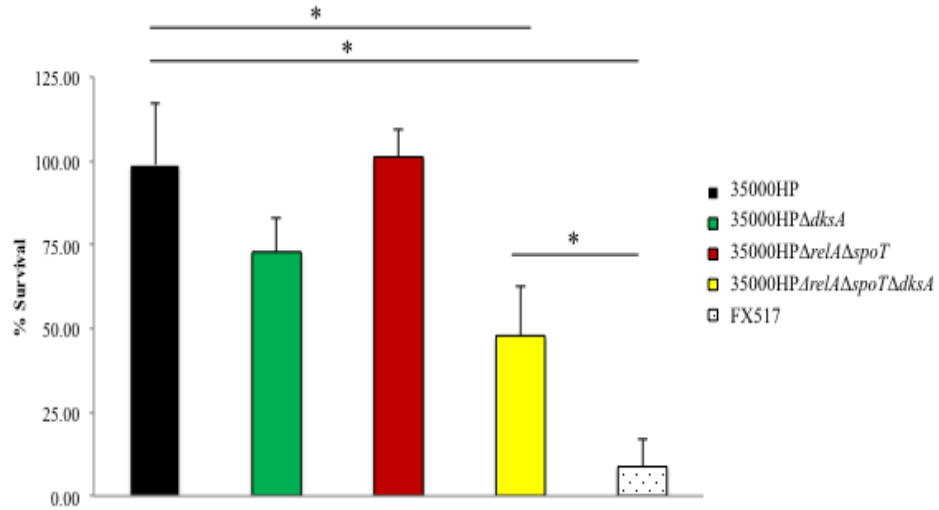
Figure 49. Sensitivity of the 35000HPΔ*relA*Δ*spoT*Δ*dksA* mutant to complement-replete human serum. Percent survival of 35000HP, 35000HPΔ*relA*Δ*spoT*, 35000HP*ΔrelAΔspoTΔdksA* and *dsrA* mutant strain FX517 in NHS. Survival was calculated as [(geometric mean CFU in NHS/geometric mean CFU in heat-inactivated NHS) × 100]. Data are means ± SD of five independent experiments. All strains were compared to 35000HP. *, $P \leq 0.05$.

The triple mutant will be useful in studies in which it is critical to identify which gene is primarily responsible for a particular phenotype. We provide some evidence that DksA can compensate for (p)ppGpp deficiency and that (p)ppGpp and DksA regulate similar gene targets. We also provide evidence that DksA and (p)ppGpp deficiencies can result in conflicting phenotypes. For example, the (p)ppGpp° mutant is more resistant to uptake by macrophages while the *dksA* mutant is less resistant. Would the (p)ppGpp° mutant exhibit even greater resistance to phagocytosis if *dksA* overexpression were not occurring? The triple mutant could provide the perfect control to answer such a question.

The triple mutant may be able to serve as a (p)ppGpp° mutant with wild type *dksA* levels. As we demonstrated in Figure 30, despite *dksA* transcripts being expressed on a multicopy plasmid with a constitutively active promoter, 35000HPΔ*dksA* (pCH24) expresses wild type levels of *dksA*. Therefore, usage of pCH24 in the triple deletion mutant might result in a (p)ppGpp° mutant that expresses *dksA* transcripts at levels equivalent to 35000HP. If this is true, this strain could be used alongside the null (35000HPΔ*relA*Δ*spoT*Δ*dksA*) and overexpressing strain (35000HPΔ*relA*Δ*spoT*)to pinpoint functional compensation of (p)ppGpp by DksA. As the triple mutant removes both regulators, it may not be directly useful in the identification of dual functional compensation.

In conclusion, we showed that the triple mutant shows cumulative effects of (p)ppGpp and DksA deficiencies. Compensation with specific stringent mediators of interest can help reveal compensatory effects in *H. ducreyi*. In summary, in the triple mutant, we have provided a unique tool to further study the stringent response in *H. ducreyi*.

Appendix II:

Inducible *relA* and *dksA* expression

An alternative approach to understanding the role of (p)ppGpp and DksA play in *H. ducreyi* pathogenesis is to overexpress these genes. To this end, we constructed plasmids to induce expression of RelA -and subsequently induce expression of (p)ppGpp- and DksA. To complement the *relA spoT* deletion mutant, the *relA* and *dksA* genes were expressed in expression vector pT.

The expression vector pT contains a tetracycline-inducible promoter on the pLS88 backbone (204).   Induction of the gene occurs by addition of 200 ng/µl of anhydrotetracycline. Preliminary analysis showed that 35000HP transformed with a pT vector containing *rpoE* had severe growth defects in broth (89). This raised the possibility that genes were being expressed in the absence of induction. To reduce the leakiness of the *tet* promoter, a 1.2-kb spectinomycin cassette from pSPECR was digested with BamHI and ligated into pT in an orientation opposite to the promoter. The orientation of the spectinomycin cassette acts to dampen the leakiness of the *tet* promoter. This construct was designated pDG10 (89).

To construct these expression vectors, the coding region of the gene was amplified. The amplicons contain an NdeI site at the 5′ end and a BamHI site at the 3′ end to ensure that the target genes are introduced into the pT backbone in the correct orientation. The *relA* open reading frame along with 21 bp of the upstream and 22 bp of the downstream regions were amplified using primers 11-P1/11-P2 (Table 11). The final plasmid was named pCH5. The *dksA* open reading frame along with 21 bp of the

upstream and 22 bp of the downstream regions were amplified using primers 11-P3/11-P4. The final plasmid was named pCH25. Plasmid maps are illustrated in Figure 50.
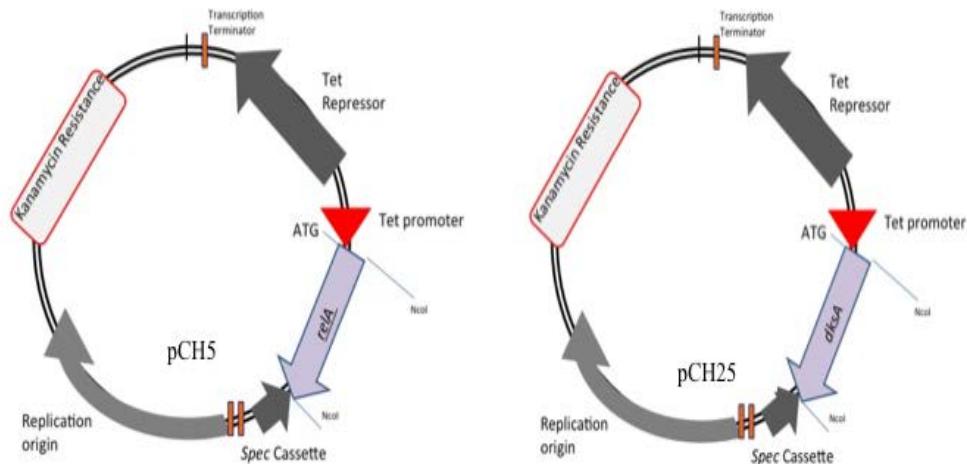
Figure 50. Plasmid maps for inducible expression of *relA* and *dksA*.

The plasmids have a spectinomycin resistance cassette in the opposite orientation of the target gene. The final constructs were confirmed by PCR and sequence analysis. The *relA* inducible plasmid, pCH5 was electroporated into 35000HP, 35000HPΔ*relA* and 35000HPΔ*relA*Δ*spoT* and the resulting strains were designated 35000HP(pCH5), 35000HPΔrelA(pCH5) and 35000HPΔ*relA*Δ*spoT*(pCH5). pCH25, the *dksA* inducible plasmid, was electroporated into 35000HP and 35000HPΔ*dksA* and the final strains designated 35000HP(pCH25) and 35000HPΔ*dksA*(pCH25). As controls, 35000HP, 35000HPΔ*relA*Δ*spoT*, and 35000HPΔ*dksA* were also electroporated with pDG10; the resulting strains were designated as 35000HP(pDG10), 35000HP Δ*relA*Δ*spoT*(pDG10), and 35000HPΔ*dksA*(pDG10).

Table 11. Plasmids and primers used for generation of inducible strains

Plasmids	Description	Source or reference
pT	A pLS88 derivative containing the tetracycline (tet) controlled expression system	(204)
pDG10	pT derivative containing the specR resistance cassette from pSPECR	(89)
pCH5	pT derivative containing the *relA* ORF	This Study
pCH25	pT derivative containing the *dksA* ORF	This Study

Primers	Purpose	Gene	5' to 3' Sequence
11-P1	For Construction of pCH5	*relA* ORF F	ATATATCCATGGTTAG TTTGCTAGCCGTTTTG
11-P2	For Construction of pCH5	*relA* ORF R	ATATATCCATGGATGG TTGCAATACGTCGTTC
11-P3	For Construction of pCH25	*dksA* ORF F	ATATATCCATGGATGG TTCAAGTGGCAACTAC
11-P4	For Construction of pCH25	*dksA* ORF R	ATATATCCATGGCTAA AGCCCCATTTGTTTCT

We next confirmed that pCH5 would induce expression of *relA* in the *relA spoT* mutant. We grew 35000HPΔ*relA*Δ*spoT*(pDG10) and 35000HPΔ*relA*Δ*spoT*(pCH5) to mid-log phase. *relA* expression was then induced by addition of 200 ng/μl anhydrotetracycyline, RNA was harvested at 0, 30, 60, 120, 180, and 240 mins after induction. Analysis showed that *relA* expression was induced after induction with anhydrotetracycline and that maximal expression occurred within 30 mins (Figure 51). As incubation progresses, induction of *relA* begins to decrease; the reason for this is unclear. Importantly, *relA* transcripts are expressed prior to induction indicating that the pCH5 was still leaky.
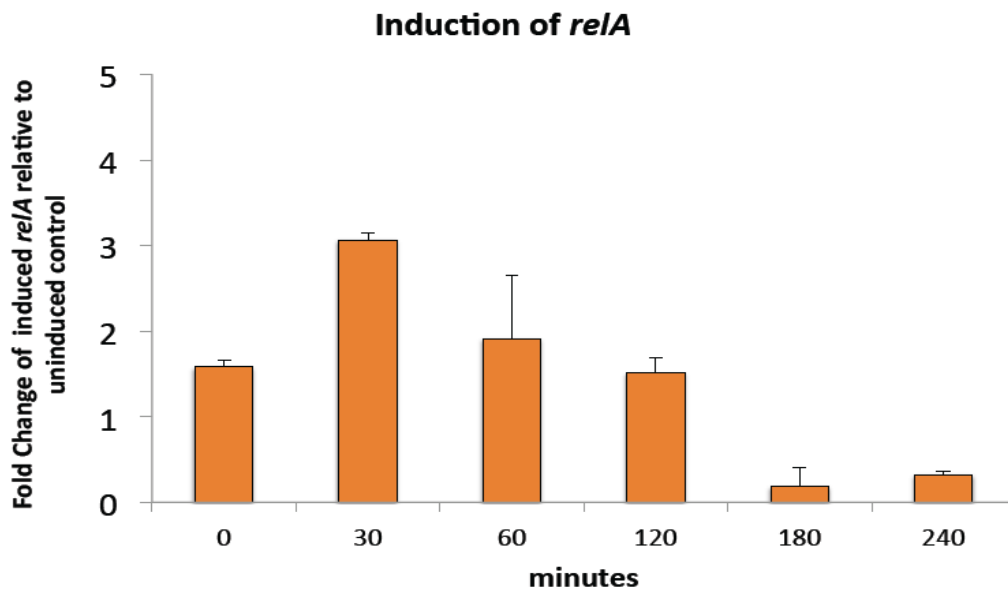
Figure 51. Validation of pCH5 plasmid induction of *relA*. Transcripts levels of *relA* were normalized to that of *dnaE*. The data represent the means ± SD of the results of three independent experiments.

SpoT is an essential gene in *E. coli* because unchecked accumulation of (p)ppGpp is often toxic. Therefore, overexpression of *relA* – and increased accumulation of (p)ppGpp – through the inducible system might prove lethal to *H. ducreyi*. We performed growth curves to determine if induction of *relA* inhibited growth of the *relA* or *relA spoT* mutant. The pCH5 containing strains and the controls were grown until they reached an OD$_{660}$ of approximately 0.2. Anhydrotetracycyline was added to the cultures and the strains were monitored for an additional 4 hours. Presence of pCH5 alone did not inhibit growth compared to the empty pDG10 vector (Figure 52). Furthermore, induction of *relA* did not inhibit growth of these strains in this limited time frame (Figure 52).
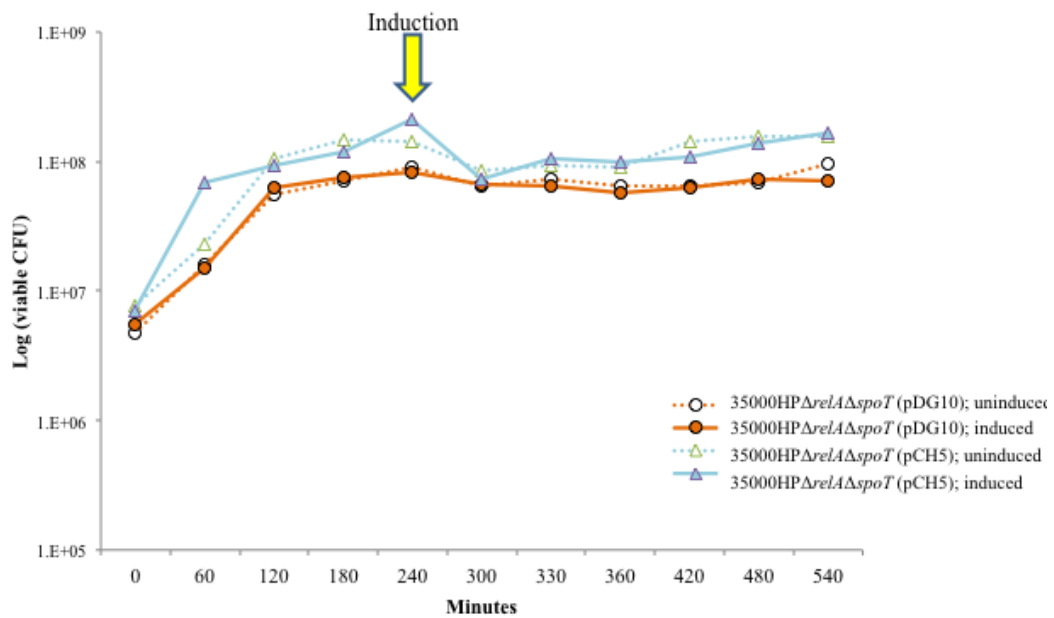
Figure 52. Growth of *relA* inducible strains. (A) Growth of 35000HPΔ*relA*Δ*spoT* (pDG10) and 35000HPΔ*relA*Δ*spoT* (pCH5) before and after induction of *relA*. The data represent the means ± SD of the results of three independent experiments.

Given that induction of *relA* did not inhibit growth of 35000HP, we utilized this strain to induce expression of (p)ppGpp in our *de novo* labeling assay. The assay was performed using cells harvested from mid-log phase since mid-log phase expressed only minor levels of (p)ppGpp. (p)ppGpp was detected in 35000HPΔ*relA*Δ*spoT* (pCH5) (Figure 53, Lanes 3-5). As expected, no expression was seen in the Δ*relA*Δ*spoT* mutant containing the empty pDG10 vector (Figure 53, Lane 1). Therefore, our inducible *relA* system led to accumulation of (p)ppGpp *in vitro*. As stated previously, the pT vector is leaky. To combat this leakiness, pDG10 was constructed with an antibiotic resistance cassette in the opposite orientation of the *tet* inducible promoter. However, (p)ppGpp can still be detected in the uninduced pCH5 containing strain (Figure 53, Lane 2). These lead us to conclude that the *tet* inducible system was still leaky; however overexpression of (p)ppGpp without expression of *spoT* was not lethal in these conditions.
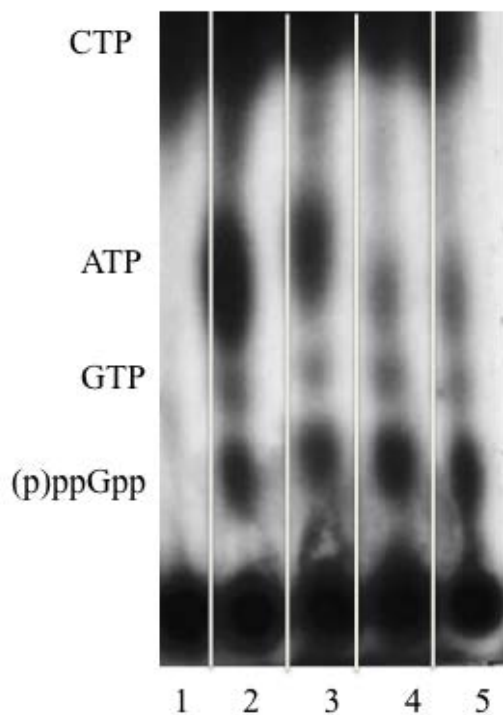
Figure 53. (p)ppGpp expression is induced by pCH5 in the absence of nutrient limitation. Bacteria were labeled with $KH_2{}^{32}PO_4$ in phosphate-limited RPMI plus 5% FBS. (p)ppGpp was extracted and detected by polyethylenimine cellulose thin layer chromatography and autoradiography. Lane 1, 35000HPΔ*relA*Δ*spoT* (pDG10); Lanes 2-5 35000HPΔ*relA*Δ*spoT* (pCH5): uninduced (2) and induced after 30 minutes (3), 1 hour (4), and 2 hours (5). Blot is representative of two independent experiments.

DksA overexpression is not linked to toxicity in bacteria. We therefore, did not expect to see any growth inhibition in the inducible *dksA* system. Prior to induction, expression of pCH25 alone did not inhibit growth compared to the empty pDG10 vector (Figure 54}. However, addition of anhydrotetracycline affected growth of all four strains. While the pT and uninduced pCH25 containing strains recovered, the induced pCH25 containing strain was severely inhibited (Figure 54). We did not assay *dksA* transcript levels after induction of pCH25; therefore we cannot confirm induction of DksA. However, addition of anhydrotetracycline to 35000HPΔ*dksA*(pCH25) did appear to inhibit growth.
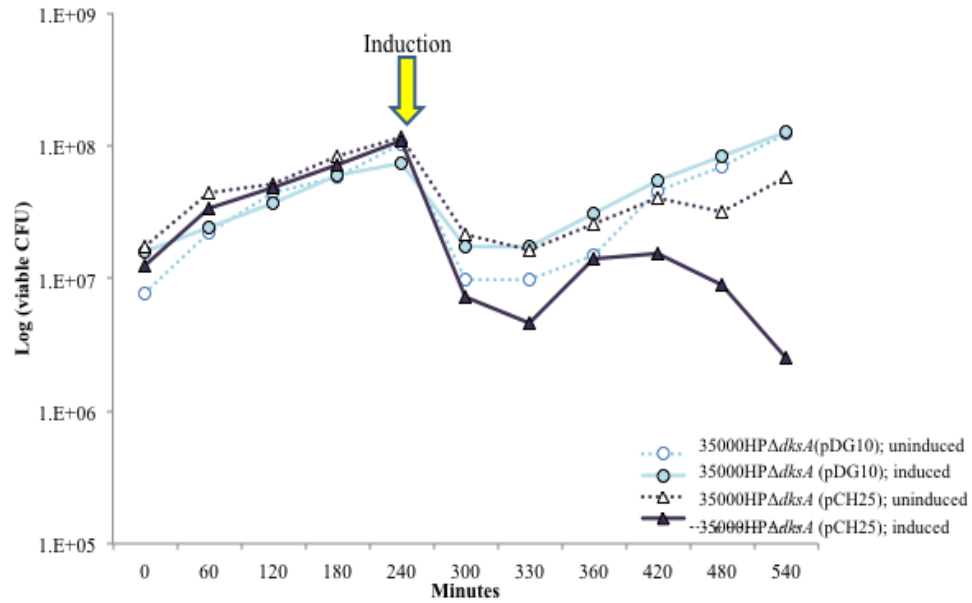
Figure 54. Growth of *dksA* inducible strains. (A) Growth of 35000HPΔ*dksA* (pDG10) and 35000HPΔ*dksA* (pCH25) before and after induction of *dksA*. The data represent the means ± SD of the results of three independent experiments.

In conclusion, we constructed inducible *relA* and *dksA* plasmids, pCH5 and pCH25, respectively. We showed that pCH5 could be used to induce expression of (p)ppGpp in the absence of any *in vitro* stringent response trigger. Overexpression of *relA* and induced accumulation of (p)ppGpp did not cause toxicity in the Δ*relA*Δ*spoT* mutant. This is surprising, as this strain should be incapable of hydrolyzing any accumulated (p)ppGpp; however, our incubation time may be too short to prove lethal Additionally, our liquid medium is rich and may counteract the effects of (p)ppGpp accumulation in the absence of hydrolase activity as the growth of the pCH5 containing strains was not inhibited *in vitro* (Figure 52). Our inducible system, therefore, may provide a mechanism for studying a hydrolase negative - *spoT* null - *H. ducreyi* strain without the necessity of a *spoT* deletion mutant.

Appendix III. Functional classification of genes differentially expressed by deletion of (p)ppGpp or DksA In Mid-Log, Transition, or Stationary Phase

Functional Category[a]	Gene	Description or homolog	35000HPΔrelAΔspoT / 35000HP[b] Fold-Change			35000HPΔdksA / 35000HP[c] Fold-Change		
			Mid-Log	Transition	Stationary	Mid-Log	Transition	Stationary
Amino acid biosynthesis								
	arcB1	Ornithine carbamoyltransferase	-2.67					
	argB	Acetylglutamate kinase		-2.61	-2.07			-2.24
	asd	Aspartate-semialdehyde dehydrogenase				2.79	3.49	3.53
	cysZ	Sulfate transporter, CysZ-type						3.26
	dapD	2,3,4,5-tetrahydropyridine-2,6-dicarboxylate N-succinyltransferase						2.06
	glnA	Glutamine synthetase type I					2.32	3.44
	HD1666	Probable phosphatase			-2.35			
	lysC	Aspartokinase			2.40			
	pheA	Chorismate mutase I / Prephenate dehydratase			2.99			3.02
	pyrD	Dihydroorotate dehydrogenase	-2.03	-2.38				
	pyrE	Orotate phosphoribosyltransferase			-3.76			
	pyrF	Orotidine 5´-phosphate decarboxylase			-3.46			
Amino acid transport and metabolism								
	aspA	Aspartate ammonia-lyase	3.06					
	brnQ	Branched-chain amino acid carrier protein			-2.40		-2.90	-2.65

Appendix III. Functional classification of genes differentially expressed by deletion of (p)ppGpp or DksA In Mid-Log, Transition, or Stationary Phase

Functional Category[a]	Gene	Description or homolog	35000HPΔrelAΔspoT / 35000HP[b] Fold-Change			35000HPΔdksA/ 35000HP[c] Fold-Change		
			Mid-Log	Transition	Stationary	Mid-Log	Transition	Stationary
	carA	Carbamoyl-phosphate synthase, small subunit	-4.29	-5.68				
	carB	Carbamoyl-phosphate synthase, large subunit	-3.97	-4.05				
	cysK	Cysteine synthase	-3.04					
	dat	Diaminobutyrate--2-oxoglutarate aminotransferase				3.80	4.90	2.81
	ddc	L-2,4-diaminobutyrate decarboxylase				3.06	3.16	
	HD1348	Nucleoside 5-triphosphatase RdgB (dHAPTP, dITP, XTP-specific)			-2.16			
	mazG	Nucleoside triphosphate pyrophosphohydrolase MazG			3.68			3.44
	nrdB	Ribonucleotide reductase of class Ia (aerobic), beta subunit			2.04			
	nudE	ADP compounds hydrolase			3.52			
	pntA	NAD(P) transhydrogenase alpha subunit	-2.39		-2.53			2.88
	pntB	NAD(P) transhydrogenase subunit beta	-2.50		-2.04		-2.44	
	potD1	Spermidine/putrescine-binding periplasmic protein (SPBP)	2.45			2.58	3.01	6.12
	potD2	ABC transporter, periplasmic spermidine putrescine-binding protein			7.01			5.06
	purA	Adenylosuccinate synthetase	-2.52		-2.24			

144

Appendix III. Functional classification of genes differentially expressed by deletion of (p)ppGpp or DksA In Mid-Log, Transition, or Stationary Phase

Functional Category[a]	Gene[a]	Description or homolog	35000HPΔrelAΔspoT / 35000HP[b] Fold-Change			35000HPΔdksA / 35000HP[c] Fold-Change		
			Mid-Log	Transition	Stationary	Mid-Log	Transition	Stationary
	purM	Phosphoribosylformylglycinamidine cyclo-ligase			2.58			2.36
	sdaC	Serine transporter	2.22					
	sucA	2-oxoglutarate dehydrogenase E1 component	-4.38					
	sucB	Dihydrolipoamide succinyltransferase component (E2) of 2-oxoglutarate dehydrogenase complex	-5.83					
	upp	Uracil phosphoribosyltransferase	-2.26		-6.29			-3.76
	uraA	Uracil permease		-2.17	5.77			5.07
Amino sugar and nucleotide metabolism								
	apt	Adenine phosphoribosyltransferase			4.56			3.87
	apbE	Thiamin biosynthesis lipoprotein			-2.29			
	dxs	1-deoxy-D-xylulose 5-phosphate synthase			-2.09			
	glmU	Glucosamine-1-phosphate N-acetyltransferase	-2.60					
	kdsA	2-Keto-3-deoxy-D-manno-octulosonate-8-phosphate synthase			-2.60			-2.16
	manA	Mannose-6-phosphate isomerase		2.30				

145

Appendix III. Functional classification of genes differentially expressed by deletion of (p)ppGpp or DksA In Mid-Log, Transition, or Stationary Phase

Functional Category[a]	Gene	Description or homolog	35000HPΔrelAΔspoT / 35000HP[b] Fold-Change			35000HPΔdksA / 35000HP[c] Fold-Change		
			Mid-Log	Transition	Stationary	Mid-Log	Transition	Stationary
	manX	Mannose-specific phosphotransferase IIAB component			-8.60			-5.21
	manY	Mannose-specific phosphotransferase system IIC component		2.35	-8.36			-6.35
	manZ	Mannose-specific phosphotransferase system IID component		2.56	-4.18			-3.27
	moaC	Molybdenum cofactor biosynthesis protein						-2.05
	moaD	Molybdenum cofactor biosynthesis protein			-2.81			-2.52
	murA	UDP-N-acetylglucosamine 1-carboxyvinyltransferase	-2.95		2.71			
	nagA	N-acetylglucosamine-6-phosphate deacetylase			-2.12			
	nanE	N-acetylmannosamine-6-phosphate 2-epimerase			-2.73			-2.96
	pta	Phosphate acetyltransferase			-2.34			
	ribH	6,7-dimethyl-8-ribityllumazine synthase			-2.54			
	thiL	Thiamine-monophosphate kinase	-2.59	-2.19	-2.31			
	thyA	Thymidylate synthase			4.53			
	uppS	Undecaprenyl pyrophosphate synthetase			3.58			2.24

Appendix III. Functional classification of genes differentially expressed by deletion of (p)ppGpp or DksA In Mid-Log, Transition, or Stationary Phase

Functional Category[a]	Gene[a]	Description or homolog	35000HPΔrelAΔspoT / 35000HP[b] Fold-Change			35000HPΔdksA / 35000HP[c] Fold-Change		
			Mid-Log	Transition	Stationary	Mid-Log	Transition	Stationary
	wecC	UDP-glucose dehydrogenase	-2.16					
Cellular carbohydrate biosynthetic process								
	alr	Alanine racemase			2.23			
	araD	L-ribulose-5-phosphate 4-epimerase		2.27				
	eno	Phosphopyruvate hydratase			3.42		-2.16	3.48
	fbp	Fructose-1,6-bisphosphatase, type I		2.09				
	frdC	Fumarate reductase subunit C			-10.48			-5.81
	frdD	Fumarate reductase subunit D		3.01	-2.59			
	gmhA	Phosphoheptose isomerase 1			2.09			
	HD0112	Negative regulator of beta-lactamase expression					3.22	
	HD0297	3-deoxy-D-manno-octulosonate 8-phosphate phosphatase			2.36			
	HD0746	Hypothetical protein				2.50	2.28	4.93
	HD0922	Tfp pilus assembly protein, pilus retraction ATPase PilT					3.04	
	kdkA	3-deoxy-D-manno-octulosonic acid kinase			2.09			
	lsgD	Lipopolysaccharide core biosynthesis glycosyltransferase WadA					2.04	
	murD	UDP-N-acetylmuramoylalanine--D-glutamate ligase			-2.74			

147

Appendix III. Functional classification of genes differentially expressed by deletion of (p)ppGpp or DksA In Mid-Log, Transition, or Stationary Phase

Functional Category[a]	Gene[a]	Description or homolog	35000HPΔrelAΔspoT / 35000HP[b] Fold-Change			35000HPΔdksA / 35000HP[c] Fold-Change		
			Mid-Log	Transition	Stationary	Mid-Log	Transition	Stationary
	murE	UDP-N-acetylmuramoylalanyl-D-glutamate--2,6-diaminopimelate ligase			-2.47			
	neuA	N-Acetylneuraminate cytidylyltransferase			2.74			
	pckA	Phosphoenolpyruvate carboxykinase [ATP]			-2.60			
	rpiA	Ribose 5-phosphate isomerase A					2.92	2.22
	sgbU	L-xylulose 5-phosphate 3-epimerase		2.07				
	tpiA	Triosephosphate isomerase			2.13			
Carbohydrate metabolism								
	aceF	Dihydrolipoamide acetyltransferase			-2.27			
	ampD	N-acetylmuramoyl-L-alanine amidase			5.80			2.24
	csrA	Carbon storage regulator			-2.34			
	rfaD	ADP-L-glycero-D-manno-heptose-6-epimerase						2.06
	suhB	Inositol-1-monophosphatase						2.44
Cell division								
	ftsI	Peptidoglycan synthetase			-2.48			
	ftsL	Cell division protein			-5.21			-3.14
	ftsW	Cell division protein			-3.95			-2.11

Appendix III. Functional classification of genes differentially expressed by deletion of (p)ppGpp or DksA In Mid-Log, Transition, or Stationary Phase

Functional Category[a]	Gene[a]	Description or homolog	35000HPΔrelAΔspoT / 35000HP[b] Fold-Change			35000HPΔdksA / 35000HP[c] Fold-Change		
			Mid-Log	Transition	Stationary	Mid-Log	Transition	Stationary
	HD1001	Z-ring-associated protein ZapA			2.47			2.02
	HD1472	Conserved hypothetical protein			2.01			
	ispZ	Intracellular septation protein IspA			-2.01			
	mreC	Rod shape-determining protein			-2.41			
Cell membrane								
	cdsA	Phosphatidate cytidylyltransferase			2.48			
	cdtA	Cytolethal distending toxin protein A	-2.49					
	cdtB	Cytolethal distending toxin protein B	-2.79		-2.59			-2.62
	cdtC	Cytolethal distending toxin protein C	-3.25		-2.93			-2.47
	crcB	putative fluoride ion transporter			-2.15			
	dppB	Dipeptide transport system permease protein			-2.22			
	dppC	Dipeptide transport system permease protein			-2.21			
	dsbB	Periplasmic thiol:disulfide oxidoreductase			2.14			
	dsrA	serum resistance protein					-2.06	
	fimA	Possible fimbrial major pilin protein	3.00	3.30	2.79	3.55		2.44
	fimB	Possible fimbrial structural subunit	2.38	2.15	3.04	2.61		2.48

149

Appendix III. Functional classification of genes differentially expressed by deletion of (p)ppGpp or DksA In Mid-Log, Transition, or Stationary Phase

Functional Category[a]	Gene	Description or homolog	35000HPΔrelAΔspoT / 35000HP[b]			35000HPΔdksA / 35000HP[c]		
			Fold-Change			Fold-Change		
			Mid-Log	Transition	Stationary	Mid-Log	Transition	Stationary
	flp1	flp operon protein Flp1		-3.22	-3.72			
	flp2	flp operon protein Flp2		-3.39	-3.81			
	flp3	flp operon protein Flp3		-3.08	-8.91			-2.33
	glpT	Glycerol 3-phosphate transporter			-3.02		-2.11	-2.43
	HD0196	Putative membrane protein					-2.71	2.74
	HD0470	Probable component of the lipoprotein assembly complex with YaeT, YfgL, and NlpB)			3.27		2.13	4.80
	HD0587	LptA, protein essential for LPS transport across the periplasm			3.21			
	HD0665	Hypothetical protein	-2.73		4.15			
	HD1071	Putative membrane protein		3.92	4.59			
	HD1123	Type IV pilin PilA						-4.76
	hgbA	Outer membrane receptor proteins, mostly Fe transport	-2.35	-2.13	-2.54			
	kefB	putative Glutathione-regulated potassium-efflux system protein		2.12				2.04
	lolC	Lipoprotein releasing system transmembrane protein			-2.19			
	momp	Major outer membrane protein			2.81			
	mrdA	Penicillin-binding protein 2 (PBP-2)			-2.31			-2.07
	oapB	opacity associated protein B	-2.92					
	ompA2	Outer membrane protein A precursor	-2.06			-2.67		

Appendix III. Functional classification of genes differentially expressed by deletion of (p)ppGpp or DksA In Mid-Log, Transition, or Stationary Phase

Functional Category[a]	Gene[a]	Description or homolog	35000HPΔrelAΔspoT / 35000HP[b] Fold-Change			35000HPΔdksA / 35000HP[c] Fold-Change		
			Mid-Log	Transition	Stationary	Mid-Log	Transition	Stationary
	ompP2A	Outer membrane protein P2 homolog	-3.05	-2.47		-2.71		
	ompP2B	Outer membrane protein P2 homolog	2.02		10.28	2.06		3.93
	ompP4	Outer membrane lipoprotein e (P4)						2.32
	pal	18K peptidoglycan-associated outer membrane lipoprotein					-2.15	
	rnfD	Putative Na-translocating NADH-quinone reductase			-2.21			
	smpA	Outer membrane lipoprotein SmpA, a component of the essential YaeT outer-membrane protein assembly complex	-2.34		9.96			5.06
	tadB	Flp pilus assembly protein			-12.05			-3.68
	tadC	Type II/IV secretion system protein TadC, associated with Flp pilus assembly			-2.19			
	yidC	Inner membrane protein translocase component YidC, long form						2.22
Cellular homeostasis								
	citD	Citrate lyase, gamma subunit						
	citE	Citrate lyase, beta chain		2.36			2.00	
	cydA	Cytochrome d ubiquinol oxidase subunit I					-2.32	

151

Appendix III. Functional classification of genes differentially expressed by deletion of (p)ppGpp or DksA In Mid-Log, Transition, or Stationary Phase

Functional Category[a]	Gene[a]	Description or homolog	35000HPΔrelAΔspoT / 35000HP[b] Fold-Change			35000HPΔdksA / 35000HP[c] Fold-Change		
			Mid-Log	Transition	Stationary	Mid-Log	Transition	Stationary
	cydB	Cytochrome d ubiquinol oxidase subunit II					-2.11	
	dsbA	Periplasmic thiol:disulfide interchange protein			4.97			2.93
	dsbE1	Cytochrome c-type biogenesis protein			-2.12			-2.27
	ftpA	Fine tangled pili major subunit	-2.15		7.79			3.03
	ftsH	Cell division protein		4.41				
	HD0697	thioredoxin-like protein			3.74			
	HD0700	Peroxiredoxin family protein/glutaredoxin			2.66		-2.24	
	lpdA	Dihydrolipoamide dehydrogenase			-2.02			
Cellular response to stress								
	cpxR	Transcriptional regulatory protein CpxR			7.19			5.89
	HD0357	Probable carbon starvation protein A			-2.23		-2.02	
	hfq	RNA-binding protein			11.67			2.64
	spoT	Guanosine-3',5'-bis(diphosphate) 3'-pyrophosphohydrolase	NA	NA	NA			2.09
DNA binding								
	HD0292	Hypothetical protein			5.41			4.00

Appendix III. Functional classification of genes differentially expressed by deletion of (p)ppGpp or DksA In Mid-Log, Transition, or Stationary Phase

Functional Category[a]	Gene[a]	Description or homolog	35000HPΔrelAΔspoT / 35000HP[b] Fold-Change			35000HPΔdksA / 35000HP[c] Fold-Change		
			Mid-Log	Transition	Stationary	Mid-Log	Transition	Stationary
	HD0509	Hypothetical protein				2.17	4.63	2.18
	HD1613	Hypothetical protein			3.84			2.37
	hupA	DNA-binding protein HU-alpha			3.04		-2.18	2.19
	ner	possible DNA-binding protein						-2.77
	uspA	Universal stress protein A			-4.57			-3.20
DNA metabolic process								
	dnaA	Chromosomal replication initiator protein			2.82			2.88
	dnaJ	Chaperone protein		7.55				
	gam	putative host-nuclease inhibitor protein					2.24	
	HD0095	Mu phage DNA transposition protein B			-2.06		2.02	
	HD1444	Hypothetical protein					2.80	2.61
	HD1452	Hypothetical protein					2.85	2.86
	HD1686	methylates LSU ribosomal protein L3p					-2.12	2.15
	ihfA	Integration host factor alpha subunit			-2.13			
	ihfB	Integration host factor, beta subunit			-3.68			
	lexA	Probable LexA repressor			2.05			-2.26
	mutM	Formamidopyrimidine-DNA glycosylase		2.15		-2.09		

153

Appendix III. Functional classification of genes differentially expressed by deletion of (p)ppGpp or DksA In Mid-Log, Transition, or Stationary Phase

Functional Category[a]	Gene	Description or homolog	35000HPΔrelAΔspoT / 35000HP[b] Fold-Change			35000HPΔdksA / 35000HP[c] Fold-Change		
			Mid-Log	Transition	Stationary	Mid-Log	Transition	Stationary
	mutT	Mutator MutT protein			2.16			
	mutY	A/G-specific adenine glycosylase					2.23	2.33
	nrdA	Ribonucleotide reductase of class Ia (aerobic), alpha subunit			-3.17			
	parC	Topoisomerase IV subunit A	2.01					
	rdgC	DNA recombination-dependent growth factor C			2.17			
	recN	DNA repair protein RecN			2.42			
	recR	Recombination protein RecR			2.99			2.07
	rep	ATP-dependent DNA helicase Rep			2.46			2.17
	ssb2	Single-stranded DNA-binding protein in PFGI-1-like cluster	-2.09					
	topB1	DNA topoisomerase III in PFGI-1-like cluster						6.19
	uvrA	Excinuclease ABC subunit A		2.02				
	xseB	Exodeoxyribonuclease VII small subunit			2.16			
Fatty acid biosynthesis and metabolism								
	accA	Acetyl-coenzyme A carboxyl transferase alpha chain			-2.97			-2.83
	acpP	Acyl carrier protein			3.08			3.12
	fabA	3-hydroxydecanoyl-[acyl-carrier-protein] dehydratase		2.53	2.61			

Appendix III. Functional classification of genes differentially expressed by deletion of (p)ppGpp or DksA In Mid-Log, Transition, or Stationary Phase

Functional Category[a]	Gene	Description or homolog	35000HPΔrelAΔspoT / 35000HP[b] Fold-Change			35000HPΔdksA / 35000HP[c] Fold-Change		
			Mid-Log	Transition	Stationary	Mid-Log	Transition	Stationary
	fabB	3-oxoacyl-[acyl-carrier-protein] synthase	3.02	6.02	2.86			
	fabH	3-oxoacyl-[acyl-carrier-protein] synthase			-2.47			
	fabI	Enoyl-[acyl-carrier-protein] reductase			4.80			3.18
	HD1711	Acyl-CoA thioesterase YciA, involved in membrane biogenesis			-3.59			-2.38
	ispB	Octaprenyl diphosphate synthase			2.27			2.56
	lst	N-acetylneuraminic acid synthase-like protein			2.83			
	waaF	ADP-heptose--lipooligosaccharide heptosyltransferase II	-2.95		2.28			2.03
Intracellular trafficking and secretion								
	HD0974	Chromosome partitioning ATPase in PFGI-1-like cluster, ParA-like	2.61					
	HD1305	Type II/IV secretion system ATPase TadZ/CpaE, associated with Flp pilus assembly			-3.47			
	HD1528	Eha					2.25	
	hhdA	Hemolysin			-3.99			
	hhdB	Channel-forming transporter/cytolysins activator of TpsB family	-2.08	-2.19				-2.09

155

Appendix III. Functional classification of genes differentially expressed by deletion of (p)ppGpp or DksA In Mid-Log, Transition, or Stationary Phase

Functional Category[a]	Gene	Description or homolog	35000HPΔrelAΔspoT / 35000HP[b] Fold-Change			35000HPΔdksA / 35000HP[c] Fold-Change		
			Mid-Log	Transition	Stationary	Mid-Log	Transition	Stationary
	hofB	Type IV fimbrial assembly, ATPase PilB						-2.25
	lspA1	Large supernatant protein 1	-2.22		-2.75			
	lspA2	Large supernatant protein 2	-3.28		-5.07			
	lspB	Large supernatant protein exporter			-5.36			
	rcpA	Type II/IV secretion system secretin RcpA/CpaC, associated with Flp pilus assembly			-4.89			
	rcpB	Flp pilus assembly protein RcpB			-5.80			-2.18
	secG	Preprotein translocase subunit			2.28			2.27
	secY	Preprotein translocase SecY subunit			-2.45			
	tadD	Flp pilus assembly protein TadD, contains TPR repeat			-2.31			
	tadF	Flp pilus assembly surface protein TadF, ATP/GTP-binding motif			-3.21			
	tatA	Twin-arginine translocation protein						-2.00
	yajC	Preprotein translocase subunit			-3.25			-2.34
Ion transport								
	corA	Magnesium and cobalt transport protein CorA	4.29	2.90				
	HD0003	ATP synthase protein I2			-3.77			-2.03
	HD0810	Conserved hypothetical protein	2.27		2.08			2.67

Appendix III. Functional classification of genes differentially expressed by deletion of (p)ppGpp or DksA In Mid-Log, Transition, or Stationary Phase

Functional Category[a]	Gene	Description or homolog	35000HPΔrelAΔspoT / 35000HP[b] Fold-Change			35000HPΔdksA / 35000HP[c] Fold-Change		
			Mid-Log	Transition	Stationary	Mid-Log	Transition	Stationary
	HD0866	Anion permease ArsB/NhaD-like	2.47					
	HD1227	Putative Na+/H+ antiporter	2.13					
	HD1621	Conserved hypothetical protein			3.48			
	nqrA	Na+-translocating NADH-ubiquinone oxidoreductase, subunit A			-10.26			
	nqrB	NADH dehydrogenase			-8.72			-2.32
	nqrC	Na+-translocating NADH-ubiquinone oxidoreductase, subunit C			-6.16			
	nqrD	Na+-translocating NADH-ubiquinone oxidoreductase, subunit D		2.00	-5.39			-2.22
	nqrE	Na+-translocating NADH-ubiquinone oxidoreductase, subunit E		2.15	-3.63			
	nqrF	Na+-translocating NADH-ubiquinone oxidoreductase, subunit F		2.85	-2.03			
	oadB	Oxaloacetate decarboxylase beta chain		2.04				
	yfeB	Manganese ABC transporter, ATP-binding protein SitB			4.97			-2.21
	znuA	Zinc ABC transporter, periplasmic-binding protein						2.89

Appendix III. Functional classification of genes differentially expressed by deletion of (p)ppGpp or DksA In Mid-Log, Transition, or Stationary Phase

Functional Category[a]	Gene	Description or homolog	35000HPΔrelAΔspoT / 35000HP[b] Fold-Change			35000HPΔdksA / 35000HP[c] Fold-Change		
			Mid-Log	Transition	Stationary	Mid-Log	Transition	Stationary
Iron sulfur cluster binding								
	bioA	Adenosylmethionine-8-amino-7-oxononanoate aminotransferase			2.05			
	bioB	Biotin synthetase		2.10				
	bioD	Dethiobiotin synthetase		-2.04				
	chuW	Putative heme iron utilization protein			-3.14			-2.01
	fdx2	Ferredoxin, 2Fe-2S			-2.37			
	HD0319	Ribosomal RNA large subunit methyltransferase N			-2.85	2.40	2.63	
	HD0684	Probable iron binding protein from the HesB_IscA_SufA family			2.38			
	HD1084	HesB family protein			-5.34			-3.16
	iscU	Iron-sulfur cluster assembly scaffold protein		2.51	-2.67			-2.05
	ykgF	Putative iron-sulfur electron transport protein			-2.39			
Lipid biosynthesis and metabolism								
	glpB	Anaerobic glycerol-3-phosphate dehydrogenase subunit B			-3.95			-2.58
	hlp	putative lipoprotein			2.17			2.48
	hlpB	lipoprotein			3.35			3.12

158

Functional Category[a]	Gene[a]	Description or homolog	35000HPΔrelAΔspoT / 35000HP[b] Fold-Change			35000HPΔdksA / 35000HP[c] Fold-Change		
			Mid-Log	Transition	Stationary	Mid-Log	Transition	Stationary
	lgtB	diadenosine tetraphosphatase						3.13
	lipB	Lipoate-protein ligase B			-2.40			
	lpxB	Lipid-A-disaccharide synthase				2.13	2.83	
	lpxD	UDP-3-O-[3-hydroxymyristoyl] glucosamine N-acyltransferase						2.16
	menB	Naphthoate synthase			-2.05			
	pgpA	Phosphatidylglycerophosphatase A	-2.06					
	pgsA	CDP-diacylglycerol--glycerol-3-phosphate 3-phosphatidyltransferase			2.49			2.16
	plsC	1-acyl-sn-glycerol-3-phosphate acyltransferase			-3.94			-2.73
Metal ion binding								
	cysQ	3'(2'),5'-bisphosphate nucleotidase			3.17			2.79
	ftnA	Ferritin-like protein 2		-2.08	2.42		-2.26	4.17
	ftnB	Ferritin-like protein 2		-2.05	3.17		-2.38	5.26
	glmM	Phosphoglucosamine mutase					2.78	2.56
	gpt	Xanthine–guanine phosphoribosyltransferase)			2.58			3.33
	HD0117	hypothetical protein					3.91	
	HD0457	Soluble cytochrome b562			5.44			5.49
	HD1365	Carbonic anhydrase			2.33			

159

Appendix III. Functional classification of genes differentially expressed by deletion of (p)ppGpp or DksA In Mid-Log, Transition, or Stationary Phase

Functional Category[a]	Gene	Description or homolog	35000HPΔrelAΔspoT / 35000HP[b] Fold-Change			35000HPΔdksA / 35000HP[c] Fold-Change		
			Mid-Log	Transition	Stationary	Mid-Log	Transition	Stationary
	HD1915	Membrane protein YedZ			2.56			
	msrB							
	napA	Periplasmic nitrate reductase precursor			-2.19		-2.09	-2.07
	napB	Nitrate reductase cytochrome c550-type subunit			-7.27	-2.05	-2.26	-5.53
	napC	Cytochrome c-type protein			-3.32		-2.24	-2.71
	napD	Possible protein		-2.48	-2.01		-2.02	
	napF	Ferredoxin-type protein		-3.04				
	napG	Ferredoxin-type protein NapG (periplasmic nitrate reductase)		-2.12	-5.26	-2.16		-4.01
	napH	Polyferredoxin NapH (periplasmic nitrate reductase)			-8.44	-2.22	-2.00	-5.89
	nrfA	Cytochrome c552 precursor					-2.27	
	nrfB	Cytochrome c-type protein NrfB precursor					-2.43	
	ppa	Inorganic pyrophosphatase			5.08			3.76
	rimO	Ribosomal protein methylthiotransferase			-2.50			
	sodA	Manganese superoxide dismutase			2.02			
	sodC	Superoxide dismutase [Cu-Zn] precursor		-2.06	2.40		-2.21	
	torZ	Trimethylamine-N-oxide reductase			-2.50			

Appendix III. Functional classification of genes differentially expressed by deletion of (p)ppGpp or DksA In Mid-Log, Transition, or Stationary Phase

Functional Category[a]	Gene	Description or homolog	35000HPΔrelAΔspoT / 35000HP[b] Fold-Change			35000HPΔdksA / 35000HP[c] Fold-Change		
			Mid-Log	Transition	Stationary	Mid-Log	Transition	Stationary
Nucelotide binding								
	atpA	ATP synthase alpha chain			-2.74			
	atpC	ATP synthase epsilon chain			-7.96			-3.16
	atpD	ATP synthase beta chain			-6.57			-2.09
	atpE	ATP synthase C chain			-9.69			-2.83
	atpF	ATP synthase B chain			-8.29			-2.65
	atpG	ATP synthase gamma chain			-4.20			
	atpH	ATP synthase delta chain			-4.63			
	coaD	Phosphopantetheine adenylyltransferase			-2.40			-2.38
	deaD	Cold-shock DEAD box protein-A	2.36					
	era	GTP-binding protein era homolog			-2.89			
	frdA	Fumarate reductase flavoprotein subunit			-6.76			-3.75
	frdB	Fumarate reductase iron-sulfur subunit			-6.61			-3.81
	guaA	GMP synthase [glutamine-hydrolyzing]	-2.40		2.13			
	guaB	Inosine-5-monophosphate dehydrogenase	-2.52	-2.16	3.02			
	HD0584	Hypothetical protein	-2.00		3.01			
	HD0586	Lipopolysaccharide ABC transporter, ATP-binding protein LptB			2.89			2.03

Appendix III. Functional classification of genes differentially expressed by deletion of (p)ppGpp or DksA In Mid-Log, Transition, or Stationary Phase

Functional Category[a]	Gene	Description or homolog	35000HPΔrelAΔspoT / 35000HP[b] Fold-Change			35000HPΔdksA / 35000HP[c] Fold-Change		
			Mid-Log	Transition	Stationary	Mid-Log	Transition	Stationary
	HD0905	Mobile element protein	-2.60		-5.45			-3.04
	hflX	GTP-binding protein			11.32			2.98
	lldD	L-lactate dehydrogenase			-2.95			
	lolD	Lipoprotein releasing system ATP-binding protein			-3.10			-2.33
	ndk	Nucleoside diphosphate kinase			2.45			
	obgE	GTP-binding protein			-2.22			
	rnfG	Electron transport complex protein RnfG			-2.72			
	sapF	Peptide transport system ATP-binding protein SapF			3.77			3.47
	selD	Selenide, water dikinase						-2.21
	surE	5-nucleotidase / Exopolyphosphatase			-2.08			
	tadA	Type II/IV secretion system ATP hydrolase TadA/VirB11/CpaF, TadA subfamily			-6.86		2.28	-2.37
	tmk	Thymidylate kinase			2.05			
	typA	GTP-binding protein TypA/BipA						2.41
	uup	ABC-type transport protein Uup			-3.04			
	visC	2-octaprenyl-3-methyl-6-methoxy-1,4-benzoquinol hydroxylase	-2.26					

Appendix III. Functional classification of genes differentially expressed by deletion of (p)ppGpp or DksA In Mid-Log, Transition, or Stationary Phase

Functional Category[a]	Gene	Description or homolog	35000HPΔrelAΔspoT / 35000HP[b] Fold-Change			35000HPΔdksA / 35000HP[c] Fold-Change		
			Mid-Log	Transition	Stationary	Mid-Log	Transition	Stationary
Protein fate								
	ccmA	ABC transporter involved in cytochrome c biogenesis, ATPase component						-2.25
	clpB	Chaperone protein	-2.41	8.36	-3.08			
	degP	Outer membrane stress sensor protease DegQ			2.50			
	dnaK	Chaperone protein	-2.09	7.70			2.00	
	fkpA	FKBP-type peptidyl-prolyl cis-trans isomerase			2.71			2.11
	gcp	TsaD/Kae1/Qri7, required for threonylcarbamoyladenosine t(6)A37 formation in tRNA						
	groEL	60 kDa chaperonin	-3.99	4.78	2.05			
	groES	10 kDa chaperonin	-3.47	5.10				
	grpE	Heat shock protein	-2.00	7.32				-7.21
	HD1278	Possible serine protease			-2.02		-2.39	
	HD1280	Possible serine protease homolog			-2.72		-2.21	
	HD1339	Cell wall endopeptidase, family M23/M37				2.07		
	HD1436	Hypothetical protein					2.11	
	HD1513	Putative RND efflux membrane fusion protein		2.81				

Appendix III. Functional classification of genes differentially expressed by deletion of (p)ppGpp or DksA In Mid-Log, Transition, or Stationary Phase

Functional Category[a]	Gene	Description or homolog	35000HPΔrelAΔspoT / 35000HP[b] Fold-Change			35000HPΔdksA / 35000HP[c] Fold-Change		
			Mid-Log	Transition	Stationary	Mid-Log	Transition	Stationary
	HD1895	putative accessory processing protein			-3.53			-2.16
	hemK	Protein-N(5)-glutamine methyltransferase PrmC			-2.07			-2.08
	hscA	Chaperone protein		2.22	-2.69			
	hscB	Chaperone protein		2.06				
	hslU	ATP-dependent hsl protease ATP-binding subunit		15.78				
	hslV	ATP-dependent protease		13.12				
	htpX	putative protease		14.26				
	icc	3',5'-cyclic-nucleotide phosphodiesterase			-2.78			-2.57
	iscS	Cysteine desulfurase		2.12				
	lepB	Signal peptidase I			-2.67			
	lon	ATP-dependent protease La, Type I		3.30				
	map	Methionine aminopeptidase						2.73
	pepB	Peptidase B	-2.51					
	pepD	Peptidase D			2.41			2.23
	ppiD	Peptidyl-prolyl cis-trans isomerase			2.42			
	prlC	Oligopeptidase A	-2.29	6.38				
	prmA	Ribosomal protein L11 methyltransferase			-2.02			

Appendix III. Functional classification of genes differentially expressed by deletion of (p)ppGpp or DksA In Mid-Log, Transition, or Stationary Phase

Functional Category[a]	Gene[a]	Description or homolog	35000HPΔrelAΔspoT / 35000HP[b] Fold-Change			35000HPΔdksA / 35000HP[c] Fold-Change		
			Mid-Log	Transition	Stationary	Mid-Log	Transition	Stationary
	proQ	influences osmotic activation of compatible solute ProP			5.81			2.49
	slyD	FKBP-type peptidyl-prolyl cis-trans isomerase SlyD		-2.12		2.01		2.05
	SohB	Possible secreted protease sohB						
	surA	Survival protein SurA homolog			4.13			2.21
RNA binding								
	HD0356	Putative deoxyribonuclease YjjV			2.06			
	HD1200	RNA binding protein			3.97			2.98
	rsuA	Ribosomal small subunit pseudouridine synthase A			3.31			
	vacB	3'-to-5' exoribonuclease RNase R			2.04			
RNA processing								
	HD0270	Putative tRNA/rRNA methyltransferase			-2.10			
	HD0448	tRNA dihydrouridine synthase B	2.23		-4.61			
	HD0478	23S rRNA (Uracil-5-) methyltransferase rumB			2.75			2.52
	HD1138	tRNA pseudouridine synthase C			2.10			2.08
	HD1664	tRNA:Cm32/Um32 methyltransferase	-2.55		-2.68			

165

Appendix III. Functional classification of genes differentially expressed by deletion of (p)ppGpp or DksA In Mid-Log, Transition, or Stationary Phase

Functional Category[a]	Gene[a]	Description or homolog	35000HPΔrelAΔspoT / 35000HP[b] Fold-Change			35000HPΔdksA / 35000HP[c] Fold-Change		
			Mid- Log	Transition	Stationary	Mid- Log	Transition	Stationary
	ksgA	Dimethyladenosine transferase			2.03			
	miaA	tRNA dimethylallyltransferase			7.64			
	mnmC	tRNA (5-methylaminomethyl-2-thiouridylate)-methyltransferase	-2.51	-2.77				
	pcnB	Poly A polymerase						2.14
	rbfA	Ribosome binding factor A	2.19	2.41	-8.10			-4.14
	rimM	16S rRNA processing protein RimM			-2.80			
	rnc	Ribonuclease III			-2.86			
	rnpA	Ribonuclease P protein component			3.80			3.54
	rrmJ	Cell division protein FtsJ / Ribosomal RNA large subunit methyltransferase E		2.32				
	rumA	23S rRNA (Uracil-5-)-methyltransferase RumA	2.21					
	sun	16S rRNA (cytosine(967)-C(5))-methyltransferase			-4.35			-3.63
	trmB	tRNA (guanine46-N7-)-methyltransferase			-2.91			-2.44
	trmD	tRNA (Guanine37-N1)-methyltransferase	2.02				-2.06	
	truA	tRNA pseudouridine synthase A						2.00
	truB	tRNA pseudouridine synthase B		2.00				

166

Appendix III. Functional classification of genes differentially expressed by deletion of (p)ppGpp or DksA In Mid-Log, Transition, or Stationary Phase

Functional Category[a]	Gene	Description or homolog	35000HPΔrelAΔspoT / 35000HP[b] Fold-Change			35000HPΔdksA / 35000HP[c] Fold-Change		
			Mid-Log	Transition	Stationary	Mid-Log	Transition	Stationary
Transcription								
	argR	Arginine pathway regulatory protein, repressor of arg regulon			2.38			
	crp	Cyclic AMP receptor protein			2.78			
	cspC	Cold shock protein CspA	2.23		9.40		-2.84	7.48
	cspD	Cold shock protein CspD			-4.06			-2.63
	fis	DNA-binding protein			-4.63			
	greA	Transcription elongation factor			2.33			
	greB	Transcription elongation factor			-2.31			-2.21
	HD0089	Transcriptional regulatory protein			-3.15			
	HD0698	Unsaturated fatty acid biosythesis repressor FabR, TetR family			3.15			
	HD1533	Transcriptional regulator, IclR family		2.07		2.15	3.34	
	HD2030	Hypothetical protein	-2.36					
	hlyX	Catabolite gene activator and regulatory subunit of cAMP-dependent protein kinases			2.14			
	lrp	Leucine-responsive regulatory protein			-2.04			
	purR	Purine nucleotide synthesis repressor			2.08			
	rpoB	DNA-directed RNA polymerase beta subunit		2.25	-2.48			

Appendix III. Functional classification of genes differentially expressed by deletion of (p)ppGpp or DksA In Mid-Log, Transition, or Stationary Phase

Functional Category[a]	Gene	Description or homolog	35000HPΔrelAΔspoT / 35000HP[b] Fold-Change			35000HPΔdksA / 35000HP[c] Fold-Change		
			Mid-Log	Transition	Stationary	Mid-Log	Transition	Stationary
	rpoC	DNA-directed RNA polymerase beta' subunit		2.92	-4.07			
	rpoE	RNA polymerase sigma-E factor			3.59			
	rpoZ	RNA polymerase omega subunit			2.88			
	rseA	Sigma factor RpoE negative regulatory protein			2.02			
	rseC	Sigma factor RpoE regulatory protein			-2.09			
	tldD	TldD protein, part of TldE/TldD proteolytic complex			-2.21			-2.07
Translation	asnA	Aspartate--ammonia ligase			4.83			
	def	Peptide deformylase			3.40		-2.08	2.21
	efp	Translation elongation factor P	2.01					4.27
	fusA	Translation elongation factor G			-2.85			
	HD1357	Conserved possible translation initiation factor	-2.38					
	hisS	Histidyl-tRNA synthetase			-3.50			
	infB	Translation initiation factor IF-2	2.03		-2.78			
	prfB	Peptide chain release factor 2; programmed frameshift-containing			2.42			-2.22
	prfC	Peptide chain release factor 3			-2.40			

Appendix III. Functional classification of genes differentially expressed by deletion of (p)ppGpp or DksA In Mid-Log, Transition, or Stationary Phase

Functional Category[a]	Gene	Description or homolog	35000HPΔrelAΔspoT / 35000HP[b] Fold-Change			35000HPΔdksA / 35000HP[c] Fold-Change		
			Mid-Log	Transition	Stationary	Mid-Log	Transition	Stationary
	pth	Peptidyl-tRNA hydrolase			2.32			3.18
	rplA	LSU ribosomal protein L1p (L10Ae)	2.31					2.46
	rplB	LSU ribosomal protein L2p (L8e)			-2.36			
	rplC	LSU ribosomal protein L3p (L3e)	2.40		-2.44			
	rplD	LSU ribosomal protein L4p (L1e)	2.30		-3.03			
	rplE	LSU ribosomal protein L5p (L11e)	2.17					
	rplF	LSU ribosomal protein L6p (L9e)			-2.24			
	rplI	LSU ribosomal protein L9p	2.39		3.11			
	rplJ	LSU ribosomal protein L10p (P0)	4.69					
	rplK	LSU ribosomal protein L11p (L12e)	2.27		-2.01			
	rplL	LSU ribosomal protein L7/L12 (P1/P2)	5.31		2.19			3.25
	rplN	LSU ribosomal protein L14p (L23e)	2.10					
	rplO	LSU ribosomal protein L15p (L27Ae)			-4.03			-2.06
	rplP	LSU ribosomal protein L16p (L10e)			-2.06			
	rplX	LSU ribosomal protein L19p	2.41					
	rplY	LSU ribosomal protein L20p			-2.75			2.19
	rplS	LSU ribosomal protein L22p (L17e)	2.03		-3.43			
	rplT	LSU ribosomal protein L23p (L23Ae)	2.16		-3.49			

169

Appendix III. Functional classification of genes differentially expressed by deletion of (p)ppGpp or DksA In Mid-Log, Transition, or Stationary Phase

Functional Category[a]	Gene	Description or homolog	35000HPΔrelAΔspoT / 35000HP[b] Fold-Change			35000HPΔdksA / 35000HP[c] Fold-Change		
			Mid-Log	Transition	Stationary	Mid-Log	Transition	Stationary
	rplV	LSU ribosomal protein L24p (L26e)	2.23					-2.13
	rplW	LSU ribosomal protein L25p	3.71		3.25			
	rpmB	LSU ribosomal protein L28p			2.35			2.58
	rpmC	LSU ribosomal protein L29p (L35e)			-2.04			
	rpmD	LSU ribosomal protein L30p (L7e)			-4.01			-2.00
	rpmE	LSU ribosomal protein L31p, zinc-dependent		-2.14	2.05			2.17
	rpmE2	50S ribosomal protein L31		2.31				
	rpmG	LSU ribosomal protein L33p, zinc-independent			3.00			3.00
	rpmH	LSU ribosomal protein L34p			2.68			2.35
	rpmI	LSU ribosomal protein L35p			-2.73			
	rpmJ	LSU ribosomal protein L36p		2.27	-3.14			
	rpsB	SSU ribosomal protein S2p (SAe)			2.19	2.90		
	rpsE	SSU ribosomal protein S5p (S2e)			-2.12			
	rpsH	SSU ribosomal protein S8p (S15Ae)			-2.02	2.81		
	rpsI	SSU ribosomal protein S9p (S16e)			2.60			
	rpsJ	SSU ribosomal protein S10p (S20e)	2.58		-2.13			
	rpsM	SSU ribosomal protein S13p (S18e)			-2.28			
	rpsN	SSU ribosomal protein S14p (S29e), zinc-independent	2.08		-2.17			
	rpsO	SSU ribosomal protein S15p (S13e)	2.18		3.54			2.47

170

Appendix III. Functional classification of genes differentially expressed by deletion of (p)ppGpp or DksA In Mid-Log, Transition, or Stationary Phase

Functional Category[a]	Gene	Description or homolog	35000HPΔrelAΔspoT / 35000HP[b] Fold-Change			35000HPΔdksA / 35000HP[c] Fold-Change		
			Mid-Log	Transition	Stationary	Mid-Log	Transition	Stationary
	rpsP	SSU ribosomal protein S16p	2.00		-2.69			
	rpsQ	SSU ribosomal protein S17p (S11e)			-2.14			
	rpsR	SSU ribosomal protein S18p, zinc-independent	2.13		2.07			
	rpsS	SSU ribosomal protein S19p (S15e)			-3.91			-2.07
	rpsT	SSU ribosomal protein S20p	3.23				-2.17	2.69
	selA	L-seryl-tRNA(Sec) selenium transferase						-2.05
	valS	Valyl-tRNA synthetase			-2.09			
Transport of proteins and carbohydrates								
	ampG	AmpG permease		2.02				
	ccmB	ABC transporter involved in cytochrome c biogenesis subunit			-3.68			-2.79
	ccmC	putative heme lyase for CcmE			-5.33			-3.32
	ccmD	Cytochrome C maturation protein D			-4.46			-2.57
	ccmF	Cytochrome c heme lyase subunit			-2.16			
	comE	Type IV pilus biogenesis protein PilQ			2.08			
	crr	PTS system, glucose-specific IIA component		2.06	5.85			4.64
	dcuB1	Anaerobic C4-dicarboxylate transporter	-2.25		3.59			

Appendix III. Functional classification of genes differentially expressed by deletion of (p)ppGpp or DksA In Mid-Log, Transition, or Stationary Phase

Functional Category[a]	Gene	Description or homolog	35000HPΔrelAΔspoT / 35000HP[b] Fold-Change			35000HPΔdksA / 35000HP[c] Fold-Change		
			Mid-Log	Transition	Stationary	Mid-Log	Transition	Stationary
	dppD	Dipeptide transport ATP-binding protein			-2.19			
	glpF	Glycerol uptake facilitator protein	4.56		-46.33			-27.32
	HD0665	Hypothetical protein	-2.73		4.15			
	HD0800	21 kDa hemolysin precursor			2.61			
	HD1859	Ascorbate-specific PTS system, EIIA component			-5.34			-2.34
	ptsH	Phosphotransferase system, phosphocarrier protein HPr			4.12			3.08
	ptsN	PTS system nitrogen-specific IIA component, PtsN			2.05			
	thiQ	Thiamin ABC transporter, ATPase component / Thiamine transport ATP-binding protein thiQ			-2.73			
	tolB	Colicin tolerance protein			-2.96			
	tolR	Tol biopolymer transport system			-2.69			
	ulaA	Ascorbate-specific PTS system, EIIC component	2.00		-6.40			-4.41
Uncharacterized conserved protein								
	HD0105	Hypothetical protein	-2.21		-2.87		2.23	
	HD0123	Hypothetical protein					2.76	
	HD0134	Mu-like prophage protein GP36				3.71	5.03	
	HD0135	hypothetical protein				3.18	4.50	2.64

172

Appendix III. Functional classification of genes differentially expressed by deletion of (p)ppGpp or DksA In Mid-Log, Transition, or Stationary Phase

Functional Category[a]	Gene[a]	Description or homolog	35000HPΔrelAΔspoT / 35000HP[b] Fold-Change			35000HPΔdksA / 35000HP[c] Fold-Change		
			Mid-Log	Transition	Stationary	Mid-Log	Transition	Stationary
	HD0136	hypothetical protein				3.77	4.99	
	HD0150	Phage FAD/FMN-containing dehydrogenase			-2.66		2.84	
	HD0250	Putative preQ0 transporter				2.11		3.69
	HD0326	Hypothetical protein co-occurring with RecR			2.27			
	HD0412	Tex			-2.52			
	HD0534	Phage FAD/FMN-containing dehydrogenase		2.55	-2.37		3.67	
	HD0588	Uncharacterized protein YrbK clustered with lipopolysaccharide transporters			2.25			
	HD0778	UPF0235 protein VC0458	-2.73	-2.42	-2.21			
	HD1218	Periplasmic lysozyme inhibitor of c-type lysozyme	-2.53		5.62			
	HD1377	Protein YeeX	-2.26	-2.46				
	HD1379	Hypothetical protein			-2.87			
	HD1386	Predicted P-loop ATPase fused to an acetyltransferase	-2.00		-2.00			
	HD1555	Phage terminase, large subunit					2.99	
	HD1556	Mu-like prophage FluMu protein gp29					2.28	
	HD1576	Phage FAD/FMN-containing dehydrogenase					2.72	

Appendix III. Functional classification of genes differentially expressed by deletion of (p)ppGpp or DksA In Mid-Log, Transition, or Stationary Phase

Functional Category[a]	Gene	Description or homolog	35000HPΔ*relA*Δ*spoT* / 35000HP[b] Fold-Change			35000HPΔ*dksA* / 35000HP[c] Fold-Change		
			Mid-Log	Transition	Stationary	Mid-Log	Transition	Stationary
	HD1622	Conserved hypothetical protein						2.89
	HD1756	Putative xanthine/uracil permease			-5.78	3.11	2.42	6.18
	phnA	Alkylphosphonate utilization operon protein PhnA			2.05			3.87
	plpR1	RstR-like phage repressor protein			3.81			3.91
	plpR2	RstR-like phage repressor protein			3.93			4.00
	sanA	SanA protein			-3.86			-4.44
	slyX	SlyX-like protein					-2.68	
	ykgE	Conserved putative dehydrogenase subunit			-2.78			

[a]Does not include genes that encode hypothetical proteins.

[b]Genes or operons differentially regulated in 35000HP Δ*relA*Δ*spoT* versus 35000HP.

[c]Genes or operons differentially regulated in 35000HPΔ*dksA* versus 35000HP.

References

1. **Morse SA.** 1989. Chancroid and *Haemophilus ducreyi*. Clin. Microbiol. Rev. **2:**137-157.

2. **Gioia J, Qin X, Jiang H, Clinkenbeard K, Lo R, Liu Y, Fox GE, Yerrapragada S, McLeod MP, McNeill TZ, Hemphill L, Sodergren E, Wang Q, Muzny DM, Homsi FJ, Weinstock GM, Highlander SK.** 2006. The genome sequence of *Mannheimia haemolytica* A1: insights into virulence, natural competence, and *Pasteurellaceae* phylogeny. Journal of bacteriology **188:**7257-7266.

3. **De Ley J, Mannheim W, Mutters R, Piechulla K, Tytgat R, Segars P, Bisgaard M, Frederikson W, Hinz K-H, Vanhoucke M.** 1990. Inter- and Intrafamilial similarities of the rRNA cistrons of the *Pasteurellaceae*. Int J Syst Bacteriol **40:**126-137.

4. **Dewhirst FE, Paster BJ, Olsen I, Fraser GJ.** 1992. Phylogeny of 54 representative strains of species in the family Pasteurellaceae as determined by comparison of 16S rRNA sequences. Journal of bacteriology **174:**2002-2013.

5. **Mbwana J, Bolin I, Lyamuya E, Mhalu F, Lagergard T.** 2006. Molecular characterization of *Haemophilus ducreyi* isolates from different geographical locations. Journal of clinical microbiology **44:**132-137.

6. **White CD, Leduc I, Jeter C, Harris C, Elkins C.** 2005. *Haemophilus ducreyi* outer membrane determinants, including DsrA, define two clonal populations. Infect. Immun. **73:**2387-2399.

7. **Post DMB, Munson RS, Jr., Baker B, Zhong H, Bozue JA, Gibson BW.** 2007. Identification of genes involved in the expression of atypical lipooligosaccharide structures from a second class of *Haemophilus ducreyi*. Infect. Immun. **75:**113-121.

175

8.   **Ricotta EE, Wang N, Cutler R, Lawrence JG, Humphreys TL.** 2011. Rapid Divergence of Two Classes of *Haemophilus ducreyi*. Journal of bacteriology **193:**2941-2947.

9.   **Ducrey A.** 1889. Experimentelle untersuchungen uber den ansteckungsstof des weichen schankers and uber die bubonen. Montash fur Prakt Dermatol **9:**387-405.

10.   **Bezancon F, Griffon V, Le Sourd L.** 1900. Culture du bacille du chancre mou. CR Soc Biol **11:**1048-1051.

11.   **Bassereau PI.** 1852. Traite de affections de la peau symptomatiques de la syphilis. Paris: JB Balliere.

12.   **Spinola SM, Bauer ME, Munson RS, Jr.** 2002. Immunopathogenesis of *Haemophilus ducreyi* infection (chancroid). Infect. Immun. **70:**1667-1676.

13.   **Sturm AW, Zanen HC.** 1984. Characteristics of *Haemophilus ducreyi* in culture. Journal of clinical microbiology **19:**672-674.

14.   **Spinola SM.** 2008. Chancroid and *Haemophilus ducreyi*, p. 689-699. *In* Holmes KK, Sparling PF, Stamm WE, Piot P, Wasserheit JN, Corey L, Cohen MS, Watts DH (ed.), Sexually transmitted diseases, 4th ed. McGraw-Hill, New York.

15.   **Orroth KK, White RG, Korenromp EL, Bakker R, Changalucha J, Habbema JDF, Hayes RJ.** 2006. Empirical observations underestimate the proportion of human immunodeficiency virus infections attributable to sexually transmitted diseases in the Mwanza and Rakai sexually transmitted disease treatment trials: Simulation results. Sex. Trans. Dis. **33:**536-544.

16. **Spinola SM, Orazi A, Arno JN, Fortney K, Kotylo P, Chen C-Y, Campagnari AA, Hood AF.** 1996. *Haemophilus ducreyi* elicits a cutaneous infiltrate of CD4 cells during experimental human infection. J. Infect. Dis. **173:**394-402.

17. **Humphreys TL, Schnizlein-Bick CT, Katz BP, Baldridge LA, Hood AF, Hromas RA, Spinola SM.** 2002. Evolution of the cutaneous immune response to experimental *Haemophilus ducreyi* infection and its relevance to HIV-1 acquisition. J. Immunol. **169:**6316-6323.

18. **King R, Choudhri SH, Nasio J, Gough J, Nagelkerke NJD, Plummer FA, Ndinya-Achola JO, Ronald AR.** 1998. Clinical and *in situ* cellular responses to *Haemophilus ducreyi* in the presence or absence of HIV infection. Int. J. STD AIDS **9:**531-536.

19. **Morse SA, Trees DL, Htun Y, Radebe F, Orle KA, Dangor Y, Beck-Sague CM, Schmid S, Fehler G, Weiss JB, Ballard RC.** 1997. Comparison of clinical diagnosis and standard laboratory and molecular methods for the diagnosis of genital ulcer disease in Lesotho: association with human immunodeficiency virus infection. J. Infect. Dis. **175:**583-589.

20. **Dyer JR, Eron JJ, Hoffman IF, Kazembe P, Vernazza PL, Nkata E, Daly CC, Fiscus SA, Cohen MS.** 1998. Association of CD4 cell depletion and elevated blood and seminal plasma human immunodeficiency virus type (HIV-1) RNA concentrations with genital ulcer disease in HIV-1-infected men in Malawi. J. Infect. Dis. **177:**224-227.

21. **Nkengasong JN, Kestens L, Ghys PD, Koblavi-Deme S, Bile C, Kalou M, Ya LK, Traore-Ettiegne V, Maurice C, Laga M, Wiktor SZ, Greenberg AE.** 2001. Human immunodeficiency virus type 1 (HIV-1) plasma virus load and markers of

immune activation among HIV-infected female sex workers with sexually transmitted diseases in Abidjan, Cote d'Ivoire. J. Infect. Dis. **183:**1405-1408.

22.   **Janowicz DM, Tenner-Racz K, Racz P, Humphreys TL, Schnizlein-Bick C, Fortney KR, Zwickl B, Katz BP, Campbell JJ, Ho DD, Spinola SM.** 2007. Experimental Infection with *Haemophilus ducreyi* in Persons Who Are Infected with HIV Does Not Cause Local or Augment Systemic Viral Replication. J Infect Dis. **195:**1443-1451.

23.   **Lewis DA.** 2014. Epidemiology, clinical features, diagnosis and treatment of *Haemophilus ducreyi* - a disappearing pathogen? Expert Rev Anti Infect Ther **12:**687-696.

24.   **Marckmann P, Hojbjerg T, von Eyben FE, Christensen I.** 1989. Imported pedal chancroid: case report. Genitourinary medicine **65:**126-127.

25.   **Ussher JE, Wilson E, Campanella S, Taylor SL, Roberts SA.** 2007. *Haemophilus ducreyi* causing chronic skin ulceration in children visiting Samoa. Clinical Infectious Diseases **44:**e85-87.

26.   **McBride WJ, Hannah RC, Le Cornec GM, Bletchly C.** 2008. Cutaneous chancroid in a visitor from Vanuatu. Australas J Dermatol. **49:**98-99.

27.   **Peel TN, Bhatti D, De Boer JC, Stratov I, Spelman DW.** 2010. Chronic cutaneous ulcers secondary to *Haemophilus ducreyi* infection. Med.J.Aust. **192:**348-350.

28.   **Mitjà O, Lukehart SA, Pokowas G, Moses P, Kapa A, Godornes C, Robson J, Cherian S, Houinei W, Kazadi W, Siba P, de Lazzari E, Bassat Q.** 2014. *Haemophilus ducreyi* as a cause of skin ulcers in children from a yaws-endemic area of Papua New Guinea: a prospective cohort study. The Lancet Global Health **2:**e235-e241.

29.   **Marks M, Chi KH, Vahi V, Pillay A, Sokana O, Pavluck A, Mabey DC, Chen CY, Solomon AW.** 2014. *Haemophilus ducreyi* Associated with Skin Ulcers among Children, Solomon Islands. Emerging infectious diseases **20:**1705-1707.

30.   **Ghinai R, El-Duah P, Chi KH, Pillay A, Solomon AW, Bailey RL, Agana N, Mabey DC, Chen CY, Adu-Sarkodie Y, Marks M.** 2015. A cross-sectional study of 'yaws' in districts of ghana which have previously undertaken azithromycin mass drug administration for trachoma control. PLoS neglected tropical diseases **9:**e0003496.

31.   **Schmid GP.** 1999. Treatment of chancroid, 1997. Clinical infectious diseases : an official publication of the Infectious Diseases Society of America **28 Suppl 1:**S14-20.

32.   **Lewis DA.** 2000. Diagnostic tests for chancroid. Sex Transm. Infect. **76:**137-141.

33.   **Motley M, Sarafian SK, Knapp JS, Zaidi AA, Schmid G.** 1992. Correlation between in vitro antimicrobial scusceptilities and b-lactamase plasmid contents of isolates of *Haemophilus ducreyi* from the United States. Antimicrobial agents and chemotherapy **36:**1639-1643.

34.   **Knapp JS, Back AF, Babst AF, Taylor D, Rice RJ.** 1993. In vitro susceptibilies of isolates of *Haemophilus ducreyi* from Thailand and the United States to currently recommended and newer agents for treatment of chancroid. Antimicrob. Agents Chemother. **37:**1552-1555.

35.   **Nicasio AM, Kuti JL, Nicolau DP.** 2008. The current state of multidrug-resistant gram-negative bacilli in North America. Pharmacotherapy **28:**235-249.

36.   **Spinola SM, Wild LM, Apicella MA, Gaspari AA, Campagnari AA.** 1994. Experimental human infection with *Haemophilus ducreyi*. J. Infect. Dis. **169:**1146-1150.

37.   **Al-Tawfiq JA, Thornton AC, Katz BP, Fortney KR, Todd KD, Hood AF, Spinola SM.** 1998. Standardization of the experimental model of *Haemophilus ducreyi* infection in human subjects. J. Infect. Dis. **178:**1684-1687.

38.   **Gaston JR, Roberts SA, Humphreys TL.** 2015. Molecular Phylogenetic Analysis of Non-Sexually Transmitted Strains of *Haemophilus ducreyi*. PloS one **10:**e0118613.

39.   **Gangaiah D, Webb KM, Humphreys TL, Fortney KR, Toh E, Tai A, Katz SS, Pillay A, Chen CY, Roberts SA, Munson RS, Jr., Spinola SM.** 2015. *Haemophilus ducreyi* Cutaneous Ulcer Strains Are Nearly Identical to Class I Genital Ulcer Strains. PLoS neglected tropical diseases **9:**e0003918.

40.   **Cohen MS, Cannon JG.** 1999. Human experimentation with *Neisseria gonorrhoeae*: Progress and goals. J. Infect. Dis. **179:**S375-S379.

41.   **McCool TL, Cate TR, Moy G, Weiser JN.** 2002. The immune response to pneumococcal proteins during experimental human carriage. The Journal of experimental medicine **195:**359-365.

42.   **McKenzie WNJ, Anderson RR.** 1981. Endotoxin induced migration of leukocytes from blood to milk. J.Dairy Sci. **64:**227-235.

43.   **Donnenberg MS, Tacket CO, Losonsky G, Frankel G, Nataro JP, Dougan G, Levine MM.** 1998. Effect of prior experimental human enteropathogenic *Escherichia coli* infection on illness following homologous and heterologous rechallenge. Infect. Immun. **66:**52-58.

44.   **Purcell BK, Richardson JA, Radolf JD, Hansen EJ.** 1991. A temperature-dependent rabbit model for production of dermal lesions by *Haemophilus ducreyi*. J. Infect. Dis. **164:**359-367.

45.   **Hobbs MM, SanMateo LR, Orndorff PE, Almond G, Kawula TH.** 1995. Swine model of *Haemophilus ducreyi* infection. Infect. Immun. **63:**3094-3100.

46.   **Totten PA, Morton WR, Knitter GH, Clark AM, Kiviat NB, Stamm WE.** 1994. A primate model for chancroid. J. Infect. Dis. **169:**1284-1290.

47.   **Janowicz DM, Ofner S, Katz BP, Spinola SM.** 2009. Experimental infection of human volunteers with *Haemophilus ducreyi*: fifteen years of clinical data and experience. The Journal of infectious diseases **199:**1671-1679.

48.   **Hansen EJ, Lumbley SR, Richardson JA, Purcell BK, Stevens MK, Cope LD, Datte J, Radolf JD.** 1994. Induction of protective immunity to *Haemophilus ducreyi* in the temperature-dependent rabbit model of experimental chancroid. J. Immunol. **152:**184-192.

49.   **Throm RE, Spinola SM.** 2001. Transcription of candidate virulence genes of *Haemophilus ducreyi* during infection of human volunteers. Infect. Immun. **69:**1483-1487.

50.   **Bauer ME, Goheen MP, Townsend CA, Spinola SM.** 2001. *Haemophilus ducreyi* associates with phagocytes, collagen, and fibrin and remains extracellular throughout infection of human volunteers. Infect. Immun. **69:**2549-2557.

51.   **Bauer ME, Townsend CA, Ronald AR, Spinola SM.** 2006. Localization of *Haemophilus ducreyi* in naturally acquired chancroidal ulcers. Microbe. Infect. **8:**2465-2468.

52. **Ahmed HJ, Johansson C, Svensson LA, Ahlman K, Verdrengh M, Lagergard T.** 2002. In vitro and in vivo interactions of *Haemophilus ducreyi* with host phagocytes. Infect. Immun. **70:**899-908.

53. **Humphreys T, Li L, Li X, Janowicz D, Fortney KR, Zhao Q, Li W, McClintick JN, Katz BP, Wilkes DS, Edenberg HJ, Spinola SM.** 2007. Dysregulated immune profiles for skin and dendritic cells are associated with increased host susceptibility to *Haemophilus ducreyi* infection in human volunteers. Infect. Immun. **75:**5686-5697.

54. **Banks KE, Humphreys T, Li W, Katz BP, Wilkes DS, Spinola SM.** 2007. *Haemophilus ducreyi* partially activates human myeloid dendritic cells. Infect. Immun. **75:**5678-5685.

55. **Palmer KL, Schnizlein-Bick CT, Orazi A, John K, Chen C-Y, Hood AF, Spinola SM.** 1998. The immune response to *Haemophilus ducreyi* resembles a delayed-type hypersensitivity reaction throughout experimental infection of human subjects. J. Infect. Dis. **178:**1688-1697.

56. **Spinola SM, Bong CTH, Faber AL, Fortney KR, Bennett SL, Townsend CA, Zwickl BE, Billings SD, Humphreys TL, Bauer ME, Katz BP.** 2003. Differences in host susceptibility to disease progression in the human challenge model of *Haemophilus ducreyi* infection. Infect. Immun. **71:**6658-6663.

57. **Fortney KR, Young RS, Bauer ME, Katz BP, Hood AF, Munson RS, Jr., Spinola SM.** 2000. Expression of peptidoglycan-associated lipoprotein is required for virulence in the human model of *Haemophilus ducreyi* infection. Infect. Immun. **68:**6441-6448.

58.   **Al-Tawfiq JA, Fortney KR, Katz BP, Elkins C, Spinola SM.** 2000. An isogenic hemoglobin receptor-deficient mutant of *Haemophilus ducreyi* is attenuated in the human model of experimental infection. J. Infect. Dis. **181:**1049-1054.

59.   **Leduc I, Banks KE, Fortney KR, Patterson KB, Billings SD, Katz BP, Spinola SM, Elkins C.** 2008. Evaluation of the repertoire of the TonB-dependent receptors of *Haemophilus ducreyi* for their role in virulence in humans. J. Infect. Dis. **197:**1103-1109.

60.   **Banks KE, Fortney KR, Baker B, Billings SD, Katz BP, Munson RS, Jr., Spinola SM.** 2008. The enterobacterial common antigen-like gene cluster of *Haemophilus ducreyi* contributes to virulence in humans. J. Infect. Dis. **197:**1531-1536.

61.   **Ward CK, Mock JR, Hansen EJ.** 2004. The LspB protein is involved in the secretion of the LspA1 and LspA2 proteins by *Haemophilus ducreyi*. Infect. Immun. **72:**1874-1884.

62.   **Vakevainen M, Greenberg S, Hansen EJ.** 2003. Inhibition of phagocytosis by *Haemophilus ducreyi* requires expression of the LspA1 and LspA2 proteins. Infect. Immun. **71:**5994-6003.

63.   **Mock JR, Vakevainen M, Deng K, Latimer JL, Young JA, van Oers NS, Greenberg S, Hansen EJ.** 2005. *Haemophilus ducreyi* targets Src family protein tyrosine kinases to inhibit phagocytic signaling. Infect. Immun. **73:**7808-7816.

64.   **Dodd DA, Worth RG, Rosen MK, Grinstein S, van Oers NS, Hansen EJ.** 2014. The *Haemophilus ducreyi* LspA1 Protein Inhibits Phagocytosis By Using a New Mechanism Involving Activation of C-Terminal Src Kinase. mBio **5**.

65.   **Ward CK, Latimer JL, Nika J, Vakevainen M, Mock JR, Deng K, Blick RJ, Hansen EJ.** 2003. Mutations in the lspA1 and lspA2 genes of *Haemophilus ducreyi* affect the virulence of this pathogen in an animal model system. Infect. Immun. **71:**2478-2486.

66.   **Janowicz DM, Fortney KR, Katz BP, Latimer JL, Deng K, Hansen EJ, Spinola SM.** 2004. Expression of the LspA1 and LspA2 proteins by *Haemophilus ducreyi* is required for virulence in human volunteers. Infect. Immun. **72:**4528-4533.

67.   **Mount KL, Townsend CA, Rinker SD, Gu X, Fortney KR, Zwickl BW, Janowicz DM, Spinola SM, Katz BP, Bauer ME.** 2010. *Haemophilus ducreyi* SapA contributes to cathelicidin resistance and virulence in humans. Infection and immunity **78:**1176-1184.

68.   **Rinker SD, Gu X, Fortney KR, Zwickl BW, Katz BP, Janowicz DM, Spinola SM, Bauer ME.** 2012. Permeases of the Sap Transporter Are Required for Cathelicidin Resistance and Virulence of *Haemophilus ducreyi* in Humans. The Journal of infectious diseases **206:**1407-1414.

69.   **Nika JR, Latimer JL, Ward CK, Blick RJ, Wagner NJ, Cope LD, Mahairas GG, Munson J, R.S., Hansen EJ.** 2002. *Haemophilus ducreyi* requires the *flp* gene cluster for microcolony formation in vitro. Infect. Immun. **70(6):**2965-2975.

70.   **Janowicz DM, Cooney SA, Walsh J, Baker B, Katz BP, Fortney KR, Zwickl B, Ellinger S, Munson J, R. S.** 2011. Expression of the flp protens by *Haemophilus ducreyi* is necessary for virulence in human volunteers. BMC Microbiology **11:**208.

71.   **Bhattacharjee MK, Kachlany SC, Fine DH, Figurski DH.** 2001. Nonspecific adherence and fibril biogenesis by *Actinobacillus actinomycetemcomitans*: tadA proteins is an ATPase. J. Bacteriol. **183:**5927-5936.

72.   **Spinola SM, Fortney KR, Katz BP, Latimer JL, Mock JR, Vakevainen M, Hansen EJ.** 2003. *Haemophilus ducreyi* requires an intact *flp* gene cluster for virulence in humans. Infect. Immun. **71:**7178-7182.

73.   **Bauer ME, Fortney KR, Harrison A, Janowicz DM, Munson RS, Jr., Spinola SM.** 2008. Identification of *Haemophilus ducreyi* genes expressed during human infection. Microbiology **154:**1152-1160.

74.   **Bauer ME, Spinola SM.** 1999. Binding of *Haemophilus ducreyi* to extracellular matrix proteins. Infect. Immun. **67:**2649-2653.

75.   **Fulcher RA, Cole LE, Janowicz DM, Toffer KL, Fortney KR, Katz BP, Orndorff PE, Spinola SM, Kawula TH.** 2006. Expression of *Haemophilus ducreyi* collagen binding outer membrane protein NcaA is required for virulence in swine and human challenge models of chancroid. Infect. Immun. **74:**2651-2658.

76.   **Bong CTH, Throm RE, Fortney KR, Katz BP, Hood AF, Elkins C, Spinola SM.** 2001. A DsrA-deficient mutant of *Haemophilus ducreyi* is impaired in its ability to infect human volunteers. Infect. Immun. **69:**1488-1491.

77.   **Elkins C, Morrow KJ, Olsen B.** 2000. Serum resistance in *Haemophilus ducreyi* requires outer membrane protein *DsrA*. Infect. Immun. **68:**1608-1619.

78.   **Leduc I, Richards P, Davis C, Schilling B, Elkins C.** 2004. A novel lectin,DltA, is required for expression of a full serum resistance phenotype in *Haemophilus ducreyi*. Infect. Immun. **72:**3418-3428.

79.   **Janowicz D, Leduc I, Fortney KR, Katz BP, Elkins C, Spinola SM.** 2006. A DltA mutant of *Haemophilus ducreyi* is partially attenuated in its ability to cause pustules in human volunteers. Infect. Immun. **74:**1394-1397.

80.   **Bauer ME, Townsend CA, Doster RS, Fortney KR, Zwickl BW, Katz BP, Spinola SM, Janowicz DM.** 2009. A fibrinogen-binding lipoprotein contributes to virulence of *Haemophilus ducreyi* in humans. J Infect Dis. **199:**684-692.

81.   **Fusco WG, Elkins C, Leduc I.** 2013. Trimeric Autotransporter DsrA Is a Major Mediator of Fibrinogen Binding in *Haemophilus ducreyi*. Infection and immunity **81:**4443-4452.

82.   **Zhu J, Miller MB, Vance RE, Dziejman M, Bassler BL, Mekalanos JJ.** 2002. Quorum-sensing regulators control virulence gene expression in *Vibrio cholerae*. Proceedings of the National Academy of Sciences of the United States of America **99:**3129-3134.

83.   **Fong KP, Chung WO, Lamont RJ, Demuth DR.** 2001. Intra- and interspecies regulation of gene expression by *Actinobacillus actinomycetemcomitans* LuxS. Infection and immunity **69:**7625-7634.

84.   **Labandeira-Rey M, Janowicz DM, Blick RJ, Fortney KR, Zwickl B, Katz BP, Spinola SM, Hansen EJ.** 2009. Inactivation of the *Haemophilus ducreyi luxS* gene affects the virulence of this pathogen in human subjects. The Journal of infectious diseases **200:**409-416.

85.   **Labandeira-Rey M, Brautigam CA, Hansen EJ.** 2010. Characterization of the CpxRA Regulon in *Haemophilus ducreyi*. Infection and immunity **78:**4779-4791.

86.   **Skerker JM, Perchuk BS, Siryaporn A, Lubin EA, Ashenberg O, Goulian M, Laub MT.** 2008. Rewiring the specificity of two-component signal transduction systems. Cell **133:**1043-1054.

87.   **Spinola SM, Fortney KR, Baker B, Janowicz DM, Zwickl B, Katz BP, Blick RJ, Munson RS, Jr.** 2010. Activation of the CpxRA system by deletion of *cpxA* impairs the ability of *Haemophilus ducreyi* to infect humans. Infection and immunity **78:**3898-3904.

88.   **Tamayo R, Pratt JT, Camilli A.** 2007. Roles of cyclic diguanylate in the regulation of bacterial pathogenesis. Annual review of microbiology **61:**131-148.

89.   **Gangaiah D, Zhang X, Baker B, Fortney KR, Liu Y, Munson RS, Jr., Spinola SM.** 2014. *Haemophilus ducreyi* RpoE and CpxRA appear to play distinct yet complementary roles in regulation of envelope-related functions. Journal of bacteriology.

90.   **Bouslimani A, Porto C, Rath CM, Wang M, Guo Y, Gonzalez A, Berg-Lyon D, Ackermann G, Moeller Christensen GJ, Nakatsuji T, Zhang L, Borkowski AW, Meehan MJ, Dorrestein K, Gallo RL, Bandeira N, Knight R, Alexandrov T, Dorrestein PC.** 2015. Molecular cartography of the human skin surface in 3D. Proceedings of the National Academy of Sciences of the United States of America.

91.   **Zhang A, Wassarman KM, Rosenow C, Tjaden BC, Storz G, Gottesman S.** 2003. Global analysis of small RNA and mRNA targets of Hfq. Molecular microbiology **50:**1111-1124.

92.   **Sittka A, Lucchini S, Papenfort K, Sharma CM, Rolle K, Binnewies TT, Hinton JC, Vogel J.** 2008. Deep sequencing analysis of small noncoding RNA and

mRNA targets of the global post-transcriptional regulator, Hfq. PLoS genetics **4:**e1000163.

93.   **Gangaiah D, Labandeira-Rey M, Zhang X, Fortney KR, Ellinger S, Zwickl B, Baker B, Liu Y, Janowicz DM, Katz BP, Brautigam CA, Munson RS, Jr., Hansen EJ, Spinola SM.** 2014. *Haemophilus ducreyi* Hfq Contributes to Virulence Gene Regulation as Cells Enter Stationary Phase. mBio **5**.

94.   **Gangaiah D, Li W, Fortney KR, Janowicz DM, Ellinger S, Zwickl B, Katz BP, Spinola SM.** 2013. Carbon Storage Regulator A Contributes to the Virulence of *Haemophilus ducreyi* in Humans by Multiple Mechanisms. Infection and immunity **81:**608-617.

95.   **Hays RC, Mandell GL.** 1974. pO_2, pH, and redox potential of experimental abscesses Proc Soc Exp Biol Med. **147:**29-30.

96.   **Costello EK, Lauber CL, Hamady M, Fierer N, Gordon JI, Knight R.** 2009. Bacterial community variation in human body habitats across space and time. Science **326:**1694-1697.

97.   **Grice EA, Segre JA.** 2011. The skin microbiome. Nature reviews. Microbiology **9:**244-253.

98.   **Jani AJ, Briggs CJ.** 2014. The pathogen Batrachochytrium dendrobatidis disturbs the frog skin microbiome during a natural epidemic and experimental infection. Proceedings of the National Academy of Sciences of the United States of America **111:**E5049-5058.

99.   **Crewe-Brown HH, Krige FK, Davel GH, Barron C, Van Vuuren JA, Shipham SO, Roux JG.** 1982. Genital ulceration in males at Ga-Rankuwa Hospital,

Pretoria. South African medical journal = Suid-Afrikaanse tydskrif vir geneeskunde **62:**861-863.

100. **Dangor Y, Fehler G, Exposto FD, Koornhof HJ.** 1989. Causes and treatment of sexually acquired genital ulceration in southern Africa. South African medical journal = Suid-Afrikaanse tydskrif vir geneeskunde **76:**339-341.

101. **Le Bacq F, Mason PR, Gwanzura L, Robertson VJ, Latif AS.** 1993. HIV and other sexually transmitted diseases at a rural hospital in Zimbabwe. Genitourinary medicine **69:**352-356.

102. **Haseltine WA, Block R.** 1973. Synthesis of guanosine tetra- and pentaphosphate requires the presence of a codon-specific, uncharged transfer ribonucleic acid in the acceptor site of ribosomes. Proceedings of the National Academy of Sciences of the United States of America **70:**1564-1568.

103. **Ostling J, Flardh K, Kjelleberg S.** 1995. Isolation of a carbon starvation regulatory mutant in a marine *Vibrio* strain. Journal of bacteriology **177:**6978-6982.

104. **Vinella D, Albrecht C, Cashel M, D'Ari R.** 2005. Iron limitation induces SpoT-dependent accumulation of ppGpp in *Escherichia coli*. Molecular microbiology **56:**958-970.

105. **Gallant J, Palmer L, Pao CC.** 1977. Anomalous synthesis of ppGpp in growing cells. Cell **11:**181-185.

106. **Perederina A, Svetlov V, Vassylyeva MN, Tahirov TH, Yokoyama S, Artsimovitch I, Vassylyev DG.** 2004. Regulation through the secondary channel--structural framework for ppGpp-DksA synergism during transcription. Cell **118:**297-309.

107.   **Paul BJ, Barker MM, Ross W, Schneider DA, Webb C, Foster JW, Gourse RL.** 2004. DksA: a critical component of the transcription initiation machinery that potentiates the regulation of rRNA promoters by ppGpp and the initiating NTP. Cell **118:**311-322.

108.   **Meddows TR, Savory AP, Grove JI, Moore T, Lloyd RG.** 2005. RecN protein and transcription factor DksA combine to promote faithful recombinational repair of DNA double-strand breaks. Molecular microbiology **57:**97-110.

109.   **Blaser MJ, Dominguez-Bello MG, Contreras M, Magris M, Hidalgo G, Estrada I, Gao Z, Clemente JC, Costello EK, Knight R.** 2013. Distinct cutaneous bacterial assemblages in a sampling of South American Amerindians and US residents. The ISME journal **7:**85-95.

110.   **Aberg A, Shingler V, Balsalobre C.** 2008. Regulation of the fimB promoter: a case of differential regulation by ppGpp and DksA in vivo. Molecular microbiology **67:**1223-1241.

111.   **Lyzen R, Kochanowska M, Wegrzyn G, Szalewska-Palasz A.** 2009. Transcription from bacteriophage lambda pR promoter is regulated independently and antagonistically by DksA and ppGpp. Nucleic acids research **37:**6655-6664.

112.   **Johnson RC, Ellis MW, Lanier JB, Schlett CD, Cui T, Merrell DS.** 2015. Correlation between nasal microbiome composition and remote purulent skin and soft tissue infections. Infection and immunity **83:**802-811.

113.   **Holley CL, Zhang X, Fortney KR, Ellinger S, Johnson P, Baker B, Liu Y, Janowicz DM, Katz BP, Munson RS, Jr., Spinola SM.** 2015. DksA and (p)ppGpp

Have Unique and Overlapping Contributions to Haemophilus ducreyi Pathogenesis in Humans. Infection and immunity.

114.   **Mitkevich VA, Ermakov A, Kulikova AA, Tankov S, Shyp V, Soosaar A, Tenson T, Makarov AA, Ehrenberg M, Hauryliuk V.** 2010. Thermodynamic characterization of ppGpp binding to EF-G or IF2 and of initiator tRNA binding to free IF2 in the presence of GDP, GTP, or ppGpp. Journal of molecular biology **402:**838-846.

115.   **Kvint K, Farewell A, Nystrom T.** 2000. RpoS-dependent promoters require guanosine tetraphosphate for induction even in the presence of high levels of sigma(s). The Journal of biological chemistry **275:**14795-14798.

116.   **Szalewska-Palasz A, Johansson LU, Bernardo LM, Skarfstad E, Stec E, Brannstrom K, Shingler V.** 2007. Properties of RNA polymerase bypass mutants: implications for the role of ppGpp and its co-factor DksA in controlling transcription dependent on sigma54. The Journal of biological chemistry **282:**18046-18056.

117.   **Costanzo A, Nicoloff H, Barchinger SE, Banta AB, Gourse RL, Ades SE.** 2008. ppGpp and DksA likely regulate the activity of the extracytoplasmic stress factor sigmaE in *Escherichia coli* by both direct and indirect mechanisms. Molecular microbiology **67:**619-632.

118.   **Gentry DR, Hernandez VJ, Nguyen LH, Jensen DB, Cashel M.** 1993. Synthesis of the stationary-phase sigma factor sigma s is positively regulated by ppGpp. Journal of bacteriology **175:**7982-7989.

119.   **Brown L, Gentry D, Elliott T, Cashel M.** 2002. DksA affects ppGpp induction of RpoS at a translational level. Journal of bacteriology **184:**4455-4465.

120. **Lennon CW, Gaal T, Ross W, Gourse RL.** 2009. *Escherichia coli* DksA binds to Free RNA polymerase with higher affinity than to RNA polymerase in an open complex. Journal of bacteriology **191:**5854-5858.

121. **Sharma AK, Payne SM.** 2006. Induction of expression of hfq by DksA is essential for Shigella flexneri virulence. Molecular microbiology **62:**469-479.

122. **Argaman L, Elgrably-Weiss M, Hershko T, Vogel J, Altuvia S.** 2012. RelA protein stimulates the activity of RyhB small RNA by acting on RNA-binding protein Hfq. Proceedings of the National Academy of Sciences of the United States of America **109:**4621-4626.

123. **Na HS, Kim HJ, Lee HC, Hong Y, Rhee JH, Choy HE.** 2006. Immune response induced by *Salmonella typhimurium* defective in ppGpp synthesis. Vaccine **24:**2027-2034.

124. **Sun W, Roland KL, Branger CG, Kuang X, Curtiss R, 3rd.** 2009. The role of relA and spoT in *Yersinia pestis* KIM5 pathogenicity. PloS one **4:**e6720.

125. **Bugrysheva JV, Bryksin AV, Godfrey HP, Cabello FC.** 2005. *Borrelia burgdorferi rel* is responsible for generation of guanosine-3'-diphosphate-5'-triphosphate and growth control. Infection and immunity **73:**4972-4981.

126. **Geiger T, Goerke C, Fritz M, Schafer T, Ohlsen K, Liebeke M, Lalk M, Wolz C.** 2010. Role of the (p)ppGpp synthase RSH, a RelA/SpoT homolog, in stringent response and virulence of *Staphylococcus aureus*. Infection and immunity **78:**1873-1883.

127. **Vogt SL, Green C, Stevens KM, Day B, Erickson DL, Woods DE, Storey DG.** 2011. The stringent response is essential for *Pseudomonas aeruginosa* virulence in the rat

lung agar bead and Drosophila melanogaster feeding models of infection. Infection and immunity **79:**4094-4104.

128.   **Dahl JL, Kraus CN, Boshoff HI, Doan B, Foley K, Avarbock D, Kaplan G, Mizrahi V, Rubin H, Barry CE, 3rd.** 2003. The role of RelMtb-mediated adaptation to stationary phase in long-term persistence of *Mycobacterium tuberculosis* in mice. Proceedings of the National Academy of Sciences of the United States of America **100:**10026-10031.

129.   **Abranches J, Martinez AR, Kajfasz JK, Chavez V, Garsin DA, Lemos JA.** 2009. The molecular alarmone (p)ppGpp mediates stress responses, vancomycin tolerance, and virulence in *Enterococcus faecalis*. Journal of bacteriology **191:**2248-2256.

130.   **Aberg A, Shingler V, Balsalobre C.** 2006. (p)ppGpp regulates type 1 fimbriation of *Escherichia coli* by modulating the expression of the site-specific recombinase FimB. Molecular microbiology **60:**1520-1533.

131.   **Haralalka S, Nandi S, Bhadra RK.** 2003. Mutation in the relA gene of *Vibrio cholerae* affects in vitro and in vivo expression of virulence factors. Journal of bacteriology **185:**4672-4682.

132.   **Mogull SA, Runyen-Janecky LJ, Hong M, Payne SM.** 2001. dksA is required for intercellular spread of *Shigella flexneri* via an RpoS-independent mechanism. Infection and immunity **69:**5742-5751.

133.   **Henard CA, Vazquez-Torres A.** 2012. DksA-dependent resistance of *Salmonella enterica* serovar Typhimurium against the antimicrobial activity of inducible nitric oxide synthase. Infection and immunity **80:**1373-1380.

134.   **Magnusson LU, Gummesson B, Joksimovic P, Farewell A, Nystrom T.** 2007. Identical, independent, and opposing roles of ppGpp and DksA in *Escherichia coli*. Journal of bacteriology **189:**5193-5202.

135.   **Pal RR, Bag S, Dasgupta S, Das B, Bhadra RK.** 2012. Functional characterization of the stringent response regulatory gene dksA of *Vibrio cholerae* and its role in modulation of virulence phenotypes. Journal of bacteriology **194:**5638-5648.

136.   **Jude F, Kohler T, Branny P, Perron K, Mayer MP, Comte R, van Delden C.** 2003. Posttranscriptional control of quorum-sensing-dependent virulence genes by DksA in *Pseudomonas aeruginosa*. Journal of bacteriology **185:**3558-3566.

137.   **Lee EC, Yu D, Martinez de Velasco J, Tessarollo L, Swing DA, Court DL, Jenkins NA, Copeland NG.** 2001. A highly efficient *Escherichia coli*-based chromosome engineering system adapted for recombinogenic targeting and subcloning of BAC DNA. Genomics **73:**56-65.

138.   **Xiao H, Kalman M, Ikehara K, Zemel S, Glaser G, Cashel M.** 1991. Residual guanosine 3',5'-bispyrophosphate synthetic activity of *relA* null mutants can be eliminated by *spoT* null mutations. The Journal of biological chemistry **266:**5980-5990.

139.   **Bong CTH, Fortney KR, Katz BP, Hood AF, San Mateo LR, Kawula TH, Spinola SM.** 2002. A superoxide dismutase C mutant of *Haemophilus ducreyi* is virulent in human volunteers. Infect. Immun. **70:**1367-1371.

140.   **Bozue JA, Tarantino L, Munson RS, Jr.** 1998. Facile construction of mutations in *Haemophilus ducreyi* using *lacz* as a counter-selectable marker. FEMS Microbiol. Lett. **164:**269-273.

141. **Tracy E, Ye F, Baker BD, Munson RS, Jr.** 2008. Construction of non-polar mutants in *Haemophilus influenzae* using FLP recombinase technology. BMC Molecular Biology **9:**101.

142. **Gibson DG, Young L, Chuang RY, Venter JC, Hutchison CA, 3rd, Smith HO.** 2009. Enzymatic assembly of DNA molecules up to several hundred kilobases. Nature methods **6:**343-345.

143. **Spinola SM, Hiltke TJ, Fortney K, Shanks K.** 1996. The conserved 18,000-molecular-weight outer membrane protein of *Haemophilus ducreyi* has homology to PAL. Infect. Immun. **64:**1950-1955.

144. **Spinola SM, Griffiths GE, Shanks KL, Blake MS.** 1993. The major outer membrane protein of *Haemophilus ducreyi* is a member of the OmpA family of proteins. Infect. Immun. **61:**1346-1351.

145. **Concepcion MB, Nelson DR.** 2003. Expression of spoT in *Borrelia burgdorferi* during serum starvation. Journal of bacteriology **185:**444-452.

146. **Gangaiah D, Liu Z, Arcos J, Kassem, II, Sanad Y, Torrelles JB, Rajashekara G.** 2010. Polyphosphate kinase 2: a novel determinant of stress responses and pathogenesis in *Campylobacter jejuni*. PloS one **5:**e12142.

147. **Naruhn S, Meissner W, Adhikary T, Kaddatz K, Klein T, Watzer B, Muller-Brusselbach S, Muller R.** 2010. 15-hydroxyeicosatetraenoic acid is a preferential peroxisome proliferator-activated receptor beta/delta agonist. Mol Pharmacol **77:**171-184.

148. **Breese MR, Liu Y.** 2013. NGSUtils: a software suite for analyzing and manipulating next-generation sequencing datasets. Bioinformatics **29:**494-496.

149. **Kanehisa M, Goto S.** 2000. KEGG: kyoto encyclopedia of genes and genomes. Nucleic acids research **28:**27-30.

150. **Caspi R, Altman T, Dreher K, Fulcher CA, Subhraveti P, Keseler IM, Kothari A, Krummenacker M, Latendresse M, Mueller LA, Ong Q, Paley S, Pujar A, Shearer AG, Travers M, Weerasinghe D, Zhang P, Karp PD.** 2012. The MetaCyc database of metabolic pathways and enzymes and the BioCyc collection of pathway/genome databases. Nucleic acids research **40:**D742-753.

151. **Weintrob AC, Murray CK, Lloyd B, Li P, Lu D, Miao Z, Aggarwal D, Carson ML, Gaskins LJ, Tribble DR.** 2013. Active surveillance for asymptomatic colonization with multidrug-resistant gram negative bacilli among injured service members--a three year evaluation. Msmr **20:**17-22.

152. **Raivio TL, Leblanc SK, Price NL.** 2013. The *Escherichia coli* Cpx envelope stress response regulates genes of diverse function that impact antibiotic resistance and membrane integrity. Journal of bacteriology **195:**2755-2767.

153. **Geiger T, Kastle B, Gratani FL, Goerke C, Wolz C.** 2014. Two small (p)ppGpp synthases in *Staphylococcus aureus* mediate tolerance against cell envelope stress conditions. Journal of bacteriology **196:**894-902.

154. **Young RS, Fortney K, Haley JC, Hood AF, Campagnari AA, Wang J, Bozue JA, Munson RSJ, Spinola SM.** 1999. Expression of sialylated or paragloboside-like lipooligosaccharides are not required for pustule formation by *Haemophilus ducreyi* in human volunteers. Infect. Immun. **67:**6335-6340.

155.   **Prather DT, Bains M, Handcock REW, Filiatrault MJ, Campagnari AA.** 2004. Differential experssion of porins OmpP2A and OmpP2B of *Haemophilus ducreyi*. Infect. Immun. **72:**6271-6278.

156.   **Tobe T, Kusukawa N, Yura T.** 1987. Suppression of rpoH (htpR) mutations of *Escherichia coli*: heat shock response in suhA revertants. Journal of bacteriology **169:**4128-4134.

157.   **Wang QP, Kaguni JM.** 1989. A novel sigma factor is involved in expression of the rpoH gene of *Escherichia coli*. Journal of bacteriology **171:**4248-4253.

158.   **Traxler MF, Summers SM, Nguyen HT, Zacharia VM, Hightower GA, Smith JT, Conway T.** 2008. The global, ppGpp-mediated stringent response to amino acid starvation in *Escherichia coli*. Molecular microbiology **68:**1128-1148.

159.   **Bauer ME, Spinola SM.** 2000. Localization of *Haemophilus ducreyi* at the pustular stage of disease in the human model of infection. Infect. Immun. **68:**2309-2314.

160.   **Khakimova M, Ahlgren HG, Harrison JJ, English AM, Nguyen D.** 2013. The stringent response controls catalases in *Pseudomonas aeruginosa* and is required for hydrogen peroxide and antibiotic tolerance. Journal of bacteriology **195:**2011-2020.

161.   **Vogt SL, Raivio TL.** 2011. Just scratching the surface: an expanding view of the Cpx envelope stress response. FEMS Microbiology Letters **326:**2-11.

162.   **Yan X, Zhao C, Budin-Verneuil A, Hartke A, Rince A, Gilmore MS, Auffray Y, Pichereau V.** 2009. The (p)ppGpp synthetase RelA contributes to stress adaptation and virulence in *Enterococcus faecalis* V583. Microbiology **155:**3226-3237.

163.   **Aberg A, Fernandez-Vazquez J, Cabrer-Panes JD, Sanchez A, Balsalobre C.** 2009. Similar and divergent effects of ppGpp and DksA deficiencies on transcription in *Escherichia coli*. Journal of bacteriology **191:**3226-3236.

164.   **Holley C, Gangaiah D, Li W, Fortney KR, Janowicz DM, Ellinger S, Zwickl B, Katz BP, Spinola SM.** 2014. A (p)ppGpp-Null Mutant of *Haemophilus ducreyi* Is Partially Attenuated in Humans Due to Multiple Conflicting Phenotypes. Infection and immunity **82:**3492-3502.

165.   **Nakanishi N, Abe H, Ogura Y, Hayashi T, Tashiro K, Kuhara S, Sugimoto N, Tobe T.** 2006. ppGpp with DksA controls gene expression in the locus of enterocyte effacement (LEE) pathogenicity island of enterohaemorrhagic *Escherichia coli* through activation of two virulence regulatory genes. Molecular microbiology **61:**194-205.

166.   **Gangaiah D, Zhang X, Fortney KR, Baker B, Liu Y, Munson RS, Jr., Spinola SM.** 2013. Activation of CpxRA in *Haemophilus ducreyi* primarily inhibits the expression of its targets, including major virulence determinants. Journal of bacteriology **195:**3486-3502.

167.   **Vogel J, Luisi BF.** 2011. Hfq and its constellation of RNA. Nature reviews. Microbiology **9:**578-589.

168.   **Sonnleitner E, Napetschnig J, Afonyushkin T, Ecker K, Vecerek B, Moll I, Kaberdin VR, Blasi U.** 2004. Functional effects of variants of the RNA chaperone Hfq. Biochemical and biophysical research communications **323:**1017-1023.

169.   **Valentin-Hansen P, Eriksen M, Udesen C.** 2004. The bacterial Sm-like protein Hfq: a key player in RNA transactions. Molecular microbiology **51:**1525-1533.

170.   **Ramachandran VK, Shearer N, Jacob JJ, Sharma CM, Thompson A.** 2012. The architecture and ppGpp-dependent expression of the primary transcriptome of *Salmonella Typhimurium* during invasion gene expression. BMC genomics **13:**25.

171.   **Vercruysse M, Fauvart M, Cloots L, Engelen K, Thijs IM, Marchal K, Michiels J.** 2010. Genome-wide detection of predicted non-coding RNAs in *Rhizobium etli* expressed during free-living and host-associated growth using a high-resolution tiling array. BMC genomics **11:**53.

172.   **Janowicz D, Luke NR, Fortney KR, Katz BP, Campagnari AA, Spinola SM.** 2006. Expression of OmpP2A and OmpP2B is not required for pustule formation by *Haemophilus ducreyi* in human volunteers. Microb. Path. **40:**110-115.

173.   **Webb C, Moreno M, Wilmes-Riesenberg M, Curtiss R, 3rd, Foster JW.** 1999. Effects of DksA and ClpP protease on sigma S production and virulence in Salmonella typhimurium. Molecular microbiology **34:**112-123.

174.   **Turner AK, Lovell MA, Hulme SD, Zhang-Barber L, Barrow PA.** 1998. Identification of Salmonella typhimurium genes required for colonization of the chicken alimentary tract and for virulence in newly hatched chicks. Infection and immunity **66:**2099-2106.

175.   **Potrykus K, Cashel M.** 2008. (p)ppGpp: still magical? Annual review of microbiology **62:**35-51.

176.   **Nystrom T.** 2003. Conditional senescence in bacteria: death of the immortals. Molecular microbiology **48:**17-23.

177.   **Aizenman E, Engelberg-Kulka H, Glaser G.** 1996. An *Escherichia coli* chromosomal "addiction module" regulated by guanosine [corrected] 3',5'-

bispyrophosphate: a model for programmed bacterial cell death. Proceedings of the National Academy of Sciences of the United States of America **93:**6059-6063.

178.   **Fernandez J, Barrett JF, Licata L, Amaratunga D, Frosco M.** 1999. Comparison of efficacies of oral levofloxacin and oral ciprofloxacin in a rabbit model of a staphylococcal abscess. Antimicrobial agents and chemotherapy **43:**667-671.

179.   **Gaca AO, Kajfasz JK, Miller JH, Liu K, Wang JD, Abranches J, Lemos JA.** 2013. Basal levels of (p)ppGpp in *Enterococcus faecalis*: the magic beyond the stringent response. mBio **4:**e00646-00613.

180.   **Grand S, Passaro G, Ziegler A, Esteve F, Boujet C, Hoffmann D, Rubin C, Segebarth C, Decorps M, Le Bas JF, Remy C.** 1999. Necrotic tumor versus brain abscess: importance of amino acids detected at 1H MR spectroscopy--initial results. Radiology **213:**785-793.

181.   **Durfee T, Hansen AM, Zhi H, Blattner FR, Jin DJ.** 2008. Transcription profiling of the stringent response in *Escherichia coli*. Journal of bacteriology **190:**1084-1096.

182.   **Edwards RL, Dalebroux ZD, Swanson MS.** 2009. *Legionella pneumophila* couples fatty acid flux to microbial differentiation and virulence. Molecular microbiology **71:**1190-1204.

183.   **Mittenhuber G.** 2001. Comparative genomics and evolution of genes encoding bacterial (p)ppGpp synthetases/hydrolases (the Rel, RelA and SpoT proteins). Journal of molecular microbiology and biotechnology **3:**585-600.

184.   **Tehranchi AK, Blankschien MD, Zhang Y, Halliday JA, Srivatsan A, Peng J, Herman C, Wang JD.** 2010. The transcription factor DksA prevents conflicts between DNA replication and transcription machinery. Cell **141:**595-605.

185.   **Tsui HC, Leung HC, Winkler ME.** 1994. Characterization of broadly pleiotropic phenotypes caused by an hfq insertion mutation in Escherichia coli K-12. Molecular microbiology **13:**35-49.

186.   **Maisonneuve E, Castro-Camargo M, Gerdes K.** 2013. (p)ppGpp controls bacterial persistence by stochastic induction of toxin-antitoxin activity. Cell **154:**1140-1150.

187.   **Murray KD, Bremer H.** 1996. Control of spoT-dependent ppGpp synthesis and degradation in *Escherichia coli*. Journal of molecular biology **259:**41-57.

188.   **Battesti A, Bouveret E.** 2006. Acyl carrier protein/SpoT interaction, the switch linking SpoT-dependent stress response to fatty acid metabolism. Molecular microbiology **62:**1048-1063.

189.   **Jishage M, Kvint K, Shingler V, Nystrom T.** 2002. Regulation of sigma factor competition by the alarmone ppGpp. Genes & development **16:**1260-1270.

190.   **Moore-Gillon JC, Eykyn SJ, Phillips I.** 1981. Microbiology of pyogenic liver abscess. Br Med J (Clin Res Ed) **283:**819-821.

191.   **Paul BJ, Berkmen MB, Gourse RL.** 2005. DksA potentiates direct activation of amino acid promoters by ppGpp. Proceedings of the National Academy of Sciences of the United States of America **102:**7823-7828.

192.   **Pelicic V.** 2008. Type IV pili: e pluribus unum? Molecular microbiology **68:**827-837.

193.   **Thanassi DG, Bliska JB, Christie PJ.** 2012. Surface organelles assembled by secretion systems of Gram-negative bacteria: diversity in structure and function. FEMS microbiology reviews **36:**1046-1082.

194.   **Darzins A.** 1993. The pilG gene product, required for *Pseudomonas aeruginosa* pilus production and twitching motility, is homologous to the enteric, single-domain response regulator CheY. Journal of bacteriology **175:**5934-5944.

195.   **Redfield RJ, Findlay WA, Bosse J, Kroll JS, Cameron AD, Nash JH.** 2006. Evolution of competence and DNA uptake specificity in the Pasteurellaceae. BMC evolutionary biology **6:**82.

196.   **Spinola SM, Abu Kwaik Y, Lesse AJ, Campagnari AA, Apicella MA.** 1990. Cloning and expression in *Escherichia coli* of a *Haemophilus influenzae* type b lipooligosaccharide synthesis gene(s) that encode a 2-keto-3-deoxyoctulosonic acid epitope. Infect. Immun. **58:**1558-1564.

197.   **Frisk A, Roggen EL, Lagergard T.** 1995. Localisation and immunological properties of a 24-kDa surface protein of *Haemophilus ducreyi*. J. Med. Microbiol. **43:**192-200.

198.   **Brentjens RJ, Ketterer M, Apicella MA, Spinola SM.** 1996. Fine tangled pili expressed by *Haemophilus ducreyi* are a novel class of pili. J. Bacteriol. **178:**808-816.

199.   **Taha M, Morand PC, Pereira Y, Eugene E, Giorgini D, Larribe M, Nassif X.** 1998. Pilus-mediated adhesion of *Neisseria meningitidis*: the essential role of cell contact-dependent transcriptional upregulation of the PilC1 protein. Molecular microbiology **28:**1153-1163.

200.   **Boddey JA, Flegg CP, Day CJ, Beacham IR, Peak IR.** 2006. Temperature-regulated microcolony formation by *Burkholderia pseudomallei* requires *pilA* and enhances association with cultured human cells. Infection and immunity **74:**5374-5381.

201.   **Egge-Jacobsen W, Salomonsson EN, Aas FE, Forslund AL, Winther-Larsen HC, Maier J, Macellaro A, Kuoppa K, Oyston PC, Titball RW, Thomas RM, Forsberg A, Prior JL, Koomey M.** 2011. O-linked glycosylation of the PilA pilin protein of *Francisella tularensis*: identification of the endogenous protein-targeting oligosaccharyltransferase and characterization of the native oligosaccharide. Journal of bacteriology **193:**5487-5497.

202.   **Jenkins SR, Winkler WG.** 1987. Descriptive epidemiology from an epizootic of raccoon rabies in the Middle Atlantic States, 1982-1983. Am.J.Epidemiol. **126:**429-437.

203.   **Richter LV, Sandler SJ, Weis RM.** 2012. Two isoforms of Geobacter sulfurreducens PilA have distinct roles in pilus biogenesis, cytochrome localization, extracellular electron transfer, and biofilm formation. Journal of bacteriology **194:**2551-2563.

204.   **Harrison A, Santana EA, Szelestey BR, Newsom DE, White P, Mason KM.** 2013. Ferric uptake regulator and its role in the pathogenesis of nontypeable Haemophilus influenzae. Infection and immunity **81:**1221-1233.

<div align="center">

Curriculum Vitae

Concerta Leigh Holley

</div>

Education

Ph.D. in Microbiology and Immunology, Indiana University   2009 – 2015
Advisor: Dr. Stanley M. Spinola
B.S. in Biological Sciences, University of Notre Dame   2009

Research Experience

Graduate Research Assistant, Indiana University   2011 – 2015
Advisor: Prof. Stanley M. Spinola, Department of Microbiology and Immunology
Project: Determine the role of the stringent response in *Haemophilus ducreyi* virulence. Constructed and characterized Δ*relA*Δ*spoT* and Δ*dksA* mutants. Evaluated response of deletion mutants in a human model of infection and correlated to *in vitro* phenotypes. Defined transcriptomes of the Δ*relA*Δ*spoT* and Δ*dksA* mutants.

Graduate Research Assistant, Indiana University   2010 – 2011
Advisor: Prof. Johnny He, Department of Microbiology and Immunology
Project: Investigated effect of the HIV Tat protein on neuropathogenesis in juvenile and adult transgenic mice. Determined interaction of the HIV Tat with the Notch signaling pathway.

Undergraduate Research Assistant, University of Notre Dame   2007 – 2009
Advisor: Profs. Hope Hollocher, Biological Sciences and Augustin Fuentes, Anthropology
Project: Analyzed the parasite species diversity of primate fecal samples across temple sites on the island of Bali, Indonesia. Isolated mitochondrial DNA and correlated data to identify parasite spread.

Research Publications

Holley C, Zhang X, Fortney KR, Ellinger S, Johnson P, Baker B, Liu Y, Janowicz DM, Katz BP, Munson RS, Spinola SM. (2015). DksA and (p)ppGpp Have Unique and Overlapping Contributions to *Haemophilus ducreyi* Pathogenesis in Humans. *In Press*, Infection and Immunity

Holley C, Gangaiah D, Li W, Fortney KR, Janowicz DM, Ellinger S, Zwickl B, Katz BP, Spinola SM. (2014). A (p)ppGpp-Null Mutant of *Haemophilus ducreyi* Is Partially Attenuated in Humans Due to Multiple Conflicting Phenotypes. *Infection and Immunity*, 82(8), 3492-3502. PMCID: PMC4136218

Lane KE, **Holley C**, Hollocher H, Fuentes A. (2011). The anthropogenic environment lessens the intensity and prevalence of gastrointestinal parasites in Balinese long-tailed macaques (*Macaca fascicularis*). *Primates* 52(2):117-128. PMCID: 21165669

Abstracts
Holley C, Gangaiah D, Li W, Fortney KR, Janowicz DM, Ellinger S, Zwickl B, Katz BP, Spinola SM. ppGpp Contributes to the Virulence of *Haemophilus ducreyi* in Humans. ASM General Meeting 2014. May 2014. Boston, MA. Poster presentation.

Teaching Experience
Graduate Teaching Assistant, Indiana University, School of Nursing   Fall 2011
Professors: Susan Karimi, Ph.D.
Course: Introduction to Microbiology J210, Laboratory
Led discussions covering major lecture and laboratory topics in two sections containing 40 students each, assisted students with weekly problem sets, homework questions, and exam preparation. Assisted course director with lesson and exam preparation.

Leadership
Chair, Randy S. Rosenthal Graduate Student Advocacy Award Committee,   2014
Department of Microbiology and Immunology, Indiana University
Organize awards, including nominations, planning, and execution. Coordinate with faculty and students.

Graduate Student Representative, Indiana University School of Medicine   2013-2015
Organize the IUSM Travel Grant application process and review submitted grants. Attend GPSG meetings and report all activities, events, and information to the IUSM Graduate Division to distribute information to all current graduate students. Discuss campus-wide, IUSM-wide, or departmental-wide issues that arise which will affect graduate students within the IUSM. Provide an open forum for graduate students to share any feedback to improve IUSM graduate student life. Collectively share information about activities, events, or anonymous student concerns to faculty member councils of each department.

Chair, Research in Progress Awards Committee,   2010-2013
Department of Microbiology and Immunology, Indiana University
Organize awards, including nominations, planning, and execution. Develop and utilize budget. Coordinate with faculty and students.

Student Mentor, Indiana University School of Medicine   2010-2014
Assist with graduate school transition. Assist with course and mentor selection. Assist with coursework.

Awards, Fellowships and Affiliations

American Society for Microbiology	2014 -
Indiana Branch, American Society for Microbiology	2014 - 2015
Travel Award, Midwest Microbial Pathogenesis Conference	2013
Harold Raidt Graduate Student Teaching Award	2013
Diversity Supplement for R01 AI27863-18S2	2012-2014
Nominated for AAAS/Science Program for Excellence in Science	2012
Invited Panelist, Responsible Conduct of Research Series – Mentoring	2011
Travel Award, Midwest Microbial Pathogenesis Conference	2011
Nominated for SREB Teaching and Mentoring Institute	2011
Association of Women in Science	2009 -
Underrepresented Professional and Graduate Student Organization	2009-2015
University Fellowship	2009-2010
Braco Award for Research Excellence	2007